



Evidence of off-shell Higgs boson production from ZZ leptonic decay channels and constraints on its total width with the ATLAS detector

The ATLAS Collaboration

This Letter reports on a search for off-shell production of the Higgs boson using 139 fb^{-1} of pp collision data at $\sqrt{s} = 13 \text{ TeV}$ collected by the ATLAS detector at the Large Hadron Collider. The signature is a pair of Z bosons, with contributions from both the production and subsequent decay of a virtual Higgs boson and the interference of that process with other processes. The two observable final states are $ZZ \rightarrow 4\ell$ and $ZZ \rightarrow 2\ell 2\nu$ with $\ell = e$ or μ . In the $ZZ \rightarrow 4\ell$ final state, a dense Neural Network is used to enhance analysis sensitivity with respect to matrix element-based discrimination. The background-only hypothesis is rejected with an observed (expected) significance of 3.3 (2.2) standard deviations, representing experimental evidence for off-shell Higgs boson production. Assuming that no new particles enter the production of the virtual Higgs boson, its total width can be deduced from the measurement of its off-shell production cross-section. The measured total width of the Higgs boson is $4.5^{+3.3}_{-2.5} \text{ MeV}$, and the observed (expected) upper limit on the total width is found to be 10.5 (10.9) MeV at 95% confidence level.

1 Introduction

The discovery of the Higgs boson in 2012 by the ATLAS and CMS collaborations at the Large Hadron Collider (LHC) [1, 2] was a major milestone in particle physics, and since then this particle has been put under the spotlight for further scrutiny to uncover its fundamental nature. Great progress has been made in measuring the properties and couplings of the Higgs boson [3, 4], and to date no deviations from the Standard Model (SM) predictions have been found. The total width of the Higgs boson (Γ_H) is a key prediction of the SM. The expected value in the SM (Γ_H^{SM}) for a 125 GeV Higgs boson is only 4.1 MeV [5], which is inaccessible via any direct measurement of the width in the resonance region due to limited detector resolution. To probe this parameter, a method relying on both off-shell and on-shell production of the Higgs boson has been developed, as documented in [6–9]. In this method, the relationship between the Higgs boson coupling constants in the on-shell and off-shell regimes is assumed to be given by the SM prediction, assuming that no new particles enter into the Higgs boson production process. On-shell Higgs boson production (only gluon-gluon fusion (ggF) is considered in the equations below, but the principle is the same in other production modes) is inversely proportional to the width:

$$\sigma_{gg \rightarrow H \rightarrow ZZ}^{\text{on-shell}} \sim \frac{g_{\text{ggF}}^2 g_{\text{HZZ}}^2}{m_H \Gamma_H}.$$

However, off-shell Higgs boson production has no width dependence:

$$\sigma_{gg \rightarrow H \rightarrow ZZ}^{\text{off-shell}} \sim \frac{g_{\text{ggF}}^2 g_{\text{HZZ}}^2}{m_Z^2}.$$

Therefore, if the HZZ and effective ggH couplings in the two regimes (where the effective coupling is obtained by treating the quark loop as a single vertex) have a known relationship, Γ_H can be extracted from the ratio of yields of observed Higgs boson events. Off-shell production is accessible in the ZZ decay channel because the available phase space for the decay increases rapidly as the off-shell mass approaches the $2m_Z$ threshold, counteracting the expected drop in the production at higher masses [10–22], where m_Z is the mass of the Z boson.

Multiple searches for off-shell Higgs boson production have been carried out by the ATLAS and CMS collaborations using LHC Run 1 and Run 2 data [23–29]. In practice the signal of off-shell Higgs boson production is a deficit in $gg \rightarrow ZZ$ or electroweak $q\bar{q} \rightarrow ZZ$ production, due to the negative interference between the off-shell Higgs boson process and the continuum background. Throughout this Letter, the notation $gg \rightarrow (H^* \rightarrow)ZZ$ is used to refer to the inclusive process that combines the Higgs boson signal $gg \rightarrow H^* \rightarrow ZZ$, the continuum background process $gg \rightarrow ZZ$, and their interference. Similarly, the notation $q\bar{q} \rightarrow (H^* \rightarrow)ZZ + 2j$ refers to the inclusive electroweak process that combines the processes $q\bar{q} \rightarrow H^* \rightarrow ZZ + 2j$, $q\bar{q} \rightarrow ZZ + 2j$, and their interference.

The corresponding leading-order Feynman diagrams for the signal and background processes are shown in Figures 1 and 2. Owing to the clean signature and accessible branching fractions, the four-lepton final states (4ℓ and $2\ell 2\nu$ with $\ell = e$ or μ), originating from the decays of a pair of on-shell Z bosons induced by a virtual Higgs boson, offer the main signal sensitivity. The latest CMS search [29], using 138 fb^{-1} in the $2\ell 2\nu$ channel and 78 fb^{-1} in the 4ℓ channel, led to an observed (expected) detection significance of about 3.6σ (2.4) standard deviations (σ) for off-shell Higgs boson production and a measured Γ_H of $3.2_{-1.7}^{+2.4}$ MeV. The analysis described in this Letter updates the previous ATLAS result [27] with more data – the full Run-2 dataset is used in both decay channels – a more powerful discriminant in the 4ℓ channel, and a

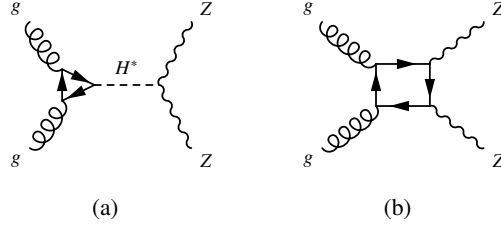


Figure 1: The leading-order Feynman diagrams for the (a) $ggZZ$ signal and (b) background processes. In the signal process the quark loop is dominated by top and bottom, while for the continuum background it is mainly light quarks.

data-driven approach to estimating the leading $q\bar{q} \rightarrow ZZ$ background. Additionally, in this analysis for the first time ggF and EW off-shell production are probed separately as well as together.

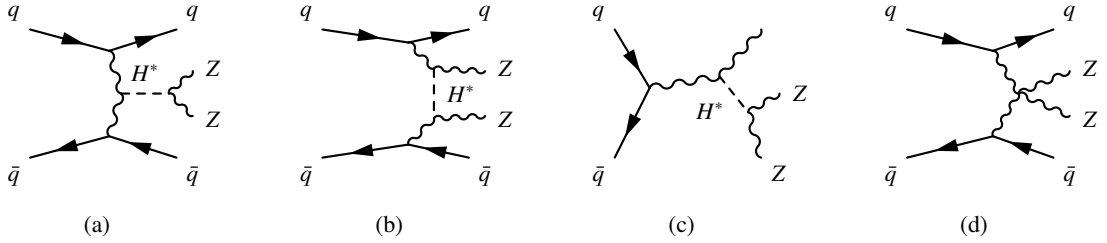


Figure 2: The leading-order Feynman diagrams for (a) the s -channel vector-boson fusion signal, (b) the t -channel vector-boson fusion signal, (c) the vector-boson associated production signal, and (d) the vector-boson scattering background.

This Letter presents a search for off-shell Higgs boson production in four-lepton final states using the full Run 2 data at a centre-of-mass energy $\sqrt{s} = 13$ TeV collected by the ATLAS detector. Two decay channels, 4ℓ and $2\ell 2\nu$, are separately analysed and then combined to obtain the final results. Events with a pair of Z bosons are categorised into several signal regions (SRs) to probe off-shell contributions from the two leading production modes, ggF and electroweak production (EW), and their respective interference with the continuum background $gg \rightarrow ZZ$ and electroweak $q\bar{q} \rightarrow ZZ + 2j$ processes. Electroweak production includes the contributions from vector-boson fusion (VBF) and vector-boson associated production (VH), since these two processes both interfere with the electroweak $q\bar{q} \rightarrow ZZ + 2j$ background and hence cannot be separated. The main irreducible background is Z boson pair production via quark–antiquark annihilation ($q\bar{q} \rightarrow ZZ$); the interfering backgrounds described above also contribute. In the 4ℓ channel, these are the only significant backgrounds, with sub-percent-level contributions from the production of Z bosons with associated jets and $t\bar{t}$ production. In the $2\ell 2\nu$ channel, background processes from diboson production (both WZ and WW), $t\bar{t}$ and single top production, and the production of Z bosons with associated jets constitute roughly half of the total background. Control regions (CRs) are defined to ensure control of the background modelling. In both channels, the background from the combination of vector-boson associated production to a top-quark pair ($t\bar{t}+V$, $V=W$ or Z) and triboson production (ZZZ , WZZ , or WWZ) is at the percent level. Distributions of discriminating variables are fitted simultaneously in all SRs to extract the off-shell contribution by measuring the signal strength $\mu_{\text{off-shell}}$, the off-shell production cross-section normalised to the SM prediction, with the CRs also included in the fit to constrain the normalisation of the main background processes. In the 4ℓ channel, an observable is constructed from the output of neural networks (NN) that are trained with kinematic variables and matrix-element discriminants sensitive to the

signal process (see Ref. [27]). The $2\ell 2\nu$ channel uses the transverse mass of the ZZ system,

$$m_{\text{T}}^{ZZ} \equiv \sqrt{\left[\sqrt{m_Z^2 + (p_{\text{T}}^{\ell\ell})^2} + \sqrt{m_Z^2 + (E_{\text{T}}^{\text{miss}})^2} \right]^2 - \left| \vec{p}_{\text{T}}^{\ell\ell} + \vec{E}_{\text{T}}^{\text{miss}} \right|^2}, \quad (1)$$

where m_Z is the Z boson mass [30], $\vec{p}_{\text{T}}^{\ell\ell}$ and $\vec{E}_{\text{T}}^{\text{miss}}$ are the transverse momentum vector of the lepton pair and the missing transverse momentum vector with magnitudes of $p_{\text{T}}^{\ell\ell}$ and $E_{\text{T}}^{\text{miss}}$, respectively. Finally, the constraint on Γ_H is derived by using both the measured $\mu_{\text{off-shell}}$ and the signal strength for on-shell Higgs boson contributions ($\mu_{\text{on-shell}}$) in the 4ℓ channel obtained from Ref. [31], relying on the equation (valid under the assumptions discussed above) $\mu_{\text{off-shell}}/\mu_{\text{on-shell}} = \Gamma_H/\Gamma_H^{\text{SM}}$. Similarly to the previous ATLAS paper [27], this search also reports the ratio of effective Higgs boson–gluon couplings (R_{gg}) and the ratio of Higgs boson and vector-boson couplings (R_{VV}) between the off-shell and on-shell regions, assuming that the Higgs boson total width takes its SM value.

2 ATLAS detector

ATLAS is a multipurpose detector with a forward–backward symmetric cylindrical geometry and a solid-angle¹ coverage of nearly 4π , described in detail in Ref. [32]. The inner tracking detector (ID), covering the region $|\eta| < 2.5$, consists of a silicon pixel detector, a silicon microstrip detector, and a transition-radiation tracker. The innermost layer of the pixel detector, the insertable B-layer [33], was installed between Run 1 and Run 2 of the LHC. The inner detector is surrounded by a thin superconducting solenoid providing a 2 T magnetic field, and by a finely segmented lead/liquid-argon (LAr) electromagnetic calorimeter covering the region $|\eta| < 3.2$. A steel/scintillator-tile hadron calorimeter provides coverage in the central region $|\eta| < 1.7$. The endcap and forward regions, covering the pseudorapidity range $1.5 < |\eta| < 4.9$, are instrumented with LAr electromagnetic and hadron calorimeters, with steel, copper, or tungsten as the absorber material. A muon spectrometer (MS) system incorporating large superconducting toroidal air-core magnets surrounds the calorimeters. Three layers of precision wire chambers provide muon tracking in the range of $|\eta| < 2.7$, while dedicated fast chambers are used for triggering in the region $|\eta| < 2.4$. The trigger system, composed of two stages, was upgraded [34] before Run 2. The first stage, implemented with custom hardware, uses information from the calorimeters and muon chambers to select events from the 40 MHz bunch crossings at a maximum rate of 100 kHz. The second stage, called the high-level trigger (HLT), reduces the data acquisition rate to about 1 kHz on average. The HLT is software-based and runs reconstruction algorithms similar to those used in offline reconstruction. An extensive software suite [35] is used in data simulation, in reconstruction and analysis of real and simulated data, in detector operations, and in the trigger and data acquisition systems of the experiment.

3 Data and Monte Carlo simulation

The proton–proton (pp) collision data used in this search were collected from 2015 to 2018, corresponding to an integrated luminosity of 139 fb^{-1} . Events in the 4ℓ final state were recorded with a combination of

¹ The ATLAS experiment uses a right-handed coordinate system with its origin at the nominal interaction point (IP) in the centre of the detector and the z -axis along the beam pipe. The x -axis points from the IP to the centre of the LHC ring, and the y -axis points upward. Cylindrical coordinates (r, ϕ) are used in the transverse plane, ϕ being the azimuthal angle around the z -axis. The pseudorapidity is defined in terms of the polar angle θ as $\eta = -\ln \tan(\theta/2)$.

single-lepton, dilepton and trilepton triggers, while the $2\ell 2\nu$ events were collected via multiple single-lepton triggers. The overall trigger efficiency for the off-shell signal process is more than 98% in each final state after the application of the SR selections defined below.

Monte Carlo (MC) simulation is used to predict the normalisation and event kinematics of the signal process and some of the backgrounds. Event samples for each process were first produced by a corresponding event generator and then passed through detector simulation [36] within the GEANT4 framework [37]. Additional inelastic pp interactions (pile-up) modelled with PYTHIA8.186 [38] were overlaid on the simulated events to mimic the real collision events, and further corrections were applied to the simulated samples to match the pile-up conditions in the data. The lepton and jet momentum scale and resolution, and the lepton reconstruction, identification, isolation and trigger efficiencies in the simulation were corrected to match those measured in data.

Separate simulated samples were generated for each of the off-shell signal from ggF production, the $gg \rightarrow ZZ$ background, and the inclusive production $gg \rightarrow (H^* \rightarrow)ZZ$, which also includes the interference between the two. These loop-induced processes were modelled by SHERPA v2.2.2 [39] with OPENLOOPS [40–42] at leading-order (LO) accuracy in quantum chromodynamics (QCD), with up to one additional parton in the final state, using the NNPDF3.0 parton distribution function (PDF) set [43]. Signal and background were simulated separately from the inclusive process for NN training and template fitting. The merging with the parton shower was performed using the MEPS@NLO prescription [44] and the SHERPA built-in algorithm was used for parton showering and hadronisation. The samples are corrected to next-to-leading order (NLO) in QCD using corrections calculated separately as a function of the invariant mass of the ZZ system (m_{ZZ}) [45, 46] for the signal, background, and inclusive processes. These corrections are similar for each process and range from 1.5 to 2. The total normalization of all three processes was then corrected to next-to-next-to-next-to-leading order (N3LO) in QCD using a constant correction of 1.32, derived for the off-shell signal [47, 48]. The use of the same correction for all processes is justified as the N3LO corrections are expected to be very similar for signal, background, and interference [49, 50].

EW production of ZZ and two jets, also denoted by $q\bar{q} \rightarrow (H^* \rightarrow) ZZ + 2j$, contains inclusively the off-shell signal from VBF production, VH production, the non-Higgs boson EW $ZZjj$ process, and their interferences. Those processes were modelled by MADGRAPH5_AMC@NLO [51] at LO QCD accuracy using the NNPDF3.0 NLO PDF set [52]. PYTHIA8.244 [38] was used for parton showering and hadronisation with the A14 set of tuned parameters (tune) for the underlying event [53]. The t -channel exchange of the Higgs boson is treated as a contribution to the VBF signal process.

The ggF- and VBF-induced contributions can be straightforwardly parameterised as a function of $\mu_{\text{off-shell}}$, where the off-shell signal and the interference depend on $\mu_{\text{off-shell}}$ and $\sqrt{\mu_{\text{off-shell}}}$, respectively. More details of this parameterisation are given in Section 8.

The $q\bar{q} \rightarrow ZZ$ background was simulated by SHERPA v2.2.2 with OPENLOOPS using the NNPDF3.0 NNLO PDF set. The matrix elements were calculated to NLO accuracy in QCD for 0- and 1-jet final states, and to LO accuracy for 2- and 3-jet final states. The merging with the SHERPA parton shower was performed using the MEPS@NLO prescription [54]. NLO EW corrections calculated on top of the LO QCD prediction were applied as a function of m_{ZZ} for the 4ℓ final state [55, 56], while the m_{ZZ} -based corrections for the $2\ell 2\nu$ channel were averaged from the additive (NLO EW + NLO QCD) and multiplicative (NLO EW \times NLO QCD) approaches following Ref. [57]. A cross-check was performed in the 4ℓ channel, and the results of the two approaches were found to agree within their uncertainties, while the uncertainties of both approaches (described in detail below) were also found to be similar.

The WZ diboson events from both QCD and EW production, with the subsequent leptonic decays of both the W and Z bosons, were simulated using SHERPA with a similar set-up to that of the $q\bar{q} \rightarrow ZZ$ background. The WZ events with the Z boson decaying leptonically and the W boson decaying hadronically were modelled with SHERPA v2.2.1. For the $2\ell 2\nu$ final state, the contribution from WW production was removed in the SHERPA simulation of the $q\bar{q} \rightarrow ZZ$ and $gg \rightarrow ZZ$ processes by requiring the charged leptons and the neutrinos to have different lepton flavours (the prediction was then scaled up by 1.5 to compensate). The $q\bar{q} \rightarrow WW$ and $gg \rightarrow WW$ processes were then modelled with POWHEG BOX v2 [58] and SHERPA v2.2.2, respectively. The interference between WW and ZZ production in the $2\ell 2\nu$ final state is expected to be negligible in the phase space of the analysis [57] and was therefore not considered.

The Z +jets background was simulated using the SHERPA v2.2.1 event generator, where the matrix elements were calculated for up to two partons at NLO and four partons at LO. The Z +jets events were normalised using the NNLO cross-sections [59]. The $t\bar{t}$ background, as well as single-top (including s-channel, t-channel, and the dominant Wt component) production, were modelled using POWHEG BOXv2 interfaced to PYTHIA8.230 with the A14 tune. The total cross-sections for $t\bar{t}$ production and single-top production were normalised to the predictions at NNLO and NLO accuracy in QCD [60–62], respectively.

The triboson backgrounds ZZZ , WZZ , and WWZ with fully leptonic decays were modelled with SHERPA v2.2.2 at NLO QCD accuracy. The $ZZZ \rightarrow 4\ell + 2j$ process is included in the $q\bar{q} \rightarrow (H^* \rightarrow) ZZ + 2j$ sample described above. The simulation of $t\bar{t} + V$ production ($V = W$ or Z) with at least one of the top quark decaying leptonically and the vector boson decaying inclusively was performed with MADGRAPH5_AMC@NLO interfaced to PYTHIA8.210 for parton showering and hadronisation with the A14 tune. The total cross-sections for the $t\bar{t} + V$ backgrounds were normalised to the NLO QCD and EW predictions from Ref. [63].

4 Reconstruction of physics objects

To describe the event signature and obtain a good signal-to-background ratio, this search relies on the successful reconstruction of collision vertices, electrons, muons, jets, \vec{E}_T^{miss} , as well as identification of jets containing b -hadrons (b -jets). The reconstruction is identical to that in Ref. [64], and briefly summarised as follows.

Events are first required to have a collision vertex associated with at least two tracks each with transverse momentum $p_T > 0.5$ GeV. The vertex with the highest sum of p_T^2 of the associated tracks is referred to as the primary vertex.

Muons are primarily identified by tracks or segments (tracks using the hits of a single MS station) reconstructed in the MS and matched to tracks reconstructed in the ID, with exceptions in areas where the MS lacks coverage. In the region $2.5 < |\eta| < 2.7$, muons can also be identified by tracks from the muon spectrometer alone (standalone muons). In the gap region ($|\eta| < 0.1$) of the MS, muons can be identified by a track from the ID associated with a compatible calorimeter energy deposit (calorimeter-tagged muons). Candidate muons are required to have $p_T > 5$ GeV and $|\eta| < 2.7$, with the exception of calorimeter-tagged muons for which the p_T threshold is raised to 15 GeV. Muons must satisfy the ‘loose’ identification criterion [65] in the 4ℓ channel with at most one standalone or calorimeter-tagged muon allowed per Higgs boson candidate. In the $2\ell 2\nu$ channel muons are selected with $|\eta| < 2.5$ and must satisfy the ‘medium’ identification criterion. Electrons are reconstructed from energy deposits in the electromagnetic calorimeter matched to a track in the ID. Candidate electrons must have $p_T > 7$ GeV and $|\eta| < 2.47$,

and satisfy the ‘loose’ and ‘medium’ identification criteria [66] in the 4ℓ and $2\ell 2\nu$ channels, respectively. All electrons and muons used in both channels must be isolated and satisfy the ‘FixedCutPFlowLoose’ isolation criteria [65, 66]. Furthermore, electrons (muons) are required to have associated tracks satisfying $|d_0/\sigma_{d_0}| < 5$ (3) and $|z_0 \times \sin \theta| < 0.5$ mm, where d_0 is the transverse impact parameter relative to the beam line, σ_{d_0} is its uncertainty, and z_0 is the z coordinate of the r - ϕ impact point, defined relative to the primary vertex. The event is rejected if the minimum angular separation between two leptons is $\Delta R_{\ell\ell} < 0.1$, where $\Delta R_{\ell\ell} = \sqrt{(\Delta\phi_{\ell\ell})^2 + (\Delta\eta_{\ell\ell})^2}$.

Jets are reconstructed from particle-flow objects [67] using the anti- k_r algorithm [68, 69] with radius parameter $R = 0.4$. The jet-energy scale is calibrated using simulation and further corrected with in situ methods [70]. Candidate jets are required to have $p_T > 30$ GeV and $|\eta| < 4.5$. A jet-vertex tagger [71] is applied to jets with $p_T < 60$ GeV and $|\eta| < 2.4$ to suppress jets that originate from pile-up. To mitigate the impact of pile-up jets in the forward region, another tagger, based on jet shapes and topological jet correlations [72], is used to suppress jets originating from the pile-up with $p_T < 50$ GeV and $2.5 < |\eta| < 4.5$. In addition, b -jets are identified using a multivariate b -tagging algorithm [73] and events containing them are rejected. The chosen b -tagging algorithm has an efficiency of 85% for b -jets and a rejection factor of 33 against light-flavour jets, measured in $t\bar{t}$ events [74].

The presence of neutrinos is identified using the missing transverse momentum vector \vec{E}_T^{miss} , which is computed as the opposite of the vector sum of transverse momenta of all the leptons and jets, as well as the tracks originating from the primary vertex but not associated with any of the leptons or jets [75]. Missing transverse momentum may also arise from the mismeasurement of the momentum of particles or jets. To avoid accepting events due to the presence of this kind of fake E_T^{miss} , the statistical significance of the E_T^{miss} , $S(E_T^{\text{miss}})$, is used. $S(E_T^{\text{miss}})$ is calculated from the resolution information of the physics objects used in the E_T^{miss} reconstruction [76].

5 $ZZ \rightarrow 4\ell$ analysis

The selection of candidate events used in the signal and control regions of the 4ℓ channel closely follows that described in Ref [64]. The four-lepton invariant mass is required to be above the on-shell ZZ production threshold, $m_{4\ell} > 180$ GeV. Candidate 4ℓ quadruplets are formed by selecting two opposite-sign, same-flavour dilepton pairs in each event. In the $4e$ and 4μ channels, in which there are two possible pairings, the one that includes the lepton pair with mass closest to the Z boson mass is chosen. The p_T thresholds for the three leading leptons are 20, 15 and 10 GeV, respectively. In each quadruplet, the lepton pair with mass closest to the Z boson mass, m_{12} , is referred to as the leading pair and required to have $50 < m_{12} < 106$ GeV. The sub-leading pair, m_{34} , must satisfy $50 < m_{34} < 115$ GeV when $m_{4\ell} > 190$ GeV. Due to the increased probability of one off-shell Z boson at lower values of $m_{4\ell}$, the lower threshold for m_{34} decreases linearly to 45 GeV for $180 < m_{4\ell} < 190$ GeV.

Three SRs are designed to provide sensitivity to both the EW and ggF production modes. The SRs are defined such that $m_{4\ell}$ is well above the Higgs boson mass, including only events with $m_{4\ell} > 220$ GeV. Events in the range $180 < m_{4\ell} < 220$ GeV are expected to have the lowest signal-to-background ratio in the $m_{4\ell}$ range of the analysis and so are reserved for the control regions defined below. Events containing two or more jets with p_T greater than 30 GeV, where the two leading jets are well separated in η , $|\Delta\eta_{jj}| > 4$, are classified into the EW SR. Events falling outside the EW SR but featuring exactly one jet in the forward direction ($|\eta_j| > 2.2$) are assigned to a mixed SR. All the remaining events are then assigned to the ggF SR.

The main background in the 4ℓ channel is the $q\bar{q} \rightarrow ZZ$ process. The overall normalisation of this background is constrained by data in three different CRs defined with $180 < m_{4\ell} < 220$ GeV and with zero, one, or ≥ 2 jets. The signal contamination in these CRs is below 2%. The kinematic distributions are modelled with simulation, described in Section 3. Events in the zero- and one-jet CRs are binned in four and two intervals of equal width in $m_{4\ell}$, respectively, to provide further information about event kinematics. The interfering background processes $gg \rightarrow ZZ$ and EW $q\bar{q} \rightarrow ZZ$, as well as the small backgrounds from triboson production and $t\bar{t}Z$, are estimated from simulation. The contribution of the reducible backgrounds where hadrons or their decay products are mis-reconstructed as prompt leptons, such as Z -jets, WZ and $t\bar{t}$ processes, are estimated by using data-driven methods described in Ref. [64] and found to be negligible.

To maximize the signal sensitivity, a multi-class dense NN is employed in the SRs to enhance events with a Higgs boson candidate. The NN, implemented using Keras [77] with TensorFlow [78] as the backend, is designed to differentiate among the three event classes: the off-shell Higgs boson signal (S), the interfering background (B), and the non-interfering (NI) background. The interfering backgrounds to the ggF and EW signals are the $gg \rightarrow ZZ$ and EW $q\bar{q} \rightarrow ZZ + 2j$ processes, respectively. The non-interfering background is the $q\bar{q} \rightarrow ZZ$ process in both production modes.

The outputs of the NN use a normalized exponential function so that they can be interpreted as probabilities of an event belonging to a particular class (P_S , P_B and P_{NI}) and their ratio is used to define the final observable:

$$O_{NN} = \log_{10} \left(\frac{P_S}{P_B + P_{NI}} \right).$$

As the analysis attempts to constrain both the ggF- and EW-induced off-shell signals independently, two separate NNs are trained, one in the ggF SR and the other in the EW SR. The observable from the first NN (O_{NN}^{ggF}) is then used as the discriminating variable in both the ggF and mixed SRs, while that of the second NN (O_{NN}^{EW}) is used in the EW SR.

The first NN is trained to discriminate among the ggF-induced signal, the $gg \rightarrow ZZ$ background, and the $q\bar{q} \rightarrow ZZ$ process. The features used by this NN include the kinematic information of the four leptons from MC simulation and also the square of the modulus of the values of the LO matrix element (ME) for the four leptons. The LO MEs are calculated for the gluon-induced signal and background processes and the $q\bar{q} \rightarrow ZZ$ process from the final-state variables in the Higgs boson rest frame using the MCFM program [8, 27]. The kinematic variables are the leading Z boson production angle and four decay angles defined in Ref [79], the three invariant masses $m_{4\ell}$, m_{12} and m_{34} . These are used as inputs to the ME calculation, and, along with the transverse momentum of the four-lepton system, as inputs to the NN as well.

The second NN is used to separate the EW-induced off-shell signal process from the non-Higgs boson EW $q\bar{q} \rightarrow ZZjj$ background and the QCD-induced $q\bar{q} \rightarrow ZZjj$ process. In addition to the variables used in the first NN, with matrix elements calculated specifically for the final state with two jets, several supplementary variables are included to exploit the kinematics of the dijet system: the invariant mass and azimuthal separation of the two leading jets, and the two Zeppenfeld angular variables, calculated for each Z boson as $\eta_{Zep} = \eta_{Z_1} - (\eta_{j_1} + \eta_{j_2})/2$ [80].

The two networks have 7 and 9 hidden layers respectively, with [90, 80, 80, 75, 75, 40, 40] and [60, 65, 70, 85, 90, 80, 75, 50, 30] neurons. The sparse categorical cross-entropy loss was used to optimize the network structure as well as the learning rate of the Adam optimizer. Input features were chosen to fully describe the event kinematics. The networks were trained on samples of the signal and the interfering and non-interfering backgrounds.

Figure 3 shows the distributions of the observed and expected NN-based observables in all three signal regions. The data is shown after the simultaneous fit described in Section 8, except that the fit is carried out only in the 4ℓ channel and the value of $\mu_{\text{off-shell}}$ is set equal to one. All systematic uncertainties, which are described in Section 7, are included.

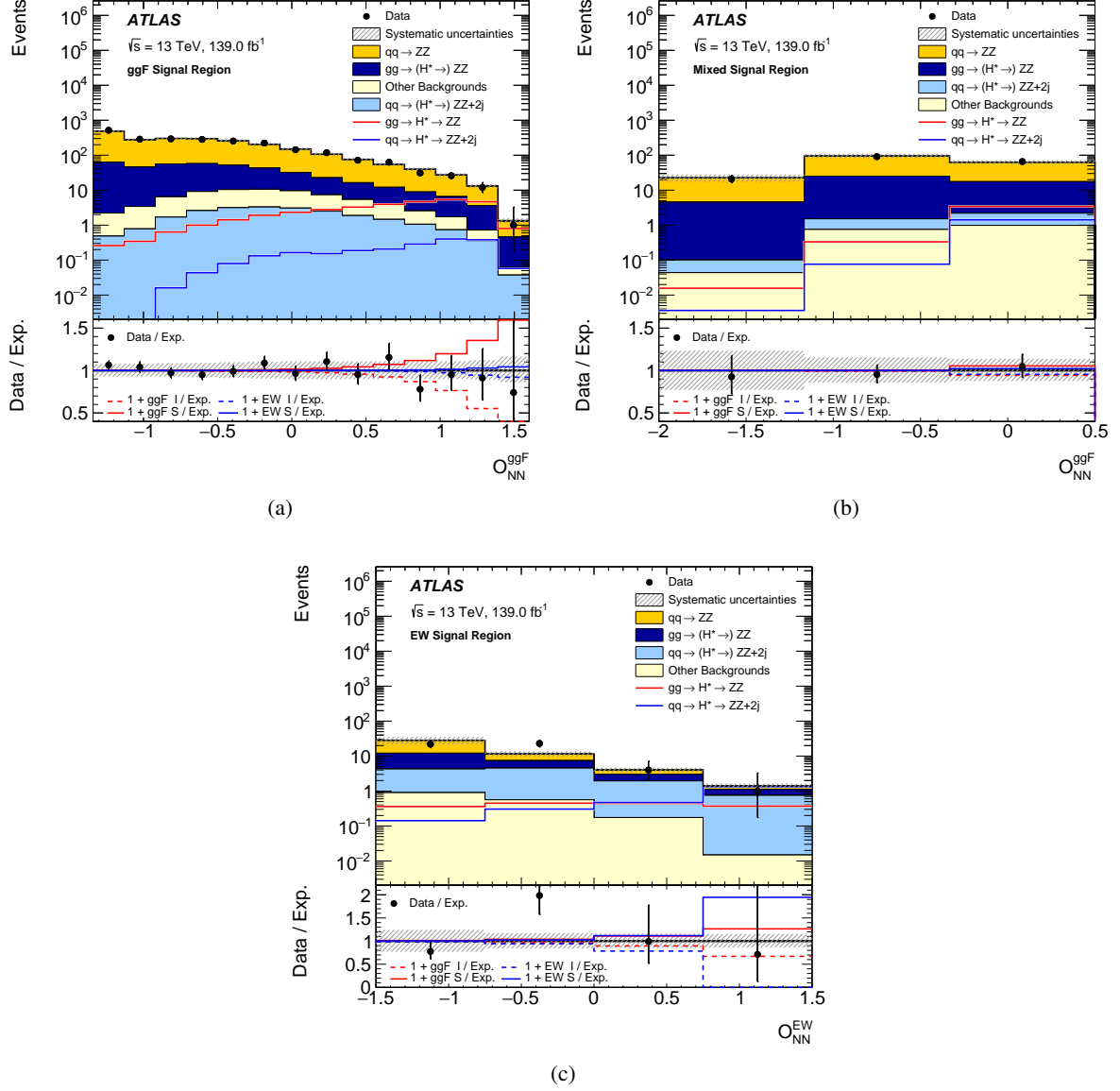


Figure 3: The observed and expected Standard Model distributions in the 4ℓ channel for (a) O_{NN}^{ggF} in the ggF signal region, (b) O_{NN}^{ggF} in the mixed signal region, and (c) O_{NN}^{EW} in the EW signal region. The observed data are shown following the fit described in Section 8, except that the fit is carried out only in the 4ℓ channel and the off-shell Higgs boson signal is fixed to the SM expectation. The total systematic uncertainty, including all uncertainties described in Section 7, is shown as the hatched area including correlations between uncertainties. The expectation includes the inclusive (signal plus background plus interference) $gg \rightarrow (H^* \rightarrow)ZZ$ (dark blue) and $q\bar{q} \rightarrow (H^* \rightarrow)ZZ + 2j$ (light blue) processes, as well as the backgrounds from QCD $q\bar{q} \rightarrow ZZ$ production (orange) and other processes (Z+jets, $t\bar{t}$, triboson and $t\bar{t}V$) (yellow). The expected $gg \rightarrow H^* \rightarrow ZZ$ and EW $q\bar{q} \rightarrow H^* \rightarrow ZZ + 2j$ signals are also shown as red and blue lines. The first and last bins include the underflow and overflow, respectively. The lower panel of each plot shows the ratio of data to expectation (black points) and the total systematic uncertainty (hatched area), as well as the ratio of the signal (solid lines) and the interference (dashed lines) to the expectation for ggF (red) and EW (blue) production. (For ease of display, for the last four curves one plus the ratio is plotted.)

6 $ZZ \rightarrow 2\ell 2\nu$ analysis

The $2\ell 2\nu$ final state consists of a pair of isolated leptons (e or μ) and large E_T^{miss} . It has a larger branching fraction than the 4ℓ channel, but is subject to larger background contamination. Candidate events are preselected by requiring exactly two electrons or muons with opposite charges and $p_T > 20$ GeV. The leading lepton must have $p_T > 30$ GeV to surpass the trigger thresholds. To suppress the WZ background, events containing any additional lepton satisfying the loose identification criteria with $p_T > 7$ GeV are rejected. Requiring the dilepton invariant mass ($m_{\ell\ell}$) to be between 76 and 106 GeV largely reduces the contamination from the non-resonant- $\ell\ell$ background, originating from $t\bar{t}$, single-top (dominated by the Wt process), and $q\bar{q} \rightarrow WW$ production. Events that satisfy this preselection are then further separated into the SRs and CRs. To suppress the remaining background dominated by the $Z + \text{jets}$ and non-resonant- $\ell\ell$ processes, further selections based on E_T^{miss} and the topology of the candidate events are applied. Candidate events are required to have $E_T^{\text{miss}} > 120$ GeV and $S(E_T^{\text{miss}}) > 10$. The azimuthal-angle difference between the dilepton system and \vec{E}_T^{miss} , $\Delta\phi(\vec{p}_T^{\ell\ell}, \vec{E}_T^{\text{miss}})$, must be larger than 2.5 radians, and the selected leptons must be close to each other, with the distance $\Delta R_{\ell\ell}$ below 1.8. Furthermore, the azimuthal-angle difference between any of the selected jets with $p_T > 100$ GeV and \vec{E}_T^{miss} must be larger than 0.4 radians to suppress events with poorly measured jet energies. Finally, events containing one or more b -jets are rejected to further suppress the $t\bar{t}$ and Wt backgrounds. The selected events are then categorised into three SRs in the same way as for the 4ℓ channel.

The shape and normalisation of the main background contribution from $q\bar{q} \rightarrow ZZ$ production are estimated from simulation, while in the combined result the overall normalisation factors are constrained by the ZZ CRs defined in the 4ℓ channel as described in the previous section. As is shown later in Table 4, the measured normalisations generally agree fairly well with the simulated ones, so this is a safe approach for developing the analysis in this final state.

To estimate the background from WZ production, control regions enriched in WZ events, with a purity of over 90%, are defined using the full event selection given above, except that the presence of a third lepton with $p_T > 20$ GeV is required. Several further selections such as $S(E_T^{\text{miss}}) > 3$, a b -jets veto, and $m_T^W > 60$ GeV, where m_T^W is constructed from the third lepton's transverse momentum and the \vec{E}_T^{miss} vector², are applied to suppress non- WZ contributions. Three separate WZ CRs are defined according to the number of jets (zero, one, and ≥ 2 jets), and the CRs are included in the statistical fit to separately constrain the normalisation of the WZ background in each N_{jets} bin. The shapes of the kinematic distributions are estimated from simulation.

To estimate the non-resonant- $\ell\ell$ background, arising from $qq \rightarrow WW$, $t\bar{t}$, and single-top production, a control region dominated by the non-resonant- $\ell\ell$ processes (with a purity of about 95%) is defined with all the event selection criteria except that the final state is required to contain an opposite-sign $e\mu$ pair. The non-resonant- $\ell\ell$ contribution with the ee ($\mu\mu$) pair is quite similar to that with the $e\mu$ pair, and the difference in lepton reconstruction is taken into account in the simulation. This CR is then used to constrain the total normalisation of the non-resonant- $\ell\ell$ background in all three SRs, and the kinematic shapes are modelled with simulation. The $Z + \text{jets}$ background contribution is estimated from simulation and constrained by a normalisation factor derived in a control region enriched in $Z + \text{jets}$ events. The control region is defined with all event selection criteria except that $S(E_T^{\text{miss}})$ is required to be less than 9, and no requirements on the azimuthal angle difference between jets with $p_T > 100$ GeV and \vec{E}_T^{miss} are made. The

² $m_T^W \equiv \sqrt{2p_T^\ell E_T^{\text{miss}} [1 - \cos \Delta\phi(\vec{p}_T^\ell, \vec{E}_T^{\text{miss}})]}$

resulting control region is about 73% pure. The kinematic distributions for the Z + jets background are modelled with simulation. The CRs for the non-resonant- $\ell\ell$ and the Z + jets backgrounds are not further divided to match the categorisation of SRs depending on jet multiplicity, due to insufficient events in the data. Finally, minor backgrounds from the VVV and $t\bar{t}V$ processes are estimated from simulation.

The distributions of the final observable m_T^{ZZ} in the $2\ell 2\nu$ channel, as defined in Eq. 1, are presented in Figure 4. The data is shown after the simultaneous fit described in Section 8, except that the fit is carried out only in the $2\ell 2\nu$ channel and the value of $\mu_{\text{off-shell}}$ is set equal to one. All three SRs are shown together with the total systematic uncertainty from the sources described in Section 7.

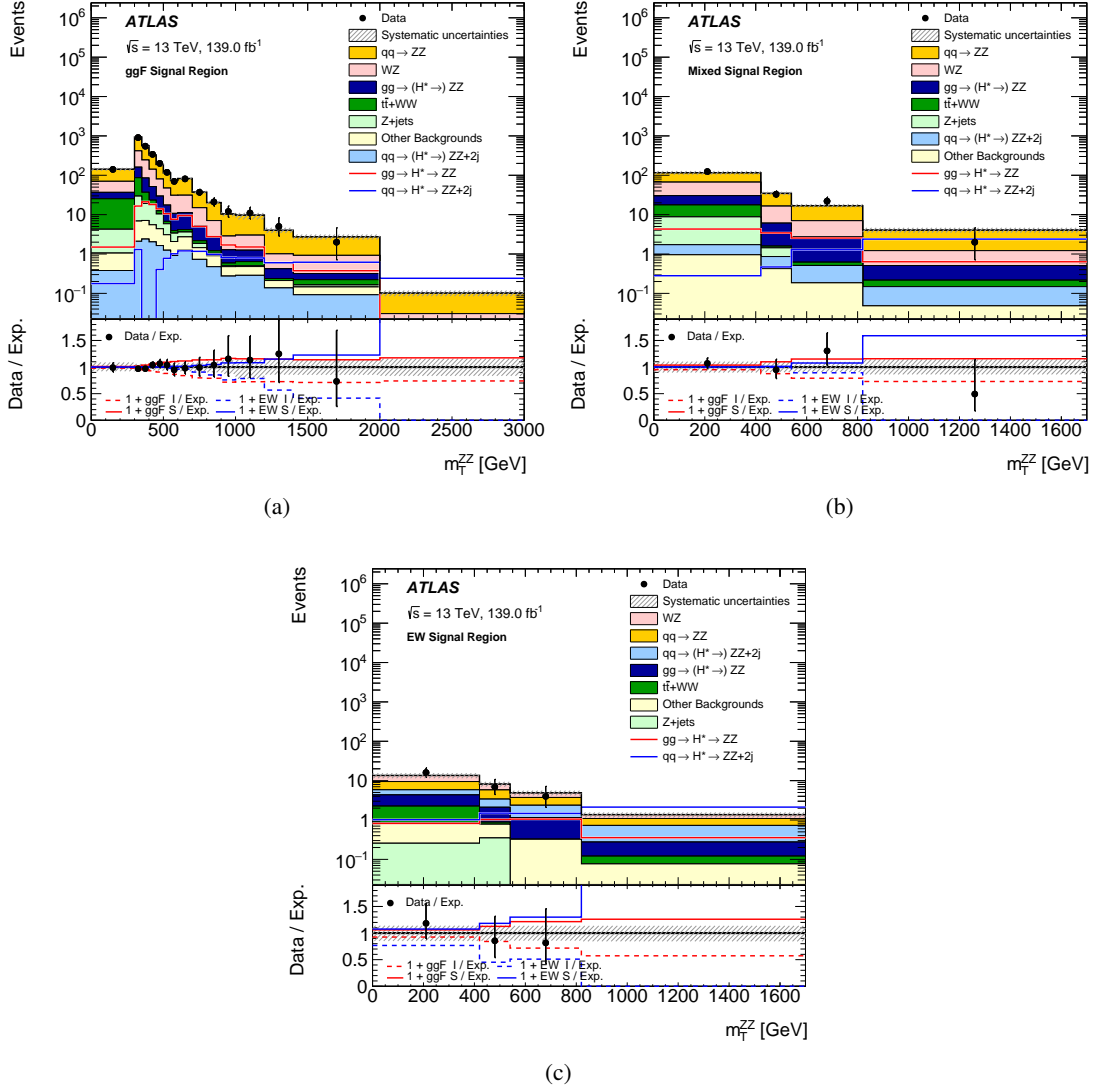


Figure 4: The observed and expected Standard Model m_T^{ZZ} distributions in the $2\ell 2\nu$ channel for (a) the ggF SR, (b) the mixed SR, and (c) the EW SR. The data are shown after the simultaneous fit described in Section 8, except that the fit is carried out only in the $2\ell 2\nu$ channel and the off-shell Higgs boson signal is fixed to the SM expectation. The hatched area shows the total systematic uncertainty after the fit, comprising all uncertainties described in Section 7 and including correlations between uncertainties. The expectation includes the inclusive (signal plus background plus interference) $gg \rightarrow (H^* \rightarrow)ZZ$ (dark blue) and EW $q\bar{q} \rightarrow (H^* \rightarrow)ZZ + 2j$ (light blue) production, as well as the backgrounds from QCD $q\bar{q} \rightarrow ZZ$ production (orange), WZ (pink), non-resonant $\ell\ell$ (dark green), Z +jets (light green), and other (triboson and $t\bar{t}V$) (yellow) processes. The expected $gg \rightarrow H^* \rightarrow ZZ$ and $q\bar{q} \rightarrow H^* \rightarrow ZZ + 2j$ signals are also shown as red and blue lines. The last bins include the overflow. The lower panel shows the ratio of data to expectation (black points) and the total systematic uncertainty (hatched area), as well as the ratio of the signal (solid lines) and the interference (dashed lines) to the expectation for ggF (red) and EW (blue) production. (For ease of display, for the last four curves one plus the ratio is plotted.)

7 Systematic uncertainties

The sources of systematic uncertainty impacting the analysis of both channels can be divided into two categories: uncertainties in the theoretical description of the signal and background processes and experimental uncertainties related to the detector response.

The largest source of systematic uncertainties arises from the theoretical modelling of the signal and background processes, including those related to the production of jets associated with the Higgs boson. Experimental uncertainties related to the reconstruction of jets are also prominent while other experimental uncertainties are generally small. To help understand the impact of the leading uncertainties, their relative size before the statistical fit for a specific process is provided in this section, with the largest uncertainties for the main processes in the signal and control regions summarized in Table 1. The impact of these uncertainties on the observed upper limits of $\mu_{\text{off-shell}}$ is given in Section 8.

The theoretical uncertainties arise from the choice of PDF, from the missing higher-order corrections in both QCD and EW perturbative calculations, and from the modelling of the parton shower.

The PDF uncertainties are evaluated using the NNPDF prescription with MC replicas. The PDF covariance matrix between each channel of the analysis is estimated from the 100 replicas from the NNPDF3.0 NNLO set. Only the principal component of the covariance matrix has a non-negligible impact on the yields and it is used as a representation of the PDF uncertainty including its bin-by-bin correlations. The uncertainties due to missing higher-order QCD corrections are estimated by varying the renormalisation and factorisation scales independently, ranging from a factor of one-half to two (excluding the cases in which one scale is varied down by one-half and the other up by two). For the $q\bar{q} \rightarrow ZZ$ background, the uncertainty is evaluated independently in bins of N_{jets} . For the gluon-induced processes, including the signal, the $gg \rightarrow ZZ$ background, and their interference, the missing higher-order uncertainties are evaluated by their impact on the respective NLO K -factors [81]. The uncertainties are increased in the kinematic regions of the SRs where the K -factor calculations are less precise due to missing effects from on-shell top quarks and high- p_T jets [27]: the uncertainty is doubled in the phase space containing a jet with $p_T > 150$ GeV and increased by 50% for m_{ZZ} around twice the top-quark mass. In both the 4ℓ and $2\ell 2\nu$ channels, the uncertainty from missing higher order corrections in the $q\bar{q} \rightarrow ZZ$ background is one of the largest uncertainties, ranging from a few percent up to 40% depending on jet multiplicity and observable bin. In both channels, the same uncertainty in the gluon–gluon processes ranges from 10% to 20%.

The uncertainties due to missing higher-order EW corrections (HOEW) are considered for the main $q\bar{q} \rightarrow ZZ$ background and handled differently in the two channels. For the $2\ell 2\nu$ channel, the difference in the NLO EW correction between the multiplicative and additive methods as a function of m_{ZZ} is assigned as the uncertainty [57]. This uncertainty ranges from 1% to at most 20% of the cross-section depending on the bins of observables. For the 4ℓ channel, the NLO EW corrections are calculated on top of the LO QCD cross-section. Therefore, a specific prescription [82], also applied in Ref. [27], is used to derive the uncertainty to account for missing NLO QCD+EW diagrams. A study of the compatibility between the two methods in the 4ℓ channel shows that the central values agree to within a few percent while the uncertainties have a similar size.

The uncertainties due to the modelling of the parton shower and hadronisation play an important role in this search, as jet multiplicity, a key variable used to define both the SRs and the CRs, is particularly sensitive to the modelling of matrix elements, parton showering, and the merging and matching between the two. The parton shower (PS) uncertainties are evaluated by varying resummation and matching scales

for the processes simulated with the SHERPA generator. These variations for SHERPA samples are expected to further account for the shape uncertainties relating to missing high-order QCD effects beyond those from the usual QCD scale variations, i.e. migrations between jet bins. For those processes simulated with the PYTHIA shower program, the uncertainty is assessed by varying the PYTHIA configurations, such as the parameter values of the A14 tune, the multi-parton models and the final-state radiation models. For ggF production, the PS uncertainties are correlated between the signal and background processes. The uncertainties are split into shape and normalization components, with the latter being more significant.

In the $2\ell 2\nu$ channel, the systematic uncertainties arising from the PS are parameterised using only the ZZ transverse momentum. In this channel, the PS uncertainty in the ggF processes is quite important: it is about 25% in the yields and ranges from a few percent to a maximum of 15% in the observable shapes. For the EW processes, this uncertainty reaches 15% in the yields and a few percent in the shapes. The PS uncertainties for the $q\bar{q} \rightarrow ZZ$ background are at percentage level for the bulk of observable bins but can reach up to 30% in some parts of the phase space.

In the 4ℓ channel, these uncertainties are parameterised using the 4ℓ invariant mass, transverse momentum, and the kinematics of the leading jets. NNs are trained to estimate the density ratio between the nominal and the varied samples in this multi-dimensional space [83]. This novel method ensures a detailed description of the systematic uncertainty while reducing statistical fluctuations due to the interpolation provided by the differentiable NN. In the 4ℓ channel, PS uncertainties are the leading source of uncertainties for the gluon–gluon processes in the SRs, and are about 30% and 40% in the yields of the signal and the background. The impact of PS uncertainties in the shape of observables is found to be no more than 10% in the 4ℓ channel. The PS uncertainties for the EW processes are less significant, ranging from a few percent to 10%. The PS uncertainties for the QCD $q\bar{q} \rightarrow ZZ$ background are generally smaller, at percentage level for most observable bins.

Experimental systematic uncertainties are generally less important than the theoretical ones. However, uncertainties related to jet reconstruction are important in the $2\ell 2\nu$ channel as mismeasurement of the jet energy can mimic E_T^{miss} . The main jet uncertainties are those in the jet energy scale (JES) and resolution (JER), which can amount to about 10% for processes in the EW SRs. The effect of pile-up and the differences between the energy responses for jets with different hadron flavour compositions are particularly important. Uncertainties originating from the electron and muon reconstruction and selection, and from E_T^{miss} reconstruction are less important. The uncertainty in the Run-2 luminosity measurement is 1.7% [84], obtained using the LUCID-2 detector [85] for the primary luminosity measurements.

Table 1: The dominant uncertainties in the leading processes in the signal and background regions. Uncertainties may depend on the value of the observable: if so, a range is given in the table. Detailed descriptions of the uncertainties are given in the text.

Process	Uncertainty	Final State	Value (%)
ggF Signal Region			
$q\bar{q} \rightarrow ZZ$	QCD Scale	$2\ell 2\nu$	4–40
$q\bar{q} \rightarrow ZZ$	QCD Scale	4ℓ	21–28
$q\bar{q} \rightarrow ZZ$	HOEW	4ℓ	1–7
$q\bar{q} \rightarrow ZZ$	HOEW	$2\ell 2\nu$	2–20
$q\bar{q} \rightarrow ZZ$	Parton Shower	$2\ell 2\nu$	1–67
$q\bar{q} \rightarrow ZZ + 2j$	Parton Shower	$2\ell 2\nu$	1–33
$q\bar{q} \rightarrow ZZ + 2j$	Parton Shower	4ℓ	2–10
$gg \rightarrow H^* \rightarrow ZZ$	Parton Shower	4ℓ	27
$gg \rightarrow H^* \rightarrow ZZ$	Parton Shower	$2\ell 2\nu$	8–45
$gg \rightarrow ZZ$	Parton Shower	4ℓ	38
$gg \rightarrow ZZ$	Parton Shower	$2\ell 2\nu$	6–43
$WZ + 0j$	QCD Scale	$2\ell 2\nu$	1–54
1-jet Signal Region			
$gg \rightarrow H^* \rightarrow ZZ$	Parton Shower	4ℓ	27
$gg \rightarrow H^* \rightarrow ZZ$	QCD Scale	$2\ell 2\nu$	13–18
$gg \rightarrow ZZ$	Parton Shower	4ℓ	38
$gg \rightarrow ZZ$	QCD Scale	$2\ell 2\nu$	18–20
$q\bar{q} \rightarrow ZZ + 2j$	QCD Scale	$2\ell 2\nu$	7–18
$q\bar{q} \rightarrow ZZ + 2j$	QCD Scale	4ℓ	3–10
2-jet Signal Region			
$q\bar{q} \rightarrow ZZ$	QCD Scale	4ℓ	18–26
$q\bar{q} \rightarrow ZZ$	QCD Scale	$2\ell 2\nu$	8–32
$gg \rightarrow H^* \rightarrow ZZ$	Parton Shower	4ℓ	27
$gg \rightarrow H^* \rightarrow ZZ$	QCD Scale	$2\ell 2\nu$	14–18
$gg \rightarrow ZZ$	Parton Shower	4ℓ	38
$gg \rightarrow ZZ$	QCD Scale	$2\ell 2\nu$	18–20
$WZ + 2j$	QCD Scale	$2\ell 2\nu$	20–22
$q\bar{q} \rightarrow ZZ + 2j$	QCD Scale	4ℓ	8–14
$q\bar{q} \rightarrow ZZ + 2j$	QCD Scale	$2\ell 2\nu$	8–16
$qq \rightarrow ZZ$ Control Regions			
$q\bar{q} \rightarrow ZZ$	QCD Scale	4ℓ	26
Three-lepton Control Regions			
$WZ + 2j$	QCD Scale	$2\ell 2\nu$	28

8 Results and interpretations

The statistical model used to translate the results into constraints on the off-shell signal strength $\mu_{\text{off-shell}}$ is based on the profile likelihood technique [86]. A binned likelihood function is constructed as a product of Poisson probability terms over all bins in all the SRs and CRs considered in the analysis, as introduced in Sections 5 and 6. The likelihood depends on the parameters of interest and a set of nuisance parameters θ that include the effects of systematic uncertainties and statistical uncertainties from the limited number of simulated events. They are constrained using Gaussian and Poisson terms, respectively. Different parameters of interest are used depending on the interpretation. The first interpretation explores two signal strength parameters ($\mu_{\text{off-shell}}^{\text{ggF}} = \kappa_{g, \text{off-shell}}^2 \kappa_{V, \text{off-shell}}^2$ and $\mu_{\text{off-shell}}^{\text{EW}} = \kappa_{V, \text{off-shell}}^4$) corresponding to the ggF- and EW-induced off-shell contributions, respectively. Here, κ_g (κ_V) refers to the Higgs boson coupling to gluons (vector bosons) normalised to the SM prediction. In the second interpretation, a single off-shell signal-strength parameter ($\mu_{\text{off-shell}}$) is applied for all production modes, assuming that $\mu_{\text{off-shell}}^{\text{ggF}} = \mu_{\text{off-shell}}^{\text{EW}} = \mu_{\text{off-shell}}$.

Given the sizeable interference effects, the off-shell signal cannot be treated independently of the interfering backgrounds. The interference term, which is proportional to $\sqrt{\mu_{\text{off-shell}}}$, must be taken into account when building the probability model. The expected number of events from the $gg \rightarrow (H^* \rightarrow)ZZ$ process for a given $\mu_{\text{off-shell}}^{\text{ggF}}$, referred as ν^{ggF} , can be obtained for a bin of the input distributions from the following parameterisation:

$$\begin{aligned} \nu^{\text{ggF}}(\mu_{\text{off-shell}}^{\text{ggF}}, \theta) &= \mu_{\text{off-shell}}^{\text{ggF}} \cdot n_{\text{S}}^{\text{ggF}}(\theta) + \sqrt{\mu_{\text{off-shell}}^{\text{ggF}}} \cdot (n_{\text{SBI}}^{\text{ggF}}(\theta) - n_{\text{S}}^{\text{ggF}}(\theta) - n_{\text{B}}^{\text{ggF}}(\theta)) + n_{\text{B}}^{\text{ggF}}(\theta) \\ &= (\mu_{\text{off-shell}}^{\text{ggF}} - \sqrt{\mu_{\text{off-shell}}^{\text{ggF}}}) \cdot n_{\text{S}}^{\text{ggF}}(\theta) + \sqrt{\mu_{\text{off-shell}}^{\text{ggF}}} \cdot n_{\text{SBI}}^{\text{ggF}}(\theta) + (1 - \sqrt{\mu_{\text{off-shell}}^{\text{ggF}}}) \cdot n_{\text{B}}^{\text{ggF}}(\theta) \end{aligned}$$

where $n_{\text{S}}^{\text{ggF}}$, $n_{\text{B}}^{\text{ggF}}$ and $n_{\text{SBI}}^{\text{ggF}}$ represent the corresponding expected yields of the signal, the $gg \rightarrow ZZ$ background and the full $gg \rightarrow (H^* \rightarrow)ZZ$ process, respectively. The expected number of events from the EW $q\bar{q} \rightarrow (H^* \rightarrow)ZZ + 2j$ process for a given $\mu_{\text{off-shell}}^{\text{EW}}$ can be modelled similarly, and the parameterisation is determined by using three simulation samples: that for the full process $q\bar{q} \rightarrow (H^* \rightarrow)ZZ + 2j$ with $\mu_{\text{off-shell}}^{\text{EW}}$ set to 1, that for the same process with $\mu_{\text{off-shell}}^{\text{EW}}$ set to 10, and the non-Higgs boson EW $q\bar{q} \rightarrow ZZ + 2j$ background³. The description in terms of a single signal component as performed for ggF production is not possible in the EW case because the requirement on high m_{ZZ} , used to ensure that the Higgs boson is off-shell, does not apply to the t -channel Higgs boson exchange in EW production, even though it is also off-shell (with $t < 0$). The parameterization described here ensures that this component scales with $\mu_{\text{off-shell}}^{\text{EW}}$.

The total normalisation of the $q\bar{q} \rightarrow ZZ$ background is left as a free parameter in the profile likelihood fit, separately for each jet multiplicity. Three parameters are introduced in the likelihood model to constrain the normalisation of this dominant background in both final states, a normalization factor for 0-jet events, μ_{qqZZ} , and two additional parameters to represent the relative contributions of higher jet multiplicities, μ_{qqZZ}^{1j} and μ_{qqZZ}^{2j} . The expected yield of 0-jet $q\bar{q} \rightarrow ZZ$ events is scaled by μ_{qqZZ} , that of 1-jet events by $\mu_{qqZZ} \cdot \mu_{qqZZ}^{1j}$, and that of events with at least two jets by $\mu_{qqZZ} \cdot \mu_{qqZZ}^{1j} \cdot \mu_{qqZZ}^{2j}$. These parameters are largely constrained by the three CRs defined in Section 5, especially at high jet multiplicity.

³ The values of $\mu_{\text{off-shell}}^{\text{EW}} = 0, 1, \text{ and } 10$ are chosen for technical reasons involving the production of simulated samples but in principle any three numbers could be used.

The normalisations of the WZ , $Z + \text{jets}$ and non-resonant- $\ell\ell$ backgrounds are also obtained from the simultaneous fit, using the dedicated control regions described in Section 6. Similarly to the $q\bar{q} \rightarrow ZZ$ background, events from the WZ process are treated separately for each jet multiplicity. Five additional free parameters, $\mu_{3\ell}$, $\mu_{3\ell}^{1j}$, $\mu_{3\ell}^{2j}$, μ_{Zj} , and $\mu_{e\mu}$, are therefore introduced in the likelihood model specifically for the $2\ell 2\nu$ channel and for its combination with the 4ℓ channel.

The likelihood function for the combination of both channels is built as a product of the likelihoods of the individual channels. Theoretical and experimental uncertainties with common sources are treated as correlated between the two channels. The NLO EW uncertainty is uncorrelated between the two channels, due to the different schemes used to derive the uncertainties. The hypothesis of systematic uncertainty correlation between the 4ℓ and $2\ell 2\nu$ channels is tested for the dominant sources of uncertainties, including the PS uncertainties that use models with different complexity in the two channels, and the NLO EW uncertainty. The difference in the result when using different correlation hypotheses is found to be negligible.

The $m_{4\ell}$ distribution for the 4ℓ channel and the m_T^{ZZ} distribution for the $2\ell 2\nu$ channel are shown in Figure 5 after the full fit to data with $\mu_{\text{off-shell}} = 1$. The total systematic uncertainty from the sources described in Section 7 are shown in the figure. The distributions of the NN observables used in the 4ℓ channel are shown in Figure 3.

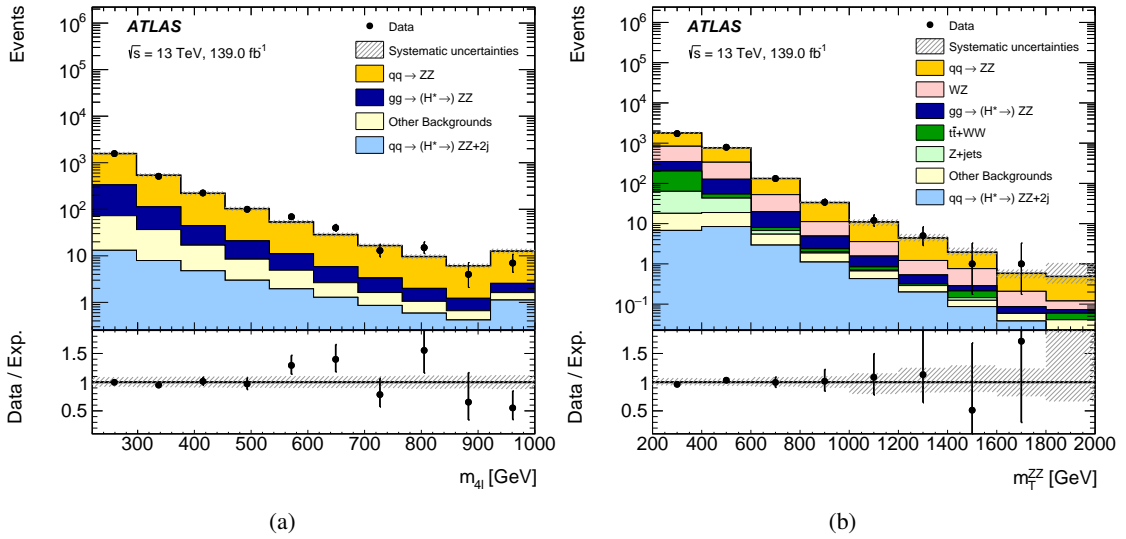


Figure 5: Comparisons between data and the SM prediction for the (a) $m_{4\ell}$ and (b) m_T^{ZZ} distributions in the inclusive off-shell signal regions in the $ZZ \rightarrow 4\ell$ and $ZZ \rightarrow 2\ell 2\nu$ channels, respectively. The scenario with the off-shell signal strength equal to one is considered in the fit. The hatched area represents the total systematic uncertainty. The last bin in both figures contains the overflow.

The expected numbers of events in the SRs after the maximum-likelihood fit to the data performed in all SRs and CRs, together with the corresponding observed yields, are shown in Tables 2 and 3 for the $ZZ \rightarrow 4\ell$ and $ZZ \rightarrow 2\ell 2\nu$ channels, respectively. The fitted background normalisation factors together with their total uncertainties are summarized in Table 4.

To obtain the results for a given parameter of interest, profile likelihood ratios (denoted by λ) are computed for different values of each parameter. The $-2 \ln \lambda$ curve as a function of $\mu_{\text{off-shell}}$ is presented in Figure 6(a).

Table 2: The observed and expected yields together with their uncertainties, for the ggF- and EW-enriched categories in the 4ℓ channel. The results are obtained after the simultaneous fit to both the 4ℓ and $2\ell 2\nu$ channels with $\mu_{\text{off-shell}} = 1$. The first row represents the inclusive ZZ process from gg production, including the signal, background, and interference components. The signal and background components are shown separately in rows 2–3: they do not add up to match the inclusive yield due to the presence of negative interference. The other backgrounds include contributions from $t\bar{t}V$ and VVV processes. The uncertainties in the expected number of events include the statistical and systematic uncertainties. The uncertainties in the $qq \rightarrow ZZ$ background are quoted as the sum in quadrature of all three jet multiplicity contributions for purposes of illustration.

Process	ggF SR	Mixed SR	EW SR
$gg \rightarrow (H^* \rightarrow)ZZ$	341 ± 117	42.5 ± 14.9	11.8 ± 4.3
$gg \rightarrow H^* \rightarrow ZZ$	32.6 ± 9.07	3.68 ± 1.03	1.58 ± 0.47
$gg \rightarrow ZZ$	345 ± 119	43.0 ± 15.2	11.9 ± 4.4
$q\bar{q} \rightarrow (H^* \rightarrow)ZZ + 2j$	23.2 ± 1.0	2.03 ± 0.16	9.89 ± 0.96
$q\bar{q} \rightarrow ZZ$	1878 ± 151	135 ± 23	22.0 ± 8.3
Other backgrounds	50.6 ± 2.5	1.79 ± 0.16	1.65 ± 0.16
Total expected (SM)	2293 ± 209	181 ± 29	45.3 ± 10.0
Observed	2327	178	50

The expected curve is constructed from a fit to an Asimov dataset which is built from the SM expectation. The expected curve is flatter than the observed due to the effect of a downward fluctuation in the data and the parabolic shape of the yield versus μ curve, which arises due to the $\sqrt{\mu}$ dependence of the interference. In particular, for electroweak production, the expected yield is minimized at the value of $\mu = 0.8$, close to the value $\mu = 1$ at which the expected $-2 \ln \lambda$ curve is minimized. In this case, a downward fluctuation in the data, observed for this production mode, does not appreciably move the minimum, because a lower yield cannot reduce the best-fit value of μ below 0.8. Instead, the lower yield makes values further from the minimum less likely, thus narrowing the profile likelihood.

Due to the quadratic parameterisation of the yield as a function of the parameter of interest, the distribution of the test statistic $-2 \ln \lambda$ is slightly different from the asymptotic χ^2 distribution predicted by Wilks' theorem [87]. Therefore confidence intervals on $\mu_{\text{off-shell}}$ are built based on the Neyman construction [88] using the distribution of $-2 \ln \lambda$ for different values of the parameter of interest. The distributions of $-2 \ln \lambda$ are estimated using simulated events sampled from the likelihood model of the analysis, profiled to the best fit results from data. The resulting confidence intervals are 5–10% more conservative than those obtained by assuming that the asymptotic assumption is correct. The intersection of the 1-sigma and 2-sigma curves in Figure 6(a) with the likelihood curves allow the true 68 and 95% confidence intervals to be estimated. The expected uncertainty in $\mu_{\text{off-shell}}$ also obtained using the 1σ confidence intervals from the Neyman construction, is ± 0.9 . The observed value of $\mu_{\text{off-shell}}$ with the 1σ confidence intervals from the Neyman construction is $\mu_{\text{off-shell}} = 1.1^{+0.7}_{-0.6}$. The observed (expected) 95% confidence level (CL) upper limit on $\mu_{\text{off-shell}}$ is 2.4 (2.6). The background-only hypothesis ($\mu_{\text{off-shell}} = 0$) is rejected at an observed (expected) significance of 3.3σ (2.2σ). The $-2 \ln \lambda = 2.30$ and $-2 \ln \lambda = 5.99$ 2D contours for $\mu_{\text{off-shell}}^{\text{ggF}}$ and $\mu_{\text{off-shell}}^{\text{EW}}$, which correspond to the 68% and 95% CL limits in the asymptotic approximation, are shown in Figure 6(b).

Table 3: The observed and expected yields together with their uncertainties, for the ggF- and EW-enriched categories in the $2\ell 2\nu$ channel. The results are obtained after the simultaneous fit to both the 4ℓ and $2\ell 2\nu$ channels with $\mu_{\text{off-shell}} = 1$. The first row represents the inclusive ZZ process from gg production, including the signal, background, and interference components. The signal and background components are shown separately in rows 2–3: they do not add up to match the inclusive yield due to the presence of negative interference. The other backgrounds include contributions from VVV , W +jets and top quark processes other than pair production. The uncertainties in the expected number of events include the statistical and systematic uncertainties. The uncertainties in the $qq \rightarrow ZZ$ and WZ backgrounds are quoted as the sum in quadrature of all three jet multiplicity contributions for purposes of illustration.

Process	ggF SR	Mixed SR	EW SR
$gg \rightarrow (H^* \rightarrow)ZZ$	210 ± 53	19.7 ± 4.9	4.29 ± 1.10
$gg \rightarrow H^* \rightarrow ZZ$	111 ± 26	10.9 ± 2.5	3.26 ± 0.82
$gg \rightarrow ZZ$	251 ± 66	23.4 ± 6.2	5.31 ± 1.46
$q\bar{q} \rightarrow (H^* \rightarrow)ZZ + 2j$	14.0 ± 3.0	1.63 ± 0.17	4.46 ± 0.50
$q\bar{q} \rightarrow ZZ$	1422 ± 112	80.4 ± 11.9	7.74 ± 2.99
WZ	678 ± 54	51.9 ± 6.9	7.89 ± 2.50
Z +jets	62.3 ± 24.3	7.51 ± 6.94	0.62 ± 0.54
Non-resonant- $\ell\ell$	106 ± 39	9.17 ± 2.73	1.55 ± 0.42
Other backgrounds	22.6 ± 5.2	1.62 ± 0.25	1.40 ± 0.10
Total expected (SM)	2515 ± 165	172 ± 17	28.0 ± 4.1
Observed	2496	181	27

Table 4: The fitted normalization factors for the dominant $q\bar{q} \rightarrow ZZ$ background as well as the WZ , Z +jets and non-resonant- $\ell\ell$ type backgrounds.

Normalization factor	Fitted value
μ_{qqZZ}	1.11 ± 0.07
μ_{qqZZ}^{1j}	0.90 ± 0.10
μ_{qqZZ}^{2j}	0.88 ± 0.26
$\mu_{3\ell}$	1.06 ± 0.03
$\mu_{3\ell}^{1j}$	0.92 ± 0.10
$\mu_{3\ell}^{2j}$	0.75 ± 0.19
μ_{Zj}	0.90 ± 0.19
$\mu_{e\mu}$	1.08 ± 0.09

To estimate the importance of the most relevant sources of systematic uncertainty to the result, Table 5 shows the value of the largest $\mu_{\text{off-shell}}$ for which $-2 \ln \lambda = 4$ when each source of uncertainty is removed one at a time. Due to the unusual shape of the yield curve, the impact of nuisance parameters on the

Table 5: The impact of most important systematic uncertainties on the observed upper value of $\mu_{\text{off-shell}}$ for which $-2 \ln \lambda = 4$, obtained by the combined fit. This value corresponds to the two standard deviation upper limit of $\mu_{\text{off-shell}}$ with the asymptotic method. The first column denotes the systematic uncertainty that was excluded from the fit. The last row gives the nominal upper limit, where all uncertainties are included. The further the upper limit is deviating from the last row value, the more important that uncertainty is.

Systematic Uncertainty Fixed	$\mu_{\text{off-shell}}$ value at which $-2 \ln \lambda(\mu_{\text{off-shell}}) = 4$
Parton shower uncertainty for $gg \rightarrow ZZ$ (normalisation)	2.26
Parton shower uncertainty for $gg \rightarrow ZZ$ (shape)	2.29
NLO EW uncertainty for $q\bar{q} \rightarrow ZZ$	2.27
NLO QCD uncertainty for $gg \rightarrow ZZ$	2.29
Parton shower uncertainty for $q\bar{q} \rightarrow ZZ$ (shape)	2.29
Jet energy scale and resolution uncertainty	2.26
None	2.30

best-fit value of $\mu_{\text{off-shell}}$ can be difficult to interpret. Additionally, the correlations between the nuisance parameters, and between the nuisance parameters and the normalization parameters for the backgrounds, make it difficult to extract uncertainty components. Table 5 indicates the magnitude of the systematic uncertainties and shows their relative importance. The most important ones are the PS uncertainties, the NLO EW uncertainties, and the jet-related uncertainties.

The combination with the on-shell $H \rightarrow ZZ^* \rightarrow 4\ell$ analysis [89], where the on-shell signal strength is measured to be $\mu_{\text{on-shell}} = 1.01 \pm 0.11$, allows these results to be translated into limits on the width of the Higgs boson normalised to its SM expectation ($\mu_{\text{off-shell}}/\mu_{\text{on-shell}} = \Gamma_H/\Gamma_H^{\text{SM}}$) as well as the ratio of off-shell to on-shell couplings for ggF ($R_{gg} \equiv \kappa_{g, \text{off-shell}}^2/\kappa_{g, \text{on-shell}}^2$) and EW ($R_{VV} \equiv \kappa_{V, \text{off-shell}}^2/\kappa_{V, \text{on-shell}}^2$) production. The experimental uncertainties are correlated between the two measurements, while the theoretical uncertainties are assumed to be uncorrelated, considering that differences could exist in the structure of high-order corrections at different mass scales. The difference in the statistical results between the correlated and uncorrelated schemes is found to be negligible. The $\Gamma_H/\Gamma_H^{\text{SM}}$ interpretation assumes that the off- and on-shell coupling modifiers are the same for both ggF and EW production modes. The R_{gg} and R_{VV} interpretations assume that the total width of the Higgs boson is equal to its SM prediction, and that the scattering phase also follows the SM. Additionally, in the R_{gg} case it is assumed that the coupling scale factors associated with the on- and off-shell EW production are the same, while in the R_{VV} case the t -channel Higgs boson exchange process is assumed to scale in the same way as for the off-shell signal.

For the combination with the on-shell analysis, the combined likelihood is built as the product of the likelihood models for the two analyses. The values of $-2 \ln \lambda$ as a function of $\Gamma_H/\Gamma_H^{\text{SM}}$, R_{gg} and R_{VV} are shown in Figures 7(a), 7(b) and 7(c), respectively. The deviation of $-2 \ln \lambda$ from a smooth parabolic curve in the region close to zero in Figure 7(b) is due to the $\sqrt{\mu}$ dependence in the yield that arises from the interference, as discussed earlier in this section, combined with a slight excess observed in the data in the 4ℓ ggH SR, which leads to a maximum near $\mu = 0$. Confidence intervals are obtained using the Neyman construction, as described above. The corresponding measured values are the following: $\Gamma_H/\Gamma_H^{\text{SM}} = 1.1_{-0.6}^{+0.7}$, $R_{gg} = 1.4_{-1.4}^{+1.1}$ and $R_{VV} = 0.9_{-0.3}^{+0.3}$. Multiplying the measured $\Gamma_H/\Gamma_H^{\text{SM}}$ by the width of the SM Higgs boson, the measured Γ_H is $4.5_{-2.5}^{+3.3}$ MeV. The total uncertainty is dominated by its statistical

component. The observed (expected) upper limit on $\Gamma_H/\Gamma_H^{\text{SM}}$ is 2.6 (2.7) at 95% confidence level using the Neyman construction, and the corresponding lower limit is 0.1 (0.01). Thus observed (expected) upper and lower limits can be placed on the total width of the Higgs boson of $0.5(0.1) < \Gamma_H < 10.5(10.9)$ MeV.

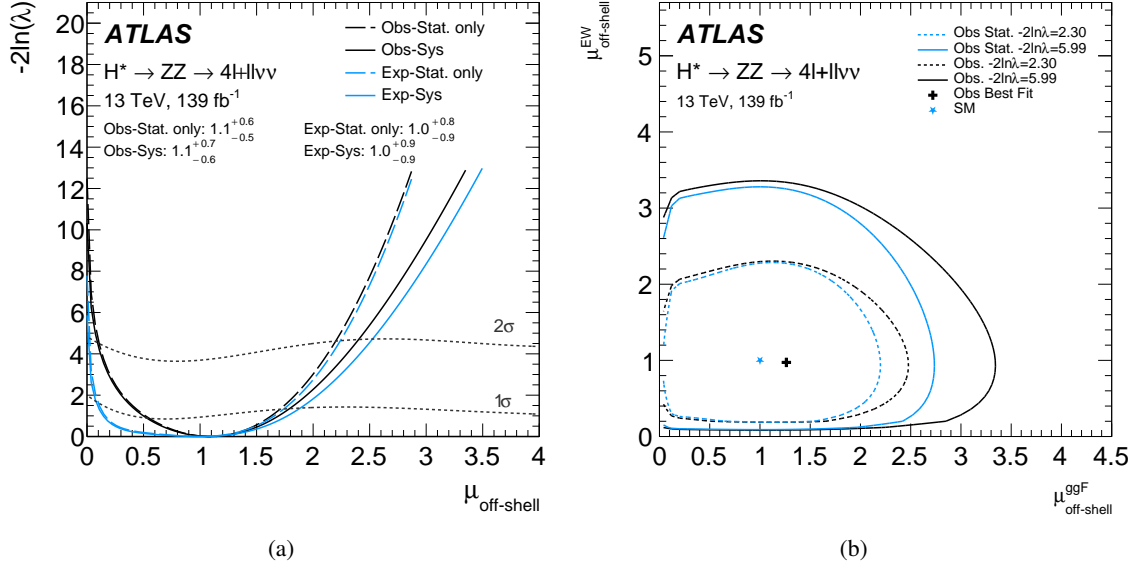
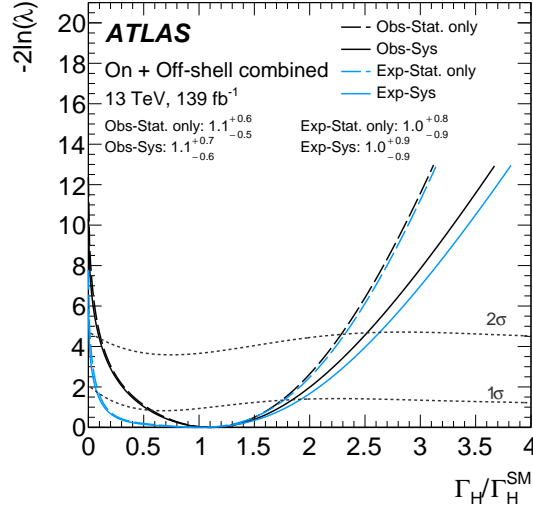
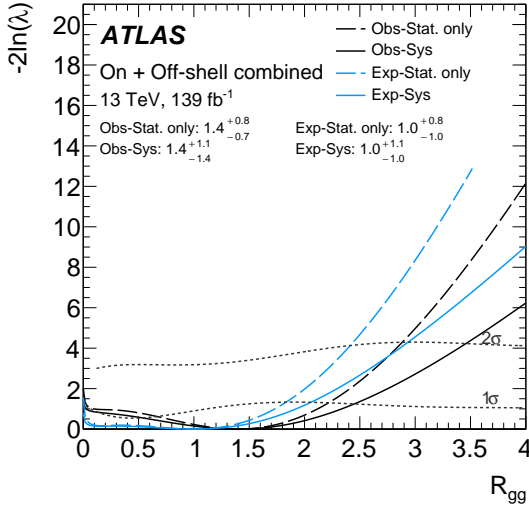


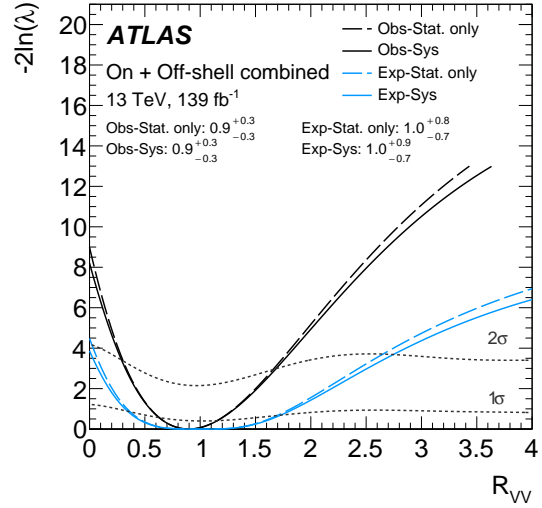
Figure 6: The likelihood profile, $-2 \ln \lambda$, as a function of (a) the off-shell Higgs boson signal strength, $\mu_{\text{off-shell}}$, for the combination of the $ZZ \rightarrow 4\ell$ and $ZZ \rightarrow 2\ell 2\nu$ off-shell analyses, and (b) two off-shell signal strength parameters for the ggF and EW production modes, plotted in a plane $(\mu_{\text{off-shell}}^{\text{ggF}}, \mu_{\text{off-shell}}^{\text{EW}})$. In (a) the dotted curves correspond to the one and two standard deviation confidence intervals on the measurement obtained using the Neyman construction while (b) shows two-dimensional contours for $\mu_{\text{off-shell}}^{\text{ggF}}$ and $\mu_{\text{off-shell}}^{\text{EW}}$ corresponding to $-2 \ln \lambda = 2.30$ and $-2 \ln \lambda = 5.99$, which correspond to the 68% and 95% CL limits in the asymptotic approximation.



(a)



(b)



(c)

Figure 7: The likelihood profile, $-2 \ln \lambda$, as a function of (a) $\Gamma_H/\Gamma_H^{\text{SM}}$, (b) R_{gg} and (c) R_{VV} for the combination with the on-shell signal strength measurement. The dotted curves correspond to the one and two standard deviation confidence intervals on the measurement obtained using the Neyman construction. For R_{gg} there are two additional negative crossings, near -1.2 and -0.84 from the best fit value: as these are very close to the $1 - \sigma$ level, they are neglected.

9 Conclusion

This Letter presents a search for off-shell Higgs boson production in the $ZZ \rightarrow 4\ell$ and the $ZZ \rightarrow 2\ell 2\nu$ final states with the ATLAS detector using 139 fb^{-1} of pp collision data. The search is optimised for sensitivity to both the ggF- and EW-induced signal, and a simultaneous fit to all SRs and CRs is performed to extract the signal contribution. No deviations from the SM prediction are observed. The data reject the background-only hypothesis with an observed (expected) significance of 3.3σ (2.2σ). The observed

(expected) upper limit at 95% confidence interval on the signal strength $\mu_{\text{off-shell}}$ is found to be 2.4 (2.6). A combination with the on-shell Higgs boson measurement gives a measured total width of the Higgs boson of $4.5^{+3.3}_{-2.5}$ MeV, and the observed (expected) upper limit on the total width is found to be 10.5 (10.9) MeV at 95% CL. These results are compatible with those previously obtained by the CMS experiment. Together with that result, this means that both experiments have observed evidence of off-shell Higgs boson production.

Acknowledgements

We thank CERN for the very successful operation of the LHC, as well as the support staff from our institutions without whom ATLAS could not be operated efficiently.

We acknowledge the support of ANPCyT, Argentina; YerPhI, Armenia; ARC, Australia; BMWFW and FWF, Austria; ANAS, Azerbaijan; CNPq and FAPESP, Brazil; NSERC, NRC and CFI, Canada; CERN; ANID, Chile; CAS, MOST and NSFC, China; Minciencias, Colombia; MEYS CR, Czech Republic; DNRF and DNSRC, Denmark; IN2P3-CNRS and CEA-DRF/IRFU, France; SRNSFG, Georgia; BMBF, HGF and MPG, Germany; GSRI, Greece; RGC and Hong Kong SAR, China; ISF and Benoziyo Center, Israel; INFN, Italy; MEXT and JSPS, Japan; CNRST, Morocco; NWO, Netherlands; RCN, Norway; MEiN, Poland; FCT, Portugal; MNE/IFA, Romania; MESTD, Serbia; MSSR, Slovakia; ARRS and MIZŠ, Slovenia; DSI/NRF, South Africa; MICINN, Spain; SRC and Wallenberg Foundation, Sweden; SERI, SNSF and Cantons of Bern and Geneva, Switzerland; MOST, Taiwan; TENMAK, Türkiye; STFC, United Kingdom; DOE and NSF, United States of America. In addition, individual groups and members have received support from BCKDF, CANARIE, Compute Canada and CRC, Canada; PRIMUS 21/SCI/017 and UNCE SCI/013, Czech Republic; COST, ERC, ERDF, Horizon 2020 and Marie Skłodowska-Curie Actions, European Union; Investissements d'Avenir Labex, Investissements d'Avenir Idex and ANR, France; DFG and AvH Foundation, Germany; Herakleitos, Thales and Aristeia programmes co-financed by EU-ESF and the Greek NSRF, Greece; BSF-NSF and MINERVA, Israel; Norwegian Financial Mechanism 2014-2021, Norway; NCN and NAWA, Poland; La Caixa Banking Foundation, CERCA Programme Generalitat de Catalunya and PROMETEO and GenT Programmes Generalitat Valenciana, Spain; Göran Gustafssons Stiftelse, Sweden; The Royal Society and Leverhulme Trust, United Kingdom.

The crucial computing support from all WLCG partners is acknowledged gratefully, in particular from CERN, the ATLAS Tier-1 facilities at TRIUMF (Canada), NDGF (Denmark, Norway, Sweden), CC-IN2P3 (France), KIT/GridKA (Germany), INFN-CNAF (Italy), NL-T1 (Netherlands), PIC (Spain), ASGC (Taiwan), RAL (UK) and BNL (USA), the Tier-2 facilities worldwide and large non-WLCG resource providers. Major contributors of computing resources are listed in Ref. [90].

References

- [1] ATLAS Collaboration, *Observation of a new particle in the search for the Standard Model Higgs boson with the ATLAS detector at the LHC*, *Phys. Lett. B* **716** (2012) 1, arXiv: [1207.7214 \[hep-ex\]](#).
- [2] CMS Collaboration, *Observation of a new boson at a mass of 125 GeV with the CMS experiment at the LHC*, *Phys. Lett. B* **716** (2012) 30, arXiv: [1207.7235 \[hep-ex\]](#).
- [3] ATLAS Collaboration, *A detailed map of Higgs boson interactions by the ATLAS experiment ten years after the discovery*, *Nature* **607** (2022) 52, arXiv: [2207.00092 \[hep-ex\]](#).
- [4] CMS Collaboration, *A portrait of the Higgs boson by the CMS experiment ten years after the discovery*, *Nature* **607** (2022) 60, arXiv: [2207.00043 \[hep-ex\]](#).
- [5] LHC Higgs Cross Section Working Group, *Handbook of LHC Higgs Cross Sections: 4. Deciphering the Nature of the Higgs Sector*, **2/2017** (2016), arXiv: [1610.07922 \[hep-ph\]](#).
- [6] N. Kauer and G. Passarino, *Inadequacy of zero-width approximation for a light Higgs boson signal*, *JHEP* **08** (2012) 116, arXiv: [1206.4803 \[hep-ph\]](#).
- [7] F. Caola and K. Melnikov, *Constraining the Higgs boson width with ZZ production at the LHC*, *Phys. Rev. D* **88** (2013) 054024, arXiv: [1307.4935 \[hep-ph\]](#).
- [8] J. M. Campbell, R. K. Ellis and C. Williams, *Bounding the Higgs width at the LHC using full analytic results for $gg \rightarrow e^-e^+\mu^-\mu^+$* , *JHEP* **04** (2014) 060, arXiv: [1311.3589 \[hep-ph\]](#).
- [9] J. M. Campbell, R. K. Ellis and C. Williams, *Bounding the Higgs width at the LHC: Complementary results from $H \rightarrow WW$* , *Phys. Rev. D* **89** (2014) 053011, arXiv: [1312.1628 \[hep-ph\]](#).
- [10] C. Englert and M. Spannowsky, *Limitations and opportunities of off-shell coupling measurements*, *Phys. Rev. D* **90** (2014) 053003, arXiv: [1405.0285 \[hep-ph\]](#).
- [11] G. Cacciapaglia, A. Deandrea, G. D. La Rochelle and J.-B. Flament, *Higgs Couplings: Disentangling New Physics with Off-Shell Measurements*, *Phys. Rev. Lett.* **113** (2014) 201802, arXiv: [1406.1757 \[hep-ph\]](#).
- [12] A. Azatov, C. Grojean, A. Paul and E. Salvioni, *Taming the off-shell Higgs boson*, *J. Exp. Theor. Phys.* **120** (2015) 354, arXiv: [1406.6338 \[hep-ph\]](#).
- [13] M. Ghezzi, G. Passarino and S. Uccirati, *Bounding the Higgs Width Using Effective Field Theory*, *PoS LL2014* **072** (2014), arXiv: [1405.1925 \[hep-ph\]](#).
- [14] M. Buschmann et al., *Mass effects in the Higgs-gluon coupling: boosted vs off-shell production*, *JHEP* **02** (2015) 038, arXiv: [1410.5806 \[hep-ph\]](#).
- [15] J. S. Gainer, J. Lykken, K. T. Matchev, S. Mrenna and M. Park, *Beyond geolocating: Constraining higher dimensional operators in $H \rightarrow 4\ell$ with off-shell production and more*, *Phys. Rev. D* **91** (2015) 035011, arXiv: [1403.4951 \[hep-ph\]](#).

- [16] C. Englert, Y. Soreq and M. Spannowsky, *Off-shell Higgs coupling measurements in BSM scenarios*, *JHEP* **05** (2015) 145, arXiv: [1410.5440 \[hep-ph\]](#).
- [17] D. Goncalves, T. Han and S. Mukhopadhyay, *Off-Shell Higgs Probe of Naturalness*, *Phys. Rev. Lett.* **120** (2018) 111801, arXiv: [1710.02149 \[hep-ph\]](#).
- [18] D. Gonçalves, T. Han, S. Ching Iris Leung and H. Qin, *Off-shell Higgs couplings in $H^* \rightarrow ZZ \rightarrow \ell\ell\nu\nu$* , *Phys. Lett. B* **817** (2021) 136329, arXiv: [2012.05272 \[hep-ph\]](#).
- [19] S. J. Lee, M. Park and Z. Qian, *Probing unitarity violation in the tail of the off-shell Higgs boson in $V_L V_L$ mode*, *Phys. Rev. D* **100** (2019) 011702, arXiv: [1812.02679 \[hep-ph\]](#).
- [20] H.-R. He, X. Wan and Y.-K. Wang, *Anomalous $H \rightarrow ZZ \rightarrow 4\ell$ decay and its interference effects on gluon–gluon contribution at the LHC*, *Chin. Phys. C* **44** (2020) 123101, arXiv: [1902.04756 \[hep-ph\]](#).
- [21] U. Haisch and G. Koole, *Off-shell Higgs production at the LHC as a probe of the trilinear Higgs coupling*, *JHEP* **02** (2022) 030, arXiv: [2111.12589 \[hep-ph\]](#).
- [22] M. Ruhdorfer, E. Salvioni and A. Weiler, *A Global View of the Off-Shell Higgs Portal*, *SciPost Phys.* **8** (2020) 027, arXiv: [1910.04170 \[hep-ph\]](#).
- [23] ATLAS Collaboration, *Constraints on the off-shell Higgs boson signal strength in the high-mass ZZ and WW final states with the ATLAS detector*, *Eur. Phys. J. C* **75** (2015) 335, arXiv: [1503.01060 \[hep-ex\]](#).
- [24] CMS Collaboration, *Constraints on the Higgs boson width from off-shell production and decay to Z-boson pairs*, *Phys. Lett. B* **736** (2014) 64, arXiv: [1405.3455 \[hep-ex\]](#).
- [25] CMS Collaboration, *Limits on the Higgs boson lifetime and width from its decay to four charged leptons*, *Phys. Rev. D* **92** (2015) 072010, arXiv: [1507.06656 \[hep-ex\]](#).
- [26] CMS Collaboration, *Search for Higgs boson off-shell production in proton–proton collisions at 7 and 8 TeV and derivation of constraints on its total decay width*, *JHEP* **09** (2016) 051, arXiv: [1605.02329 \[hep-ex\]](#).
- [27] ATLAS Collaboration, *Constraints on off-shell Higgs boson production and the Higgs boson total width in $ZZ \rightarrow 4\ell$ and $ZZ \rightarrow 2\ell 2\nu$ final states with the ATLAS detector*, *Phys. Lett. B* **786** (2018) 223, arXiv: [1808.01191 \[hep-ex\]](#).
- [28] CMS Collaboration, *Measurements of the Higgs boson width and anomalous HVV couplings from on-shell and off-shell production in the four-lepton final state*, *Phys. Rev. D* **99** (2019) 112003, arXiv: [1901.00174 \[hep-ex\]](#).
- [29] CMS Collaboration, *Measurement of the Higgs boson width and evidence of its off-shell contributions to ZZ production*, *Nature Phys.* **18** (2022) 1329, eprint: [2202.06923](#).
- [30] S. Schael et al., *Precision electroweak measurements on the Z resonance*, *Phys. Rept.* **427** (2006) 257, arXiv: [hep-ex/0509008](#).

- [31] ATLAS Collaboration, *Measurements of the Higgs boson inclusive and differential fiducial cross sections in the 4ℓ decay channel at $\sqrt{s} = 13$ TeV*, *Eur. Phys. J. C* **80** (2020) 942, arXiv: [2004.03969](https://arxiv.org/abs/2004.03969) [[hep-ex](#)].
- [32] ATLAS Collaboration, *The ATLAS Experiment at the CERN Large Hadron Collider*, *JINST* **3** (2008) S08003.
- [33] ATLAS Collaboration, *ATLAS Insertable B-Layer Technical Design Report*, CERN-LHCC-2010-013, ATLAS-TDR-19, 2010, URL: <https://cds.cern.ch/record/1291633>, *ATLAS Insertable B-Layer Technical Design Report Addendum*, ATLAS-TDR-19-ADD-1, 2012, URL: <https://cds.cern.ch/record/1451888>.
- [34] ATLAS Collaboration, *Performance of the ATLAS Trigger System in 2015*, *Eur. Phys. J. C* **77** (2017) 317, arXiv: [1611.09661](https://arxiv.org/abs/1611.09661) [[hep-ex](#)].
- [35] ATLAS Collaboration, *The ATLAS Collaboration Software and Firmware*, ATL-SOFT-PUB-2021-001, 2021, URL: <https://cds.cern.ch/record/2767187>.
- [36] ATLAS Collaboration, *The ATLAS Simulation Infrastructure*, *Eur. Phys. J. C* **70** (2010) 823, arXiv: [1005.4568](https://arxiv.org/abs/1005.4568) [[physics.ins-det](#)].
- [37] S. Agostinelli et al., *GEANT4: A simulation toolkit*, *Nucl. Instrum. Meth. A* **506** (2003) 250.
- [38] T. Sjöstrand, S. Mrenna and P. Z. Skands, *A brief introduction to PYTHIA 8.1*, *Comput. Phys. Commun.* **178** (2008) 852, arXiv: [0710.3820](https://arxiv.org/abs/0710.3820) [[hep-ph](#)].
- [39] E. Bothmann et al., *Event generation with Sherpa 2.2*, *SciPost Phys.* **7** (2019) 034, arXiv: [1905.09127](https://arxiv.org/abs/1905.09127) [[hep-ph](#)].
- [40] F. Buccioni et al., *OpenLoops 2*, *Eur. Phys. J. C* **79** (2019) 866, arXiv: [1907.13071](https://arxiv.org/abs/1907.13071) [[hep-ph](#)].
- [41] F. Cascioli, P. Maieröfer and S. Pozzorini, *Scattering Amplitudes with Open Loops*, *Phys. Rev. Lett.* **108** (2012) 111601, arXiv: [1111.5206](https://arxiv.org/abs/1111.5206) [[hep-ph](#)].
- [42] A. Denner, S. Dittmaier and L. Hofer, *Collier: A fortran-based complex one-loop library in extended regularizations*, *Comput. Phys. Commun.* **212** (2017) 220, arXiv: [1604.06792](https://arxiv.org/abs/1604.06792) [[hep-ph](#)].
- [43] R. D. Ball et al., *Parton distributions for the LHC Run II*, *JHEP* **04** (2015) 040, arXiv: [1410.8849](https://arxiv.org/abs/1410.8849) [[hep-ph](#)].
- [44] F. Cascioli et al., *Precise Higgs-background predictions: merging NLO QCD and squared quark-loop corrections to four-lepton + 0,1 jet production*, *JHEP* **01** (2014) 046, arXiv: [1309.0500](https://arxiv.org/abs/1309.0500) [[hep-ph](#)].
- [45] F. Caola, K. Melnikov, R. Röntsch and L. Tancredi, *QCD corrections to ZZ production in gluon fusion at the LHC*, *Phys. Rev. D* **92** (2015) 18, arXiv: [1509.06734](https://arxiv.org/abs/1509.06734) [[hep-ph](#)].
- [46] F. Caola, M. Dowling, K. Melnikov, R. Röntsch and L. Tancredi, *QCD corrections to vector boson pair production in gluon fusion including interference effects with off-shell Higgs at the LHC*, *JHEP* **07** (2016) 087, arXiv: [1605.04610](https://arxiv.org/abs/1605.04610) [[hep-ph](#)].
- [47] G. Passarino, *Higgs CAT*, *Eur. Phys. J. C* **74** (2014) 2866, arXiv: [1312.2397](https://arxiv.org/abs/1312.2397) [[hep-ph](#)].
- [48] LHC Higgs Cross Section Working Group, D. de Florian et al., *Handbook of LHC Higgs Cross Sections: 4. Deciphering the nature of the Higgs sector*, CERN-2017-002-M (CERN, Geneva, 2016), arXiv: [1610.07922](https://arxiv.org/abs/1610.07922) [[hep-ph](#)].

- [49] M. Bonvini, F. Caola, S. Forte, K. Melnikov and G. Ridolfi, *Signal-background interference effects for $gg \rightarrow H \rightarrow W^+W^-$ beyond leading order*, *Phys. Rev. D* **88** (3 2013) 034032, URL: <https://link.aps.org/doi/10.1103/PhysRevD.88.034032>.
- [50] F. Caola, K. Melnikov, R. Röntsch and L. Tancredi, *QCD corrections to W^+W^- production through gluon fusion*, *Physics Letters B* **754** (2016) 275, ISSN: 0370-2693.
- [51] J. Alwall et al., *The automated computation of tree-level and next-to-leading order differential cross sections, and their matching to parton shower simulations*, *JHEP* **07** (2014) 079, arXiv: [1405.0301](https://arxiv.org/abs/1405.0301) [hep-ph].
- [52] R. D. Ball et al., *Parton distributions with LHC data*, *Nucl. Phys. B* **867** (2013) 244, arXiv: [1207.1303](https://arxiv.org/abs/1207.1303) [hep-ph].
- [53] ATLAS Collaboration, *ATLAS Pythia 8 tunes to 7 TeV data*, ATL-PHYS-PUB-2014-021, 2014, URL: <https://cds.cern.ch/record/1966419>.
- [54] S. Höche, F. Krauss, M. Schönherr and F. Siegert, *QCD matrix elements + parton showers. The NLO case*, *JHEP* **04** (2013) 027, arXiv: [1207.5030](https://arxiv.org/abs/1207.5030) [hep-ph].
- [55] B. Biedermann, A. Denner, S. Dittmaier, L. Hofer and B. Jäger, *Electroweak Corrections to $pp \rightarrow \mu^+\mu^-e^+e^- + X$ at the LHC: A Higgs Boson Background Study*, *Phys. Rev. Lett.* **116** (2016) 161803, arXiv: [1601.07787](https://arxiv.org/abs/1601.07787) [hep-ph].
- [56] B. Biedermann, A. Denner, S. Dittmaier, L. Hofer and B. Jäger, *Next-to-leading-order electroweak corrections to the production of four charged leptons at the LHC*, *JHEP* **01** (2017) 033, arXiv: [1611.05338](https://arxiv.org/abs/1611.05338) [hep-ph].
- [57] S. Kallweit, J. Lindert, S. Pozzorini and M. Schönherr, *NLO QCD+EW predictions for $2\ell 2\nu$ diboson signatures at the LHC*, *JHEP* **11** (2017) 120, arXiv: [1705.00598](https://arxiv.org/abs/1705.00598) [hep-ph].
- [58] P. Nason and G. Zanderighi, *W^+W^- , WZ and ZZ production in the POWHEG-BOX-V2*, *Eur. Phys. J. C* **74** (2014) 2702, arXiv: [1311.1365](https://arxiv.org/abs/1311.1365) [hep-ph].
- [59] R. Gavin, Y. Li, F. Petriello and S. Quackenbush, *FEWZ 2.0: A code for hadronic Z production at next-to-next-to-leading order*, *Comput. Phys. Commun.* **182** (2011) 2388, arXiv: [1011.3540](https://arxiv.org/abs/1011.3540) [hep-ph].
- [60] M. Czakon and A. Mitov, *Top++: A Program for the Calculation of the Top-Pair Cross-Section at Hadron Colliders*, *Comput. Phys. Commun.* **185** (2014) 2930, arXiv: [1112.5675](https://arxiv.org/abs/1112.5675) [hep-ph].
- [61] P. Kant et al., *HatHor for single top-quark production: Updated predictions and uncertainty estimates for single top-quark production in hadronic collisions*, *Comput. Phys. Commun.* **191** (2015) 74, arXiv: [1406.4403](https://arxiv.org/abs/1406.4403) [hep-ph].
- [62] M. Aliev et al., *HATHOR: HAdronic Top and Heavy quarks crOss section calculatoR*, *Comput. Phys. Commun.* **182** (2011) 1034, arXiv: [1007.1327](https://arxiv.org/abs/1007.1327) [hep-ph].
- [63] S. Frixione, V. Hirschi, D. Pagani, H.-S. Shao and M. Zaro, *Electroweak and QCD corrections to top-pair hadroproduction in association with heavy bosons*, *JHEP* **06** (2015) 184, arXiv: [1504.03446](https://arxiv.org/abs/1504.03446) [hep-ph].

- [64] ATLAS Collaboration, *Search for heavy resonances decaying into a pair of Z bosons in the $\ell^+\ell^-\ell'^+\ell'^-$ and $\ell^+\ell^-\nu\bar{\nu}$ final states using 139fb^{-1} of proton–proton collisions at $\sqrt{s} = 13$, TeV with the ATLAS detector*, *Eur. Phys. J. C* **81** (2020) 332, arXiv: [2009.14791 \[hep-ex\]](#).
- [65] ATLAS Collaboration, *Muon reconstruction performance of the ATLAS detector in proton–proton collision data at $\sqrt{s} = 13$ TeV*, *Eur. Phys. J. C* **76** (2016) 292, arXiv: [1603.05598 \[hep-ex\]](#).
- [66] ATLAS Collaboration, *Electron reconstruction and identification in the ATLAS experiment using the 2015 and 2016 LHC proton–proton collision data at $\sqrt{s} = 13$ TeV*, *Eur. Phys. J. C* **79** (2019) 639, arXiv: [1902.04655 \[hep-ex\]](#).
- [67] ATLAS Collaboration, *Jet reconstruction and performance using particle flow with the ATLAS Detector*, *Eur. Phys. J. C* **77** (2017) 466, arXiv: [1703.10485 \[hep-ex\]](#).
- [68] M. Cacciari, G. P. Salam and G. Soyez, *The anti- k_t jet clustering algorithm*, *JHEP* **04** (2008) 063, arXiv: [0802.1189 \[hep-ph\]](#).
- [69] M. Cacciari, G. P. Salam and G. Soyez, *FastJet user manual*, *Eur. Phys. J. C* **72** (2012) 1896, arXiv: [1111.6097 \[hep-ph\]](#).
- [70] ATLAS Collaboration, *Jet energy scale measurements and their systematic uncertainties in proton–proton collisions at $\sqrt{s} = 13$ TeV with the ATLAS detector*, *Phys. Rev. D* **96** (2017) 072002, arXiv: [1703.09665 \[hep-ex\]](#).
- [71] ATLAS Collaboration, *Performance of pile-up mitigation techniques for jets in pp collisions at $\sqrt{s} = 8$ TeV using the ATLAS detector*, *Eur. Phys. J. C* **76** (2016) 581, arXiv: [1510.03823 \[hep-ex\]](#).
- [72] ATLAS Collaboration, *Identification and rejection of pile-up jets at high pseudorapidity with the ATLAS detector*, *Eur. Phys. J. C* **77** (2017) 580, [Erratum: *Eur.Phys.J.C* 77, 712 (2017)], arXiv: [1705.02211 \[hep-ex\]](#).
- [73] ATLAS Collaboration, *ATLAS b-jet identification performance and efficiency measurement with $t\bar{t}$ events in pp collisions at $\sqrt{s} = 13$ TeV*, *Eur. Phys. J. C* **79** (2019) 970, arXiv: [1907.05120 \[hep-ex\]](#).
- [74] *ATLAS flavour-tagging algorithms for the LHC Run 2 pp collision dataset*, (2022), arXiv: [2211.16345 \[physics.data-an\]](#).
- [75] ATLAS Collaboration, *Performance of missing transverse momentum reconstruction with the ATLAS detector in the first proton–proton collisions at $\sqrt{s} = 13$ TeV*, ATL-PHYS-PUB-2015-027, 2015, URL: <https://cds.cern.ch/record/2037904>.
- [76] ATLAS Collaboration, *Object-based missing transverse momentum significance in the ATLAS Detector*, ATL-CONF-2018-038, 2018, URL: <https://cds.cern.ch/record/2630948>.
- [77] F. Chollet et al., *Keras*, 2015, URL: <https://github.com/fchollet/keras>.
- [78] Martín Abadi et al., *TensorFlow: Large-Scale Machine Learning on Heterogeneous Systems*, Software available from tensorflow.org, 2015, URL: <https://www.tensorflow.org/>.
- [79] ATLAS Collaboration, *Evidence for the spin-0 nature of the Higgs boson using ATLAS data*, *Phys. Lett. B* **726** (2013) 120, arXiv: [1307.1432 \[hep-ex\]](#).

- [80] D. Rainwater, R. Szalapski and D. Zeppenfeld,
Probing color-singlet exchange in $Z + 2$ -jet events at the CERN LHC,
Phys. Rev. D **54** (11 1996) 6680,
URL: <https://link.aps.org/doi/10.1103/PhysRevD.54.6680>.
- [81] D. de Florian et al.,
Handbook of LHC Higgs Cross Sections: 4. Deciphering the Nature of the Higgs Sector, (2016),
arXiv: [1610.07922](https://arxiv.org/abs/1610.07922) [[hep-ph](#)].
- [82] S. Gieseke, T. Kasprzik and J. H. Kühn,
Vector-boson pair production and electroweak corrections in HERWIG++,
Eur. Phys. J. C **74** (2014) 2988, arXiv: [1401.3964](https://arxiv.org/abs/1401.3964) [[hep-ph](#)].
- [83] B. Nachman and J. Thaler, *Neural conditional reweighting*, *Phys. Rev. D* **105** (2022) 076015,
arXiv: [2107.08979](https://arxiv.org/abs/2107.08979) [[physics.data-an](#)].
- [84] ATLAS Collaboration,
Luminosity determination in pp collisions at $\sqrt{s} = 13$ TeV using the ATLAS detector at the LHC,
ATLAS-CONF-2019-021, 2019, URL: <https://cds.cern.ch/record/2677054>.
- [85] G. Avoni et al., *The new LUCID-2 detector for luminosity measurement and monitoring in ATLAS*,
JINST **13** (2018) P07017.
- [86] G. Cowan, K. Cranmer, E. Gross and O. Vitells,
Asymptotic formulae for likelihood-based tests of new physics, *Eur. Phys. J. C* **71** (2011).
- [87] S. S. Wilks,
The Large-Sample Distribution of the Likelihood Ratio for Testing Composite Hypotheses,
Annals Math. Statist. **9** (1938) 60.
- [88] J. Neyman,
Outline of a Theory of Statistical Estimation Based on the Classical Theory of Probability,
Philosophical Transactions of the Royal Society of London. Series A, Mathematical and Physical
Sciences **236** (1937) 333, ISSN: 00804614.
- [89] ATLAS Collaboration, *Higgs boson production cross-section measurements and their EFT
interpretation in the 4ℓ decay channel at $\sqrt{s} = 13$ TeV with the ATLAS detector*,
Eur. Phys. J. C **80** (2020) 957, arXiv: [2004.03447](https://arxiv.org/abs/2004.03447) [[hep-ex](#)],
Erratum: *Eur. Phys. J. C* **81** (2021) 29, Erratum: *Eur. Phys. J. C* **81** (2021) 398.
- [90] ATLAS Collaboration, *ATLAS Computing Acknowledgements*, ATL-SOFT-PUB-2023-001, 2023,
URL: <https://cds.cern.ch/record/2869272>.

The ATLAS Collaboration

G. Aad ¹⁰², B. Abbott ¹²⁰, K. Abeling ⁵⁵, S.H. Abidi ²⁹, A. Aboulhorma ^{35e},
H. Abramowicz ¹⁵¹, H. Abreu ¹⁵⁰, Y. Abulaiti ¹¹⁷, A.C. Abusleme Hoffman ^{137a},
B.S. Acharya ^{69a,69b,p}, C. Adam Bourdarios ⁴, L. Adamczyk ^{85a}, L. Adamek ¹⁵⁵,
S.V. Addepalli ²⁶, J. Adelman ¹¹⁵, A. Adiguzel ^{21c}, S. Adorni ⁵⁶, T. Adye ¹³⁴, A.A. Affolder ¹³⁶,
Y. Afik ³⁶, M.N. Agaras ¹³, J. Agarwala ^{73a,73b}, A. Aggarwal ¹⁰⁰, C. Agheorghiesei ^{27c},
J.A. Aguilar-Saavedra ^{130f}, A. Ahmad ³⁶, F. Ahmadov ^{38,ab}, W.S. Ahmed ¹⁰⁴, S. Ahuja ⁹⁵,
X. Ai ⁴⁸, G. Aielli ^{76a,76b}, M. Ait Tamlihat ^{35e}, B. Aitbenkikh ^{35a}, I. Aizenberg ¹⁶⁹,
M. Akbiyik ¹⁰⁰, T.P.A. Åkesson ⁹⁸, A.V. Akimov ³⁷, N.N. Akolkar ²⁴, K. Al Houry ⁴¹,
G.L. Alberghi ^{23b}, J. Albert ¹⁶⁵, P. Albicocco ⁵³, S. Alderweireldt ⁵², M. Aleksa ³⁶,
I.N. Aleksandrov ³⁸, C. Alexa ^{27b}, T. Alexopoulos ¹⁰, A. Alfonsi ¹¹⁴, F. Alfonsi ^{23b},
M. Alhroob ¹²⁰, B. Ali ¹³², S. Ali ¹⁴⁸, M. Aliev ³⁷, G. Alimonti ^{71a}, W. Alkakhki ⁵⁵,
C. Allaire ⁶⁶, B.M.M. Allbrooke ¹⁴⁶, C.A. Allendes Flores ^{137f}, P.P. Allport ²⁰, A. Aloisio ^{72a,72b},
F. Alonso ⁹⁰, C. Alpigiani ¹³⁸, M. Alvarez Estevez ⁹⁹, A. Alvarez Fernandez ¹⁰⁰,
M.G. Alvigi ^{72a,72b}, M. Aly ¹⁰¹, Y. Amaral Coutinho ^{82b}, A. Ambler ¹⁰⁴, C. Amelung ³⁶,
M. Amerl ¹⁰¹, C.G. Ames ¹⁰⁹, D. Amidei ¹⁰⁶, S.P. Amor Dos Santos ^{130a}, K.R. Amos ¹⁶³,
V. Ananiev ¹²⁵, C. Anastopoulos ¹³⁹, T. Andeen ¹¹, J.K. Anders ³⁶, S.Y. Andrean ^{47a,47b},
A. Andreazza ^{71a,71b}, S. Angelidakis ⁹, A. Angerami ^{41,ae}, A.V. Anisenkov ³⁷, A. Annovi ^{74a},
C. Antel ⁵⁶, M.T. Anthony ¹³⁹, E. Antipov ¹⁴⁵, M. Antonelli ⁵³, D.J.A. Antrim ^{17a}, F. Anulli ^{75a},
M. Aoki ⁸³, T. Aoki ¹⁵³, J.A. Aparisi Pozo ¹⁶³, M.A. Aparo ¹⁴⁶, L. Aperio Bella ⁴⁸,
C. Appelt ¹⁸, N. Aranzabal ³⁶, V. Araujo Ferraz ^{82a}, C. Arcangeletti ⁵³, A.T.H. Arce ⁵¹,
E. Arena ⁹², J-F. Arguin ¹⁰⁸, S. Argyropoulos ⁵⁴, J.-H. Arling ⁴⁸, A.J. Armbruster ³⁶,
O. Arnaez ⁴, H. Arnold ¹¹⁴, Z.P. Arrubarrena Tame ¹⁰⁹, G. Artoni ^{75a,75b}, H. Asada ¹¹¹,
K. Asai ¹¹⁸, S. Asai ¹⁵³, N.A. Asbah ⁶¹, K. Assamagan ²⁹, R. Astalos ^{28a}, R.J. Atkin ^{33a},
M. Atkinson ¹⁶², N.B. Atlay ¹⁸, H. Atmani ^{62b}, P.A. Atlasiddha ¹⁰⁶, K. Augsten ¹³²,
S. Auricchio ^{72a,72b}, A.D. Auriol ²⁰, V.A. Austrup ¹⁷¹, G. Avner ¹⁵⁰, G. Avolio ³⁶, K. Axiotis ⁵⁶,
G. Azuelos ^{108,ai}, D. Babal ^{28b}, H. Bachacou ¹³⁵, K. Bachas ^{152,s}, A. Bachiu ³⁴,
F. Backman ^{47a,47b}, A. Badea ⁶¹, P. Bagnaia ^{75a,75b}, M. Bahmani ¹⁸, A.J. Bailey ¹⁶³,
V.R. Bailey ¹⁶², J.T. Baines ¹³⁴, C. Bakalis ¹⁰, O.K. Baker ¹⁷², E. Bakos ¹⁵, D. Bakshi Gupta ⁸,
R. Balasubramanian ¹¹⁴, E.M. Baldin ³⁷, P. Balek ¹³³, E. Ballabene ^{71a,71b}, F. Balli ¹³⁵,
L.M. Baltes ^{63a}, W.K. Balunas ³², J. Balz ¹⁰⁰, E. Banas ⁸⁶, M. Bandieramonte ¹²⁹,
A. Bandyopadhyay ²⁴, S. Bansal ²⁴, L. Barak ¹⁵¹, E.L. Barberio ¹⁰⁵, D. Barberis ^{57b,57a},
M. Barbero ¹⁰², G. Barbour ⁹⁶, K.N. Barends ^{33a}, T. Barillari ¹¹⁰, M-S. Barisits ³⁶, T. Barklow ¹⁴³,
P. Baron ¹²², D.A. Baron Moreno ¹⁰¹, A. Baroncelli ^{62a}, G. Barone ²⁹, A.J. Barr ¹²⁶,
L. Barranco Navarro ^{47a,47b}, F. Barreiro ⁹⁹, J. Barreiro Guimarães da Costa ^{14a}, U. Barron ¹⁵¹,
M.G. Barros Teixeira ^{130a}, S. Barsov ³⁷, F. Bartels ^{63a}, R. Bartoldus ¹⁴³, A.E. Barton ⁹¹,
P. Bartos ^{28a}, A. Basan ¹⁰⁰, M. Baselga ⁴⁹, I. Bashta ^{77a,77b}, A. Bassalat ^{66,b}, M.J. Basso ¹⁵⁵,
C.R. Basson ¹⁰¹, R.L. Bates ⁵⁹, S. Batlamous ^{35e}, J.R. Batley ³², B. Batool ¹⁴¹, M. Battaglia ¹³⁶,
D. Battulga ¹⁸, M. Bauge ^{75a,75b}, M. Bauer ³⁶, P. Bauer ²⁴, J.B. Beacham ⁵¹, T. Beau ¹²⁷,
P.H. Beauchemin ¹⁵⁸, F. Becherer ⁵⁴, P. Bechtel ²⁴, H.P. Beck ^{19,r}, K. Becker ¹⁶⁷,
A.J. Beddall ^{21d}, V.A. Bednyakov ³⁸, C.P. Bee ¹⁴⁵, L.J. Beemster ¹⁵, T.A. Beermann ³⁶,
M. Begalli ^{82d}, M. Begel ²⁹, A. Behera ¹⁴⁵, J.K. Behr ⁴⁸, C. Beirao Da Cruz E Silva ³⁶,
J.F. Beirer ^{55,36}, F. Beisiegel ²⁴, M. Belfkir ¹⁵⁹, G. Bella ¹⁵¹, L. Bellagamba ^{23b}, A. Bellerive ³⁴,
P. Bellos ²⁰, K. Beloborodov ³⁷, N.L. Belyaev ³⁷, D. Benchebroun ^{35a}, F. Bendebba ^{35a},
Y. Benhammou ¹⁵¹, M. Benoit ²⁹, J.R. Bensinger ²⁶, S. Bentvelsen ¹¹⁴, L. Beresford ⁴⁸,

M. Beretta ⁵³, E. Bergeaas Kuutmann ¹⁶¹, N. Berger ⁴, B. Bergmann ¹³², J. Beringer ^{17a},
S. Berlendis ⁷, G. Bernardi ⁵, C. Bernius ¹⁴³, F.U. Bernlochner ²⁴, T. Berry ⁹⁵, P. Berta ¹³³,
A. Berthold ⁵⁰, I.A. Bertram ⁹¹, S. Bethke ¹¹⁰, A. Betti ^{75a,75b}, A.J. Bevan ⁹⁴, M. Bhamjee ^{33c},
S. Bhatta ¹⁴⁵, D.S. Bhattacharya ¹⁶⁶, P. Bhattarai ²⁶, V.S. Bhopatkar ¹²¹, R. Bi ^{29,ak},
R.M. Bianchi ¹²⁹, O. Biebel ¹⁰⁹, R. Bielski ¹²³, M. Biglietti ^{77a}, T.R.V. Billoud ¹³², M. Bindi ⁵⁵,
A. Bingul ^{21b}, C. Bini ^{75a,75b}, A. Biondini ⁹², C.J. Birch-sykes ¹⁰¹, G.A. Bird ^{20,134},
M. Birman ¹⁶⁹, M. Biroš ¹³³, T. Bisanz ³⁶, E. Bisceglie ^{43b,43a}, D. Biswas ¹⁷⁰, A. Bitadze ¹⁰¹,
K. Bjørke ¹²⁵, I. Bloch ⁴⁸, C. Blocker ²⁶, A. Blue ⁵⁹, U. Blumenschein ⁹⁴, J. Blumenthal ¹⁰⁰,
G.J. Bobbink ¹¹⁴, V.S. Bobrovnikov ³⁷, M. Boehler ⁵⁴, D. Bogavac ³⁶, A.G. Bogdanchikov ³⁷,
C. Bohm ^{47a}, V. Boisvert ⁹⁵, P. Bokan ⁴⁸, T. Bold ^{85a}, M. Bomben ⁵, M. Bona ⁹⁴,
M. Boonekamp ¹³⁵, C.D. Booth ⁹⁵, A.G. Borbély ⁵⁹, H.M. Borecka-Bielska ¹⁰⁸, L.S. Borgna ⁹⁶,
G. Borissov ⁹¹, D. Bortoletto ¹²⁶, D. Boscherini ^{23b}, M. Bosman ¹³, J.D. Bossio Sola ³⁶,
K. Bouaouda ^{35a}, N. Bouchhar ¹⁶³, J. Boudreau ¹²⁹, E.V. Bouhova-Thacker ⁹¹, D. Boumediene ⁴⁰,
R. Bouquet ⁵, A. Boveia ¹¹⁹, J. Boyd ³⁶, D. Boye ²⁹, I.R. Boyko ³⁸, J. Bracinik ²⁰,
N. Brahimí ^{62d}, G. Brandt ¹⁷¹, O. Brandt ³², F. Braren ⁴⁸, B. Brau ¹⁰³, J.E. Brau ¹²³,
K. Brendlinger ⁴⁸, R. Brenner ¹⁶⁹, L. Brenner ¹¹⁴, R. Brenner ¹⁶¹, S. Bressler ¹⁶⁹, D. Britton ⁵⁹,
D. Britzger ¹¹⁰, I. Brock ²⁴, G. Brooijmans ⁴¹, W.K. Brooks ^{137f}, E. Brost ²⁹, L.M. Brown ¹⁶⁵,
T.L. Bruckler ¹²⁶, P.A. Bruckman de Renstrom ⁸⁶, B. Brüers ⁴⁸, D. Bruncko ^{28b,*}, A. Bruni ^{23b},
G. Bruni ^{23b}, M. Bruschi ^{23b}, N. Brusino ^{75a,75b}, T. Buanes ¹⁶, Q. Buat ¹³⁸, A.G. Buckley ⁵⁹,
I.A. Budagov ^{38,*}, M.K. Bugge ¹²⁵, O. Bulekov ³⁷, B.A. Bullard ¹⁴³, S. Burdin ⁹²,
C.D. Burgard ⁴⁹, A.M. Burger ⁴⁰, B. Burghgrave ⁸, O. Burlayenko ⁵⁴, J.T.P. Burr ³²,
C.D. Burton ¹¹, J.C. Burzynski ¹⁴², E.L. Busch ⁴¹, V. Büscher ¹⁰⁰, P.J. Bussey ⁵⁹,
J.M. Butler ²⁵, C.M. Buttar ⁵⁹, J.M. Butterworth ⁹⁶, W. Buttinger ¹³⁴, C.J. Buxo Vazquez ¹⁰⁷,
A.R. Buzykaev ³⁷, G. Cabras ^{23b}, S. Cabrera Urbán ¹⁶³, D. Caforio ⁵⁸, H. Cai ¹²⁹, Y. Cai ^{14a,14e},
V.M.M. Cairo ³⁶, O. Cakir ^{3a}, N. Calace ³⁶, P. Calafiura ^{17a}, G. Calderini ¹²⁷, P. Calfayan ⁶⁸,
G. Callea ⁵⁹, L.P. Caloba ^{82b}, D. Calvet ⁴⁰, S. Calvet ⁴⁰, T.P. Calvet ¹⁰², M. Calvetti ^{74a,74b},
R. Camacho Toro ¹²⁷, S. Camarda ³⁶, D. Camarero Munoz ²⁶, P. Camarri ^{76a,76b},
M.T. Camerlingo ^{72a,72b}, D. Cameron ¹²⁵, C. Camincher ¹⁶⁵, M. Campanelli ⁹⁶, A. Camplani ⁴²,
V. Canale ^{72a,72b}, A. Canesse ¹⁰⁴, M. Cano Bret ⁸⁰, J. Cantero ¹⁶³, Y. Cao ¹⁶², F. Capocasa ²⁶,
M. Capua ^{43b,43a}, A. Carbone ^{71a,71b}, R. Cardarelli ^{76a}, J.C.J. Cardenas ⁸, F. Cardillo ¹⁶³,
T. Carli ³⁶, G. Carlino ^{72a}, J.I. Carlotto ¹³, B.T. Carlson ^{129,t}, E.M. Carlson ^{165,156a},
L. Carminati ^{71a,71b}, M. Carnesale ^{75a,75b}, S. Caron ¹¹³, E. Carquin ^{137f}, S. Carrá ^{71a},
G. Carratta ^{23b,23a}, F. Carrio Argos ^{33g}, J.W.S. Carter ¹⁵⁵, T.M. Carter ⁵², M.P. Casado ^{13,j},
A.F. Casha ¹⁵⁵, M. Caspar ⁴⁸, E.G. Castiglia ¹⁷², F.L. Castillo ^{63a}, L. Castillo Garcia ¹³,
V. Castillo Gimenez ¹⁶³, N.F. Castro ^{130a,130e}, A. Catinaccio ³⁶, J.R. Catmore ¹²⁵, V. Cavaliere ²⁹,
N. Cavalli ^{23b,23a}, V. Cavalinni ^{74a,74b}, E. Celebi ^{21a}, F. Celli ¹²⁶, M.S. Centonze ^{70a,70b},
K. Cerny ¹²², A.S. Cerqueira ^{82a}, A. Cerri ¹⁴⁶, L. Cerrito ^{76a,76b}, F. Cerutti ^{17a}, A. Cervelli ^{23b},
G. Cesarini ⁵³, S.A. Cetin ^{21d}, Z. Chadi ^{35a}, D. Chakraborty ¹¹⁵, M. Chala ^{130f}, J. Chan ¹⁷⁰,
W.Y. Chan ¹⁵³, J.D. Chapman ³², B. Chargeishvili ^{149b}, D.G. Charlton ²⁰, T.P. Charman ⁹⁴,
M. Chatterjee ¹⁹, C. Chauhan ¹³³, S. Chekanov ⁶, S.V. Chekulaev ^{156a}, G.A. Chelkov ^{38,a},
A. Chen ¹⁰⁶, B. Chen ¹⁵¹, B. Chen ¹⁶⁵, H. Chen ^{14c}, H. Chen ²⁹, J. Chen ^{62c}, J. Chen ¹⁴²,
S. Chen ¹⁵³, S.J. Chen ^{14c}, X. Chen ^{62c}, X. Chen ^{14b,ah}, Y. Chen ^{62a}, C.L. Cheng ¹⁷⁰,
H.C. Cheng ^{64a}, S. Cheong ¹⁴³, A. Cheplakov ³⁸, E. Cheremushkina ⁴⁸, E. Cherepanova ¹¹⁴,
R. Cherkaoui El Moursli ^{35e}, E. Cheu ⁷, K. Cheung ⁶⁵, L. Chevalier ¹³⁵, V. Chiarella ⁵³,
G. Chiarelli ^{74a}, N. Chiedde ¹⁰², G. Chiodini ^{70a}, A.S. Chisholm ²⁰, A. Chitan ^{27b},
M. Chitishvili ¹⁶³, M.V. Chizhov ³⁸, K. Choi ¹¹, A.R. Chomont ^{75a,75b}, Y. Chou ¹⁰³,
E.Y.S. Chow ¹¹⁴, T. Chowdhury ^{33g}, L.D. Christopher ^{33g}, K.L. Chu ^{64a}, M.C. Chu ^{64a},

X. Chu ^{14a,14e}, J. Chudoba ¹³¹, J.J. Chwastowski ⁸⁶, D. Cieri ¹¹⁰, K.M. Ciesla ^{85a}, V. Cindro ⁹³, A. Ciocio ^{17a}, F. Cirotto ^{72a,72b}, Z.H. Citron ^{169,m}, M. Citterio ^{71a}, D.A. Ciubotaru ^{27b}, B.M. Ciungu ¹⁵⁵, A. Clark ⁵⁶, P.J. Clark ⁵², J.M. Clavijo Columbie ⁴⁸, S.E. Clawson ¹⁰¹, C. Clement ^{47a,47b}, J. Clercx ⁴⁸, L. Clissa ^{23b,23a}, Y. Coadou ¹⁰², M. Cobal ^{69a,69c}, A. Cocco ^{57b}, R.F. Coelho Barrue ^{130a}, R. Coelho Lopes De Sa ¹⁰³, S. Coelli ^{71a}, H. Cohen ¹⁵¹, A.E.C. Coimbra ^{71a,71b}, B. Cole ⁴¹, J. Collot ⁶⁰, P. Conde Muiño ^{130a,130g}, M.P. Connell ^{33c}, S.H. Connell ^{33c}, I.A. Connelly ⁵⁹, E.I. Conroy ¹²⁶, F. Conventi ^{72a,aj}, H.G. Cooke ²⁰, A.M. Cooper-Sarkar ¹²⁶, F. Cormier ¹⁶⁴, L.D. Corpe ³⁶, M. Corradi ^{75a,75b}, F. Corriveau ^{104,z}, A. Cortes-Gonzalez ¹⁸, M.J. Costa ¹⁶³, F. Costanza ⁴, D. Costanzo ¹³⁹, B.M. Cote ¹¹⁹, G. Cowan ⁹⁵, K. Cranmer ¹¹⁷, S. Crépe-Renaudin ⁶⁰, F. Crescioli ¹²⁷, M. Cristinziani ¹⁴¹, M. Cristoforetti ^{78a,78b,d}, V. Croft ¹¹⁴, G. Crosetti ^{43b,43a}, A. Cueto ³⁶, T. Cuhadar Donszelmann ¹⁶⁰, H. Cui ^{14a,14e}, Z. Cui ⁷, W.R. Cunningham ⁵⁹, F. Curcio ^{43b,43a}, P. Czodrowski ³⁶, M.M. Czurylo ^{63b}, M.J. Da Cunha Sargedas De Sousa ^{62a}, J.V. Da Fonseca Pinto ^{82b}, C. Da Via ¹⁰¹, W. Dabrowski ^{85a}, T. Dado ⁴⁹, S. Dahbi ^{33g}, T. Dai ¹⁰⁶, C. Dallapiccola ¹⁰³, M. Dam ⁴², G. D'amen ²⁹, V. D'Amico ¹⁰⁹, J. Damp ¹⁰⁰, J.R. Dandoy ¹²⁸, M.F. Daneri ³⁰, M. Danninger ¹⁴², V. Dao ³⁶, G. Darbo ^{57b}, S. Darmora ⁶, S.J. Das ^{29,ak}, S. D'Auria ^{71a,71b}, C. David ^{156b}, T. Davidek ¹³³, B. Davis-Purcell ³⁴, I. Dawson ⁹⁴, K. De ⁸, R. De Asmundis ^{72a}, N. De Biase ⁴⁸, S. De Castro ^{23b,23a}, N. De Groot ¹¹³, P. de Jong ¹¹⁴, H. De la Torre ¹⁰⁷, A. De Maria ^{14c}, A. De Salvo ^{75a}, U. De Sanctis ^{76a,76b}, A. De Santo ¹⁴⁶, J.B. De Vivie De Regie ⁶⁰, D.V. Dedovich ³⁸, J. Degens ¹¹⁴, A.M. Deiana ⁴⁴, F. Del Corso ^{23b,23a}, J. Del Peso ⁹⁹, F. Del Rio ^{63a}, F. Deliot ¹³⁵, C.M. Delitzsch ⁴⁹, M. Della Pietra ^{72a,72b}, D. Della Volpe ⁵⁶, A. Dell'Acqua ³⁶, L. Dell'Asta ^{71a,71b}, M. Delmastro ⁴, P.A. Delsart ⁶⁰, S. Demers ¹⁷², M. Demichev ³⁸, S.P. Denisov ³⁷, L. D'Eramo ¹¹⁵, D. Derendarz ⁸⁶, F. Derue ¹²⁷, P. Dervan ⁹², K. Desch ²⁴, K. Dette ¹⁵⁵, C. Deutsch ²⁴, F.A. Di Bello ^{57b,57a}, A. Di Ciaccio ^{76a,76b}, L. Di Ciaccio ⁴, A. Di Domenico ^{75a,75b}, C. Di Donato ^{72a,72b}, A. Di Girolamo ³⁶, G. Di Gregorio ⁵, A. Di Luca ^{78a,78b}, B. Di Micco ^{77a,77b}, R. Di Nardo ^{77a,77b}, C. Diaconu ¹⁰², F.A. Dias ¹¹⁴, T. Dias Do Vale ¹⁴², M.A. Diaz ^{137a,137b}, F.G. Diaz Capriles ²⁴, M. Didenko ¹⁶³, E.B. Diehl ¹⁰⁶, L. Diehl ⁵⁴, S. Díez Cornell ⁴⁸, C. Diez Pardos ¹⁴¹, C. Dimitriadi ^{24,161}, A. Dimitrievska ^{17a}, J. Dingfelder ²⁴, I-M. Dinu ^{27b}, S.J. Dittmeier ^{63b}, F. Dittus ³⁶, F. Djama ¹⁰², T. Djobava ^{149b}, J.I. Djuvsland ¹⁶, C. Doglioni ^{101,98}, J. Dolejsi ¹³³, Z. Dolezal ¹³³, M. Donadelli ^{82c}, B. Dong ¹⁰⁷, J. Donini ⁴⁰, A. D'Onofrio ^{77a,77b}, M. D'Onofrio ⁹², J. Dopke ¹³⁴, A. Doria ^{72a}, M.T. Dova ⁹⁰, A.T. Doyle ⁵⁹, M.A. Draguet ¹²⁶, E. Drechsler ¹⁴², E. Dreyer ¹⁶⁹, I. Drivas-koulouris ¹⁰, A.S. Drobac ¹⁵⁸, M. Drozdova ⁵⁶, D. Du ^{62a}, T.A. du Pree ¹¹⁴, F. Dubinin ³⁷, M. Dubovsky ^{28a}, E. Duchovni ¹⁶⁹, G. Duckeck ¹⁰⁹, O.A. Ducu ^{27b}, D. Duda ¹¹⁰, A. Dudarev ³⁶, E.R. Duden ²⁶, M. D'uffizi ¹⁰¹, L. Duflost ⁶⁶, M. Dührssen ³⁶, C. Dülsen ¹⁷¹, A.E. Dumitriu ^{27b}, M. Dunford ^{63a}, S. Dungs ⁴⁹, K. Dunne ^{47a,47b}, A. Duperrin ¹⁰², H. Duran Yildiz ^{3a}, M. Düren ⁵⁸, A. Durglishvili ^{149b}, B.L. Dwyer ¹¹⁵, G.I. Dyckes ^{17a}, M. Dyndal ^{85a}, S. Dysch ¹⁰¹, B.S. Dziedzic ⁸⁶, Z.O. Earnshaw ¹⁴⁶, B. Eckerova ^{28a}, S. Eggebrecht ⁵⁵, M.G. Eggleston ⁵¹, E. Egidio Purcino De Souza ¹²⁷, L.F. Ehrke ⁵⁶, G. Eigen ¹⁶, K. Einsweiler ^{17a}, T. Ekelof ¹⁶¹, P.A. Ekman ⁹⁸, Y. El Ghazali ^{35b}, H. El Jarrari ^{35e,148}, A. El Moussaouy ^{35a}, V. Ellajosyula ¹⁶¹, M. Ellert ¹⁶¹, F. Ellinghaus ¹⁷¹, A.A. Elliot ⁹⁴, N. Ellis ³⁶, J. Elmsheuser ²⁹, M. Elsing ³⁶, D. Emelianov ¹³⁴, Y. Enari ¹⁵³, I. Ene ^{17a}, S. Epari ¹³, J. Erdmann ⁴⁹, P.A. Erland ⁸⁶, M. Errenst ¹⁷¹, M. Escalier ⁶⁶, C. Escobar ¹⁶³, E. Etzion ¹⁵¹, G. Evans ^{130a}, H. Evans ⁶⁸, L.S. Evans ⁹⁵, M.O. Evans ¹⁴⁶, A. Ezhilov ³⁷, S. Ezzarqtouni ^{35a}, F. Fabbri ⁵⁹, L. Fabbri ^{23b,23a}, G. Facini ⁹⁶, V. Fadeyev ¹³⁶, R.M. Fakhruddinov ³⁷, S. Falciano ^{75a}, L.F. Falda Ulhoa Coelho ³⁶, P.J. Falke ²⁴, S. Falke ³⁶, J. Faltova ¹³³, C. Fan ¹⁶², Y. Fan ^{14a}, Y. Fang ^{14a,14e}, M. Fanti ^{71a,71b},

M. Faraj [ID 69a,69b](#), Z. Farazpay [ID 97](#), A. Farbin [ID 8](#), A. Farilla [ID 77a](#), T. Farooque [ID 107](#), S.M. Farrington [ID 52](#),
F. Fassi [ID 35e](#), D. Fassouliotis [ID 9](#), M. Faucci Giannelli [ID 76a,76b](#), W.J. Fawcett [ID 32](#), L. Fayard [ID 66](#),
P. Federic [ID 133](#), P. Federicova [ID 131](#), O.L. Fedin [ID 37,a](#), G. Fedotov [ID 37](#), M. Feickert [ID 170](#),
L. Feligioni [ID 102](#), A. Fell [ID 139](#), D.E. Fellers [ID 123](#), C. Feng [ID 62b](#), M. Feng [ID 14b](#), Z. Feng [ID 114](#),
M.J. Fenton [ID 160](#), A.B. Fenyuk [ID 37](#), L. Ferencz [ID 48](#), R.A.M. Ferguson [ID 91](#), S.I. Fernandez Luengo [ID 137f](#),
M.J.V. Fernoux [ID 102](#), J. Ferrando [ID 48](#), A. Ferrari [ID 161](#), P. Ferrari [ID 114,113](#), R. Ferrari [ID 73a](#), D. Ferrere [ID 56](#),
C. Ferretti [ID 106](#), F. Fiedler [ID 100](#), A. Filipčič [ID 93](#), E.K. Filmer [ID 1](#), F. Filthaut [ID 113](#),
M.C.N. Fiolhais [ID 130a,130c,c](#), L. Fiorini [ID 163](#), W.C. Fisher [ID 107](#), T. Fitschen [ID 101](#), I. Fleck [ID 141](#),
P. Fleischmann [ID 106](#), T. Flick [ID 171](#), L. Flores [ID 128](#), M. Flores [ID 33d,af](#), L.R. Flores Castillo [ID 64a](#),
F.M. Follega [ID 78a,78b](#), N. Fomin [ID 16](#), J.H. Foo [ID 155](#), B.C. Forland [ID 68](#), A. Formica [ID 135](#), A.C. Forti [ID 101](#),
E. Fortin [ID 36](#), A.W. Fortman [ID 61](#), M.G. Foti [ID 17a](#), L. Fountas [ID 9,k](#), D. Fournier [ID 66](#), H. Fox [ID 91](#),
P. Francavilla [ID 74a,74b](#), S. Francescato [ID 61](#), S. Franchellucci [ID 56](#), M. Franchini [ID 23b,23a](#), S. Franchino [ID 63a](#),
D. Francis [ID 36](#), L. Franco [ID 113](#), L. Franconi [ID 48](#), M. Franklin [ID 61](#), G. Frattari [ID 26](#), A.C. Freegard [ID 94](#),
W.S. Freund [ID 82b](#), Y.Y. Frid [ID 151](#), N. Fritzsche [ID 50](#), A. Froch [ID 54](#), D. Froidevaux [ID 36](#), J.A. Frost [ID 126](#),
Y. Fu [ID 62a](#), M. Fujimoto [ID 118](#), E. Fullana Torregrosa [ID 163,*](#), E. Furtado De Simas Filho [ID 82b](#),
J. Fuster [ID 163](#), A. Gabrielli [ID 23b,23a](#), A. Gabrielli [ID 155](#), P. Gadow [ID 48](#), G. Gagliardi [ID 57b,57a](#),
L.G. Gagnon [ID 17a](#), E.J. Gallas [ID 126](#), B.J. Gallop [ID 134](#), K.K. Gan [ID 119](#), S. Ganguly [ID 153](#), J. Gao [ID 62a](#),
Y. Gao [ID 52](#), F.M. Garay Walls [ID 137a,137b](#), B. Garcia [ID 29](#), C. García [ID 163](#), A. Garcia Alonso [ID 114](#),
J.E. García Navarro [ID 163](#), M. Garcia-Sciveres [ID 17a](#), R.W. Gardner [ID 39](#), D. Garg [ID 80](#), R.B. Garg [ID 143,q](#),
C.A. Garner [ID 155](#), S.J. Gasiorowski [ID 138](#), P. Gaspar [ID 82b](#), G. Gaudio [ID 73a](#), V. Gautam [ID 13](#), P. Gauzzi [ID 75a,75b](#),
I.L. Gavrilenko [ID 37](#), A. Gavriyuk [ID 37](#), C. Gay [ID 164](#), G. Gaycken [ID 48](#), E.N. Gazis [ID 10](#),
A.A. Geanta [ID 27b,27e](#), C.M. Gee [ID 136](#), C. Gemme [ID 57b](#), M.H. Genest [ID 60](#), S. Gentile [ID 75a,75b](#),
S. George [ID 95](#), W.F. George [ID 20](#), T. Gerialis [ID 46](#), L.O. Gerlach [ID 55](#), P. Gessinger-Befurt [ID 36](#),
M.E. Geyik [ID 171](#), M. Ghneimat [ID 141](#), K. Ghorbanian [ID 94](#), A. Ghosal [ID 141](#), A. Ghosh [ID 160](#), A. Ghosh [ID 7](#),
B. Giacobbe [ID 23b](#), S. Giagu [ID 75a,75b](#), P. Giannetti [ID 74a](#), A. Giannini [ID 62a](#), S.M. Gibson [ID 95](#),
M. Gignac [ID 136](#), D.T. Gil [ID 85b](#), A.K. Gilbert [ID 85a](#), B.J. Gilbert [ID 41](#), D. Gillberg [ID 34](#), G. Gilles [ID 114](#),
N.E.K. Gillwald [ID 48](#), L. Ginabat [ID 127](#), D.M. Gingrich [ID 2,ai](#), M.P. Giordani [ID 69a,69c](#), P.F. Giraud [ID 135](#),
G. Giugliarelli [ID 69a,69c](#), D. Giugni [ID 71a](#), F. Giuli [ID 36](#), I. Gkialas [ID 9,k](#), L.K. Gladilin [ID 37](#), C. Glasman [ID 99](#),
G.R. Gledhill [ID 123](#), M. Glisic [ID 123](#), I. Gnesi [ID 43b,g](#), Y. Go [ID 29,ak](#), M. Goblirsch-Kolb [ID 36](#), B. Gocke [ID 49](#),
D. Godin [ID 108](#), B. Gokturk [ID 21a](#), S. Goldfarb [ID 105](#), T. Golling [ID 56](#), M.G.D. Gololo [ID 33g](#), D. Golubkov [ID 37](#),
J.P. Gombas [ID 107](#), A. Gomes [ID 130a,130b](#), G. Gomes Da Silva [ID 141](#), A.J. Gomez Delegido [ID 163](#),
R. Gonçalves [ID 130a,130c](#), G. Gonella [ID 123](#), L. Gonella [ID 20](#), A. Gongadze [ID 38](#), F. Gonnella [ID 20](#),
J.L. Gonski [ID 41](#), R.Y. González Andana [ID 52](#), S. González de la Hoz [ID 163](#), S. Gonzalez Fernandez [ID 13](#),
R. Gonzalez Lopez [ID 92](#), C. Gonzalez Renteria [ID 17a](#), R. Gonzalez Suarez [ID 161](#), S. Gonzalez-Sevilla [ID 56](#),
G.R. Gonzalvo Rodriguez [ID 163](#), L. Goossens [ID 36](#), P.A. Gorbounov [ID 37](#), B. Gorini [ID 36](#), E. Gorini [ID 70a,70b](#),
A. Gorišek [ID 93](#), T.C. Gosart [ID 128](#), A.T. Goshaw [ID 51](#), M.I. Gostkin [ID 38](#), S. Goswami [ID 121](#),
C.A. Gottardo [ID 36](#), M. Goughri [ID 35b](#), V. Goumarre [ID 48](#), A.G. Goussiou [ID 138](#), N. Govender [ID 33c](#),
I. Grabowska-Bold [ID 85a](#), K. Graham [ID 34](#), E. Gramstad [ID 125](#), S. Grancagnolo [ID 70a,70b](#), M. Grandi [ID 146](#),
V. Gratchev [ID 37,*](#), P.M. Gravila [ID 27f](#), F.G. Gravili [ID 70a,70b](#), H.M. Gray [ID 17a](#), M. Greco [ID 70a,70b](#),
C. Grefe [ID 24](#), I.M. Gregor [ID 48](#), P. Grenier [ID 143](#), C. Grieco [ID 13](#), A.A. Grillo [ID 136](#), K. Grimm [ID 31,n](#),
S. Grinstein [ID 13,v](#), J.-F. Grivaz [ID 66](#), E. Gross [ID 169](#), J. Grosse-Knetter [ID 55](#), C. Grud [ID 106](#), J.C. Grundy [ID 126](#),
L. Guan [ID 106](#), W. Guan [ID 29](#), C. Gubbels [ID 164](#), J.G.R. Guerrero Rojas [ID 163](#), G. Guerrieri [ID 69a,69b](#),
F. Guescini [ID 110](#), R. Gugel [ID 100](#), J.A.M. Guhit [ID 106](#), A. Guida [ID 48](#), T. Guillemain [ID 4](#),
E. Guilloton [ID 167,134](#), S. Guindon [ID 36](#), F. Guo [ID 14a,14e](#), J. Guo [ID 62c](#), L. Guo [ID 66](#), Y. Guo [ID 106](#),
R. Gupta [ID 48](#), S. Gurbuz [ID 24](#), S.S. Gurdasani [ID 54](#), G. Gustavino [ID 36](#), M. Guth [ID 56](#), P. Gutierrez [ID 120](#),
L.F. Gutierrez Zagazeta [ID 128](#), C. Gutschow [ID 96](#), C. Gwenlan [ID 126](#), C.B. Gwilliam [ID 92](#), E.S. Haaland [ID 125](#),
A. Haas [ID 117](#), M. Habedank [ID 48](#), C. Haber [ID 17a](#), H.K. Hadavand [ID 8](#), A. Hadeef [ID 100](#), S. Hadzic [ID 110](#),

E.H. Haines ¹⁹⁶, M. Haleem ¹⁶⁶, J. Haley ¹²¹, J.J. Hall ¹³⁹, G.D. Hallewell ¹⁰², L. Halser ¹⁹, K. Hamano ¹⁶⁵, H. Hamdaoui ^{35e}, M. Hamer ²⁴, G.N. Hamity ⁵², E.J. Hampshire ⁹⁵, J. Han ^{62b}, K. Han ^{62a}, L. Han ^{14c}, L. Han ^{62a}, S. Han ^{17a}, Y.F. Han ¹⁵⁵, K. Hanagaki ⁸³, M. Hance ¹³⁶, D.A. Hangal ^{41,ae}, H. Hanif ¹⁴², M.D. Hank ¹²⁸, R. Hankache ¹⁰¹, J.B. Hansen ⁴², J.D. Hansen ⁴², P.H. Hansen ⁴², K. Hara ¹⁵⁷, D. Harada ⁵⁶, T. Harenberg ¹⁷¹, S. Harkusha ³⁷, Y.T. Harris ¹²⁶, N.M. Harrison ¹¹⁹, P.F. Harrison ¹⁶⁷, N.M. Hartman ¹⁴³, N.M. Hartmann ¹⁰⁹, Y. Hasegawa ¹⁴⁰, A. Hasib ⁵², S. Haug ¹⁹, R. Hauser ¹⁰⁷, M. Havranek ¹³², C.M. Hawkes ²⁰, R.J. Hawkings ³⁶, S. Hayashida ¹¹¹, D. Hayden ¹⁰⁷, C. Hayes ¹⁰⁶, R.L. Hayes ¹¹⁴, C.P. Hays ¹²⁶, J.M. Hays ⁹⁴, H.S. Hayward ⁹², F. He ^{62a}, Y. He ¹⁵⁴, Y. He ¹²⁷, N.B. Heatley ⁹⁴, V. Hedberg ⁹⁸, A.L. Heggelund ¹²⁵, N.D. Hehir ⁹⁴, C. Heidegger ⁵⁴, K.K. Heidegger ⁵⁴, W.D. Heidorn ⁸¹, J. Heilman ³⁴, S. Heim ⁴⁸, T. Heim ^{17a}, J.G. Heinlein ¹²⁸, J.J. Heinrich ¹²³, L. Heinrich ^{110,ag}, J. Hejbal ¹³¹, L. Helary ⁴⁸, A. Held ¹⁷⁰, S. Hellesund ¹⁶, C.M. Helling ¹⁶⁴, S. Hellman ^{47a,47b}, C. Helsens ³⁶, R.C.W. Henderson ⁹¹, L. Henkelmann ³², A.M. Henriques Correia ³⁶, H. Herde ⁹⁸, Y. Hernández Jiménez ¹⁴⁵, L.M. Herrmann ²⁴, T. Herrmann ⁵⁰, G. Herten ⁵⁴, R. Hertenberger ¹⁰⁹, L. Hervas ³⁶, N.P. Hessey ^{156a}, H. Hibi ⁸⁴, S.J. Hillier ²⁰, F. Hinterkeuser ²⁴, M. Hirose ¹²⁴, S. Hirose ¹⁵⁷, D. Hirschbuehl ¹⁷¹, T.G. Hitchings ¹⁰¹, B. Hiti ⁹³, J. Hobbs ¹⁴⁵, R. Hobincu ^{27e}, N. Hod ¹⁶⁹, M.C. Hodgkinson ¹³⁹, B.H. Hodgkinson ³², A. Hoecker ³⁶, J. Hofer ⁴⁸, T. Holm ²⁴, M. Holzbock ¹¹⁰, L.B.A.H. Hommels ³², B.P. Honan ¹⁰¹, J. Hong ^{62c}, T.M. Hong ¹²⁹, J.C. Honig ⁵⁴, B.H. Hooberman ¹⁶², W.H. Hopkins ⁶, Y. Horii ¹¹¹, S. Hou ¹⁴⁸, A.S. Howard ⁹³, J. Howarth ⁵⁹, J. Hoya ⁶, M. Hrabovsky ¹²², A. Hrynevich ⁴⁸, T. Hryn'ova ⁴, P.J. Hsu ⁶⁵, S.-C. Hsu ¹³⁸, Q. Hu ⁴¹, Y.F. Hu ^{14a,14e}, D.P. Huang ⁹⁶, S. Huang ^{64b}, X. Huang ^{14c}, Y. Huang ^{62a}, Y. Huang ^{14a}, Z. Huang ¹⁰¹, Z. Hubacek ¹³², M. Huebner ²⁴, F. Huegging ²⁴, T.B. Huffman ¹²⁶, M. Huhtinen ³⁶, S.K. Huiberts ¹⁶, R. Hulsken ¹⁰⁴, N. Huseynov ^{12,a}, J. Huston ¹⁰⁷, J. Huth ⁶¹, R. Hyneman ¹⁴³, G. Iacobucci ⁵⁶, G. Iakovidis ²⁹, I. Ibragimov ¹⁴¹, L. Iconomidou-Fayard ⁶⁶, P. Iengo ^{72a,72b}, R. Iguchi ¹⁵³, T. Iizawa ⁵⁶, Y. Ikegami ⁸³, A. Ilg ¹⁹, N. Ilic ¹⁵⁵, H. Imam ^{35a}, T. Ingebretsen Carlson ^{47a,47b}, G. Introzzi ^{73a,73b}, M. Iodice ^{77a}, V. Ippolito ^{75a,75b}, M. Ishino ¹⁵³, W. Islam ¹⁷⁰, C. Issever ^{18,48}, S. Istin ^{21a,am}, H. Ito ¹⁶⁸, J.M. Iturbe Ponce ^{64a}, R. Iuppa ^{78a,78b}, A. Ivina ¹⁶⁹, J.M. Izen ⁴⁵, V. Izzo ^{72a}, P. Jacka ^{131,132}, P. Jackson ¹, R.M. Jacobs ⁴⁸, B.P. Jaeger ¹⁴², C.S. Jagfeld ¹⁰⁹, P. Jain ⁵⁴, G. Jäkel ¹⁷¹, K. Jakobs ⁵⁴, T. Jakoubek ¹⁶⁹, J. Jamieson ⁵⁹, K.W. Janas ^{85a}, A.E. Jaspan ⁹², M. Javurkova ¹⁰³, F. Jeanneau ¹³⁵, L. Jeanty ¹²³, J. Jejelava ^{149a,ac}, P. Jenni ^{54,h}, C.E. Jessiman ³⁴, S. Jézéquel ⁴, C. Jia ^{62b}, J. Jia ¹⁴⁵, X. Jia ⁶¹, X. Jia ^{14a,14e}, Z. Jia ^{14c}, Y. Jiang ^{62a}, S. Jiggins ⁴⁸, J. Jimenez Pena ¹¹⁰, S. Jin ^{14c}, A. Jinaru ^{27b}, O. Jinnouchi ¹⁵⁴, P. Johansson ¹³⁹, K.A. Johns ⁷, J.W. Johnson ¹³⁶, D.M. Jones ³², E. Jones ⁴⁸, P. Jones ³², R.W.L. Jones ⁹¹, T.J. Jones ⁹², R. Joshi ¹¹⁹, J. Jovicevic ¹⁵, X. Ju ^{17a}, J.J. Junggeburth ³⁶, T. Junkermann ^{63a}, A. Juste Rozas ^{13,v}, S. Kabana ^{137e}, A. Kaczmariska ⁸⁶, M. Kado ¹¹⁰, H. Kagan ¹¹⁹, M. Kagan ¹⁴³, A. Kahn ⁴¹, A. Kahn ¹²⁸, C. Kahra ¹⁰⁰, T. Kaji ¹⁶⁸, E. Kajomovitz ¹⁵⁰, N. Kakati ¹⁶⁹, C.W. Kalderon ²⁹, A. Kamenshchikov ¹⁵⁵, S. Kanayama ¹⁵⁴, N.J. Kang ¹³⁶, D. Kar ^{33g}, K. Karava ¹²⁶, M.J. Kareem ^{156b}, E. Karentzos ⁵⁴, I. Karkanias ^{152,f}, S.N. Karpov ³⁸, Z.M. Karpova ³⁸, V. Kartvelishvili ⁹¹, A.N. Karyukhin ³⁷, E. Kasimi ^{152,f}, J. Katzy ⁴⁸, S. Kaur ³⁴, K. Kawade ¹⁴⁰, T. Kawamoto ¹³⁵, G. Kawamura ⁵⁵, E.F. Kay ¹⁶⁵, F.I. Kaya ¹⁵⁸, S. Kazakos ¹³, V.F. Kazanin ³⁷, Y. Ke ¹⁴⁵, J.M. Keaveney ^{33a}, R. Keeler ¹⁶⁵, G.V. Kehris ⁶¹, J.S. Keller ³⁴, A.S. Kelly ⁹⁶, D. Kelsey ¹⁴⁶, J.J. Kempster ¹⁴⁶, K.E. Kennedy ⁴¹, P.D. Kennedy ¹⁰⁰, O. Kepka ¹³¹, B.P. Kerridge ¹⁶⁷, S. Kersten ¹⁷¹, B.P. Kerševan ⁹³, S. Keshri ⁶⁶, L. Keszezhova ^{28a}, S. Ketabchi Haghghat ¹⁵⁵, M. Khandoga ¹²⁷, A. Khanov ¹²¹, A.G. Kharlamov ³⁷, T. Kharlamova ³⁷, E.E. Khoda ¹³⁸, T.J. Khoo ¹⁸, G. Khorauli ¹⁶⁶, J. Khubua ^{149b}, Y.A.R. Khwaira ⁶⁶, M. Kiehn ³⁶, A. Kilgallon ¹²³, D.W. Kim ^{47a,47b},

Y.K. Kim ³⁹, N. Kimura ⁹⁶, A. Kirchhoff ⁵⁵, C. Kirfel ²⁴, J. Kirk ¹³⁴, A.E. Kiryunin ¹¹⁰,
 T. Kishimoto ¹⁵³, D.P. Kisliuk ¹⁵⁵, C. Kitsaki ¹⁰, O. Kivernyk ²⁴, M. Klassen ^{63a}, C. Klein ³⁴,
 L. Klein ¹⁶⁶, M.H. Klein ¹⁰⁶, M. Klein ⁹², S.B. Klein ⁵⁶, U. Klein ⁹², P. Klimek ³⁶,
 A. Klimentov ²⁹, T. Klioutchnikova ³⁶, P. Kluit ¹¹⁴, S. Kluth ¹¹⁰, E. Kneringer ⁷⁹,
 T.M. Knight ¹⁵⁵, A. Knue ⁵⁴, R. Kobayashi ⁸⁷, M. Kocian ¹⁴³, P. Kodyš ¹³³, D.M. Koeck ¹²³,
 P.T. Koenig ²⁴, T. Koffas ³⁴, M. Kolb ¹³⁵, I. Koletsou ⁴, T. Komarek ¹²², K. Köneke ⁵⁴,
 A.X.Y. Kong ¹, T. Kono ¹¹⁸, N. Konstantinidis ⁹⁶, B. Konya ⁹⁸, R. Kopeliansky ⁶⁸,
 S. Koperny ^{85a}, K. Korcyl ⁸⁶, K. Kordas ^{152,f}, G. Koren ¹⁵¹, A. Korn ⁹⁶, S. Korn ⁵⁵,
 I. Korolkov ¹³, N. Korotkova ³⁷, B. Kortman ¹¹⁴, O. Kortner ¹¹⁰, S. Kortner ¹¹⁰,
 W.H. Kostecka ¹¹⁵, V.V. Kostyukhin ¹⁴¹, A. Kotsokechagia ¹³⁵, A. Kotwal ⁵¹, A. Koulouris ³⁶,
 A. Kourkoumeli-Charalampidi ^{73a,73b}, C. Kourkoumelis ⁹, E. Kourlitis ⁶, O. Kovanda ¹⁴⁶,
 R. Kowalewski ¹⁶⁵, W. Kozanecki ¹³⁵, A.S. Kozhin ³⁷, V.A. Kramarenko ³⁷, G. Kramberger ⁹³,
 P. Kramer ¹⁰⁰, M.W. Krasny ¹²⁷, A. Krasznahorkay ³⁶, J.A. Kremer ¹⁰⁰, T. Kresse ⁵⁰,
 J. Kretschmar ⁹², K. Kreul ¹⁸, P. Krieger ¹⁵⁵, S. Krishnamurthy ¹⁰³, M. Krivos ¹³³,
 K. Krizka ²⁰, K. Kroeninger ⁴⁹, H. Kroha ¹¹⁰, J. Kroll ¹³¹, J. Kroll ¹²⁸, K.S. Krowpman ¹⁰⁷,
 U. Kruchonak ³⁸, H. Krüger ²⁴, N. Krumnack ⁸¹, M.C. Kruse ⁵¹, J.A. Krzysiak ⁸⁶,
 O. Kuchinskaia ³⁷, S. Kuday ^{3a}, S. Kuehn ³⁶, R. Kuesters ⁵⁴, T. Kuhl ⁴⁸, V. Kukhtin ³⁸,
 Y. Kulchitsky ^{37,a}, S. Kuleshov ^{137d,137b}, M. Kumar ^{33g}, N. Kumari ¹⁰², A. Kupco ¹³¹,
 T. Kupfer ⁴⁹, A. Kupich ³⁷, O. Kuprash ⁵⁴, H. Kurashige ⁸⁴, L.L. Kurchaninov ^{156a}, O. Kurdysh ⁶⁶,
 Y.A. Kurochkin ³⁷, A. Kurova ³⁷, M. Kuze ¹⁵⁴, A.K. Kvam ¹⁰³, J. Kvita ¹²², T. Kwan ¹⁰⁴,
 N.G. Kyriacou ¹⁰⁶, L.A.O. Laatu ¹⁰², C. Lacasta ¹⁶³, F. Lacava ^{75a,75b}, H. Lacker ¹⁸,
 D. Lacour ¹²⁷, N.N. Lad ⁹⁶, E. Ladygin ³⁸, B. Laforge ¹²⁷, T. Lagouri ^{137e}, S. Lai ⁵⁵,
 I.K. Lakomic ^{85a}, N. Lalloue ⁶⁰, J.E. Lambert ¹²⁰, S. Lammers ⁶⁸, W. Lampl ⁷,
 C. Lampoudis ^{152,f}, A.N. Lancaster ¹¹⁵, E. Lançon ²⁹, U. Landgraf ⁵⁴, M.P.J. Landon ⁹⁴,
 V.S. Lang ⁵⁴, R.J. Langenberg ¹⁰³, A.J. Lankford ¹⁶⁰, F. Lanni ³⁶, K. Lantzsch ²⁴, A. Lanza ^{73a},
 A. Lapertosa ^{57b,57a}, J.F. Laporte ¹³⁵, T. Lari ^{71a}, F. Lasagni Manghi ^{23b}, M. Lassnig ³⁶,
 V. Latonova ¹³¹, A. Laudrain ¹⁰⁰, A. Laurier ¹⁵⁰, S.D. Lawlor ⁹⁵, Z. Lawrence ¹⁰¹,
 M. Lazzaroni ^{71a,71b}, B. Le ¹⁰¹, E.M. Le Boulicaut ⁵¹, B. Leban ⁹³, A. Lebedev ⁸¹, M. LeBlanc ³⁶,
 F. Ledroit-Guillon ⁶⁰, A.C.A. Lee ⁹⁶, G.R. Lee ¹⁶, S.C. Lee ¹⁴⁸, S. Lee ^{47a,47b}, T.F. Lee ⁹²,
 L.L. Leeuw ^{33c}, H.P. Lefebvre ⁹⁵, M. Lefebvre ¹⁶⁵, C. Leggett ^{17a}, K. Lehmann ¹⁴²,
 G. Lehmann Miotto ³⁶, M. Leigh ⁵⁶, W.A. Leight ¹⁰³, A. Leisos ^{152,u}, M.A.L. Leite ^{82c},
 C.E. Leitgeb ⁴⁸, R. Leitner ¹³³, K.J.C. Leney ⁴⁴, T. Lenz ²⁴, S. Leone ^{74a}, C. Leonidopoulos ⁵²,
 A. Leopold ¹⁴⁴, C. Leroy ¹⁰⁸, R. Les ¹⁰⁷, C.G. Lester ³², M. Levchenko ³⁷, J. Levêque ⁴,
 D. Levin ¹⁰⁶, L.J. Levinson ¹⁶⁹, M.P. Lewicki ⁸⁶, D.J. Lewis ⁴, A. Li ⁵, B. Li ^{62b}, C. Li ^{62a},
 C-Q. Li ^{62c}, H. Li ^{62a}, H. Li ^{62b}, H. Li ^{14c}, H. Li ^{62b}, J. Li ^{62c}, K. Li ¹³⁸, L. Li ^{62c},
 M. Li ^{14a,14e}, Q.Y. Li ^{62a}, S. Li ^{14a,14e}, S. Li ^{62d,62c,e}, T. Li ^{62b}, X. Li ¹⁰⁴, Z. Li ^{62b}, Z. Li ¹²⁶,
 Z. Li ¹⁰⁴, Z. Li ⁹², Z. Li ^{14a,14e}, Z. Liang ^{14a}, M. Liberatore ⁴⁸, B. Liberti ^{76a}, K. Lie ^{64c},
 J. Lieber Marin ^{82b}, H. Lien ⁶⁸, K. Lin ¹⁰⁷, R.A. Linck ⁶⁸, R.E. Lindley ⁷, J.H. Lindon ²,
 A. Linss ⁴⁸, E. Lipeles ¹²⁸, A. Lipniacka ¹⁶, A. Lister ¹⁶⁴, J.D. Little ⁴, B. Liu ^{14a},
 B.X. Liu ¹⁴², D. Liu ^{62d,62c}, J.B. Liu ^{62a}, J.K.K. Liu ³², K. Liu ^{62d,62c}, M. Liu ^{62a},
 M.Y. Liu ^{62a}, P. Liu ^{14a}, Q. Liu ^{62d,138,62c}, X. Liu ^{62a}, Y. Liu ^{14d,14e}, Y.L. Liu ¹⁰⁶, Y.W. Liu ^{62a},
 J. Llorente Merino ¹⁴², S.L. Lloyd ⁹⁴, E.M. Lobodzinska ⁴⁸, P. Loch ⁷, S. Loffredo ^{76a,76b},
 T. Lohse ¹⁸, K. Lohwasser ¹³⁹, E. Loiacono ⁴⁸, M. Lokajicek ^{131,*}, J.D. Lomas ²⁰,
 J.D. Long ¹⁶², I. Longarini ¹⁶⁰, L. Longo ^{70a,70b}, R. Longo ¹⁶², I. Lopez Paz ⁶⁷,
 A. Lopez Solis ⁴⁸, J. Lorenz ¹⁰⁹, N. Lorenzo Martinez ⁴, A.M. Lory ¹⁰⁹, G. Löschcke Centeno ¹⁴⁶,
 X. Lou ^{47a,47b}, X. Lou ^{14a,14e}, A. Lounis ⁶⁶, J. Love ⁶, P.A. Love ⁹¹, G. Lu ^{14a,14e}, M. Lu ⁸⁰,
 S. Lu ¹²⁸, Y.J. Lu ⁶⁵, H.J. Lubatti ¹³⁸, C. Luci ^{75a,75b}, F.L. Lucio Alves ^{14c}, A. Lucotte ⁶⁰,

F. Luehring ⁶⁸, I. Luise ¹⁴⁵, O. Lukianchuk ⁶⁶, O. Lundberg ¹⁴⁴, B. Lund-Jensen ¹⁴⁴, N.A. Luongo ¹²³, M.S. Lutz ¹⁵¹, D. Lynn ²⁹, H. Lyons ⁹², R. Lysak ¹³¹, E. Lytken ⁹⁸, V. Lyubushkin ³⁸, T. Lyubushkina ³⁸, M.M. Lyukova ¹⁴⁵, H. Ma ²⁹, L.L. Ma ^{62b}, Y. Ma ⁹⁶, D.M. Mac Donell ¹⁶⁵, G. Maccarrone ⁵³, J.C. MacDonald ¹³⁹, R. Madar ⁴⁰, W.F. Mader ⁵⁰, J. Maeda ⁸⁴, T. Maeno ²⁹, M. Maerker ⁵⁰, H. Maguire ¹³⁹, A. Maio ^{130a,130b,130d}, K. Maj ^{85a}, O. Majersky ⁴⁸, S. Majewski ¹²³, N. Makovec ⁶⁶, V. Maksimovic ¹⁵, B. Malaescu ¹²⁷, Pa. Malecki ⁸⁶, V.P. Maleev ³⁷, F. Malek ⁶⁰, D. Malito ^{43b,43a}, U. Mallik ⁸⁰, C. Malone ³², S. Maltezos ¹⁰, S. Malyukov ³⁸, J. Mamuzic ¹³, G. Mancini ⁵³, G. Manco ^{73a,73b}, J.P. Mandalia ⁹⁴, I. Mandić ⁹³, L. Manhaes de Andrade Filho ^{82a}, I.M. Maniatis ¹⁶⁹, J. Manjarres Ramos ^{102,ad}, D.C. Mankad ¹⁶⁹, A. Mann ¹⁰⁹, B. Mansoulie ¹³⁵, S. Manzoni ³⁶, A. Marantis ^{152,u}, G. Marchiori ⁵, M. Marcisovsky ¹³¹, C. Marcon ^{71a}, M. Marinescu ²⁰, M. Marjanovic ¹²⁰, E.J. Marshall ⁹¹, Z. Marshall ^{17a}, S. Marti-Garcia ¹⁶³, T.A. Martin ¹⁶⁷, V.J. Martin ⁵², B. Martin dit Latour ¹⁶, L. Martinelli ^{75a,75b}, M. Martinez ^{13,v}, P. Martinez Agullo ¹⁶³, V.I. Martinez Outschoorn ¹⁰³, P. Martinez Suarez ¹³, S. Martin-Haugh ¹³⁴, V.S. Martoiu ^{27b}, A.C. Martyniuk ⁹⁶, A. Marzin ³⁶, S.R. Maschek ¹¹⁰, D. Mascione ^{78a,78b}, L. Masetti ¹⁰⁰, T. Mashimo ¹⁵³, J. Masik ¹⁰¹, A.L. Maslennikov ³⁷, L. Massa ^{23b}, P. Massarotti ^{72a,72b}, P. Mastrandrea ^{74a,74b}, A. Mastroberardino ^{43b,43a}, T. Masubuchi ¹⁵³, T. Mathisen ¹⁶¹, N. Matsuzawa ¹⁵³, J. Maurer ^{27b}, B. Maček ⁹³, D.A. Maximov ³⁷, R. Mazini ¹⁴⁸, I. Maznas ^{152,f}, M. Mazza ¹⁰⁷, S.M. Mazza ¹³⁶, C. Mc Ginn ²⁹, J.P. Mc Gowan ¹⁰⁴, S.P. Mc Kee ¹⁰⁶, E.F. McDonald ¹⁰⁵, A.E. McDougall ¹¹⁴, J.A. Mcfayden ¹⁴⁶, R.P. McGovern ¹²⁸, G. Mchedlidze ^{149b}, R.P. Mckenzie ^{33g}, T.C. Mclachlan ⁴⁸, D.J. Mclaughlin ⁹⁶, K.D. McLean ¹⁶⁵, S.J. McMahon ¹³⁴, P.C. McNamara ¹⁰⁵, C.M. Mcpartland ⁹², R.A. McPherson ^{165,z}, T. Megy ⁴⁰, S. Mehlhase ¹⁰⁹, A. Mehta ⁹², D. Melini ¹⁵⁰, B.R. Mellado Garcia ^{33g}, A.H. Melo ⁵⁵, F. Meloni ⁴⁸, A.M. Mendes Jacques Da Costa ¹⁰¹, H.Y. Meng ¹⁵⁵, L. Meng ⁹¹, S. Menke ¹¹⁰, M. Mentink ³⁶, E. Meoni ^{43b,43a}, C. Merlassino ¹²⁶, L. Merola ^{72a,72b}, C. Meroni ^{71a,71b}, G. Merz ¹⁰⁶, O. Meshkov ³⁷, J. Metcalfe ⁶, A.S. Mete ⁶, C. Meyer ⁶⁸, J-P. Meyer ¹³⁵, R.P. Middleton ¹³⁴, L. Mijović ⁵², G. Mikenberg ¹⁶⁹, M. Mikestikova ¹³¹, M. Mikuž ⁹³, H. Mildner ¹³⁹, A. Milic ³⁶, C.D. Milke ⁴⁴, D.W. Miller ³⁹, L.S. Miller ³⁴, A. Milov ¹⁶⁹, D.A. Milstead ^{47a,47b}, T. Min ^{14c}, A.A. Minaenko ³⁷, I.A. Minashvili ^{149b}, L. Mince ⁵⁹, A.I. Mincer ¹¹⁷, B. Mindur ^{85a}, M. Mineev ³⁸, Y. Mino ⁸⁷, L.M. Mir ¹³, M. Miralles Lopez ¹⁶³, M. Mironova ^{17a}, M.C. Missio ¹¹³, T. Mitani ¹⁶⁸, A. Mitra ¹⁶⁷, V.A. Mitsou ¹⁶³, O. Miu ¹⁵⁵, P.S. Miyagawa ⁹⁴, Y. Miyazaki ⁸⁹, A. Mizukami ⁸³, T. Mkrtchyan ^{63a}, M. Mlinarevic ⁹⁶, T. Mlinarevic ⁹⁶, M. Mlynarikova ³⁶, S. Mobius ⁵⁵, K. Mochizuki ¹⁰⁸, P. Moder ⁴⁸, P. Mogg ¹⁰⁹, A.F. Mohammed ^{14a,14e}, S. Mohapatra ⁴¹, G. Mokgatitwane ^{33g}, B. Mondal ¹⁴¹, S. Mondal ¹³², K. Mönig ⁴⁸, E. Monnier ¹⁰², L. Monsonis Romero ¹⁶³, J. Montejo Berlingen ⁸³, M. Montella ¹¹⁹, F. Monticelli ⁹⁰, N. Morange ⁶⁶, A.L. Moreira De Carvalho ^{130a}, M. Moreno Llácer ¹⁶³, C. Moreno Martinez ⁵⁶, P. Morettini ^{57b}, S. Morgenstern ³⁶, M. Morii ⁶¹, M. Morinaga ¹⁵³, A.K. Morley ³⁶, F. Morodei ^{75a,75b}, L. Morvaj ³⁶, P. Moschovakos ³⁶, B. Moser ³⁶, M. Mosidze ^{149b}, T. Moskalets ⁵⁴, P. Moskvitina ¹¹³, J. Moss ^{31,o}, E.J.W. Moyse ¹⁰³, O. Mtintsilana ^{33g}, S. Muanza ¹⁰², J. Mueller ¹²⁹, D. Muenstermann ⁹¹, R. Müller ¹⁹, G.A. Mullier ¹⁶¹, J.J. Mullin ¹²⁸, D.P. Mungo ¹⁵⁵, J.L. Munoz Martinez ¹³, D. Munoz Perez ¹⁶³, F.J. Munoz Sanchez ¹⁰¹, M. Murin ¹⁰¹, W.J. Murray ^{167,134}, A. Murrone ^{71a,71b}, J.M. Muse ¹²⁰, M. Muškinja ^{17a}, C. Mwewa ²⁹, A.G. Myagkov ^{37,a}, A.J. Myers ⁸, A.A. Myers ¹²⁹, G. Myers ⁶⁸, M. Myska ¹³², B.P. Nachman ^{17a}, O. Nackenhorst ⁴⁹, A. Nag ⁵⁰, K. Nagai ¹²⁶, K. Nagano ⁸³, J.L. Nagle ^{29,ak}, E. Nagy ¹⁰², A.M. Nairz ³⁶, Y. Nakahama ⁸³, K. Nakamura ⁸³, H. Nanjo ¹²⁴, R. Narayan ⁴⁴, E.A. Narayanan ¹¹², I. Naryshkin ³⁷, M. Naseri ³⁴, C. Nass ²⁴, G. Navarro ^{22a}, J. Navarro-Gonzalez ¹⁶³, R. Nayak ¹⁵¹, A. Nayaz ¹⁸, P.Y. Nechaeva ³⁷, F. Nechansky ⁴⁸,

L. Nedic ¹²⁶, T.J. Neep ²⁰, A. Negri ^{73a,73b}, M. Negrini ^{23b}, C. Nellist ¹¹⁴, C. Nelson ¹⁰⁴,
 K. Nelson ¹⁰⁶, S. Nemecek ¹³¹, M. Nessi ^{36,i}, M.S. Neubauer ¹⁶², F. Neuhaus ¹⁰⁰,
 J. Neundorf ⁴⁸, R. Newhouse ¹⁶⁴, P.R. Newman ²⁰, C.W. Ng ¹²⁹, Y.W.Y. Ng ⁴⁸, B. Ngair ^{35e},
 H.D.N. Nguyen ¹⁰⁸, R.B. Nickerson ¹²⁶, R. Nicolaidou ¹³⁵, J. Nielsen ¹³⁶, M. Niemeyer ⁵⁵,
 N. Nikiforou ³⁶, V. Nikolaenko ^{37,a}, I. Nikolic-Audit ¹²⁷, K. Nikolopoulos ²⁰, P. Nilsson ²⁹,
 I. Ninca ⁴⁸, H.R. Nindhito ⁵⁶, G. Ninio ¹⁵¹, A. Nisati ^{75a}, N. Nishu ², R. Nisius ¹¹⁰,
 J-E. Nitschke ⁵⁰, E.K. Nkadimeng ^{33g}, S.J. Noacco Rosende ⁹⁰, T. Nobe ¹⁵³, D.L. Noel ³²,
 T. Nommensen ¹⁴⁷, M.A. Nomura ²⁹, M.B. Norfolk ¹³⁹, R.R.B. Norisam ⁹⁶, B.J. Norman ³⁴,
 J. Novak ⁹³, T. Novak ⁴⁸, L. Novotny ¹³², R. Novotny ¹¹², L. Nozka ¹²², K. Ntekas ¹⁶⁰,
 N.M.J. Nunes De Moura Junior ^{82b}, E. Nurse ⁹⁶, J. Ocariz ¹²⁷, A. Ochi ⁸⁴, I. Ochoa ^{130a},
 S. Oerdeek ¹⁶¹, J.T. Offermann ³⁹, A. Ogrodnik ^{85a}, A. Oh ¹⁰¹, C.C. Ohm ¹⁴⁴, H. Oide ⁸³,
 R. Oishi ¹⁵³, M.L. Ojeda ⁴⁸, Y. Okazaki ⁸⁷, M.W. O'Keefe ⁹², Y. Okumura ¹⁵³,
 L.F. Oleiro Seabra ^{130a}, S.A. Olivares Pino ^{137d}, D. Oliveira Damazio ²⁹, D. Oliveira Goncalves ^{82a},
 J.L. Oliver ¹⁶⁰, M.J.R. Olsson ¹⁶⁰, A. Olszewski ⁸⁶, Ö.O. Öncel ⁵⁴, D.C. O'Neil ¹⁴²,
 A.P. O'Neill ¹⁹, A. Onofre ^{130a,130e}, P.U.E. Onyisi ¹¹, M.J. Oreglia ³⁹, G.E. Orellana ⁹⁰,
 D. Orestano ^{77a,77b}, N. Orlando ¹³, R.S. Orr ¹⁵⁵, V. O'Shea ⁵⁹, R. Ospanov ^{62a},
 G. Otero y Garzon ³⁰, H. Otono ⁸⁹, P.S. Ott ^{63a}, G.J. Ottino ^{17a}, M. Ouchrif ^{35d}, J. Ouellette ²⁹,
 F. Ould-Saada ¹²⁵, M. Owen ⁵⁹, R.E. Owen ¹³⁴, K.Y. Oyulmaz ^{21a}, V.E. Ozcan ^{21a}, N. Ozturk ⁸,
 S. Ozturk ^{21d}, H.A. Pacey ³², A. Pacheco Pages ¹³, C. Padilla Aranda ¹³, G. Padovano ^{75a,75b},
 S. Pagan Griso ^{17a}, G. Palacino ⁶⁸, A. Palazzo ^{70a,70b}, S. Palestini ³⁶, J. Pan ¹⁷², T. Pan ^{64a},
 D.K. Panchal ¹¹, C.E. Pandini ¹¹⁴, J.G. Panduro Vazquez ⁹⁵, H. Pang ^{14b}, P. Pani ⁴⁸,
 G. Panizzo ^{69a,69c}, L. Paolozzi ⁵⁶, C. Papadatos ¹⁰⁸, S. Parajuli ⁴⁴, A. Paramonov ⁶,
 C. Paraskevopoulos ¹⁰, D. Paredes Hernandez ^{64b}, T.H. Park ¹⁵⁵, M.A. Parker ³², F. Parodi ^{57b,57a},
 E.W. Parrish ¹¹⁵, V.A. Parrish ⁵², J.A. Parsons ⁴¹, U. Parzefall ⁵⁴, B. Pascual Dias ¹⁰⁸,
 L. Pascual Dominguez ¹⁵¹, F. Pasquali ¹¹⁴, E. Pasqualucci ^{75a}, S. Passaggio ^{57b}, F. Pastore ⁹⁵,
 P. Pasuwan ^{47a,47b}, P. Patel ⁸⁶, U.M. Patel ⁵¹, J.R. Pater ¹⁰¹, T. Pauly ³⁶, J. Pearkes ¹⁴³,
 M. Pedersen ¹²⁵, R. Pedro ^{130a}, S.V. Peleganchuk ³⁷, O. Penc ³⁶, E.A. Pender ⁵², H. Peng ^{62a},
 K.E. Penski ¹⁰⁹, M. Penzin ³⁷, B.S. Peralva ^{82d}, A.P. Pereira Peixoto ⁶⁰, L. Pereira Sanchez ^{47a,47b},
 D.V. Perepelitsa ^{29,ak}, E. Perez Codina ^{156a}, M. Perganti ¹⁰, L. Perini ^{71a,71b,*}, H. Pernegger ³⁶,
 A. Perrevoort ¹¹³, O. Perrin ⁴⁰, K. Peters ⁴⁸, R.F.Y. Peters ¹⁰¹, B.A. Petersen ³⁶,
 T.C. Petersen ⁴², E. Petit ¹⁰², V. Petousis ¹³², C. Petridou ^{152,f}, A. Petrukhin ¹⁴¹, M. Pettee ^{17a},
 N.E. Pettersson ³⁶, A. Petukhov ³⁷, K. Petukhova ¹³³, A. Peyaud ¹³⁵, R. Pezoa ^{137f},
 L. Pezzotti ³⁶, G. Pezzullo ¹⁷², T.M. Pham ¹⁷⁰, T. Pham ¹⁰⁵, P.W. Phillips ¹³⁴, M.W. Phipps ¹⁶²,
 G. Piacquadio ¹⁴⁵, E. Pianori ^{17a}, F. Piazza ^{71a,71b}, R. Piegaia ³⁰, D. Pietreanu ^{27b},
 A.D. Pilkington ¹⁰¹, M. Pinamonti ^{69a,69c}, J.L. Pinfeld ², B.C. Pinheiro Pereira ^{130a},
 C. Pitman Donaldson ⁹⁶, D.A. Pizzi ³⁴, L. Pizzimento ^{76a,76b}, A. Pizzini ¹¹⁴, M.-A. Pleier ²⁹,
 V. Plesanovs ⁵⁴, V. Pleskot ¹³³, E. Plotnikova ³⁸, G. Poddar ⁴, R. Poettgen ⁹⁸, L. Poggioli ¹²⁷,
 D. Pohl ²⁴, I. Pokharel ⁵⁵, S. Polacek ¹³³, G. Polesello ^{73a}, A. Poley ^{142,156a}, R. Polifka ¹³²,
 A. Polini ^{23b}, C.S. Pollard ¹⁶⁷, Z.B. Pollock ¹¹⁹, V. Polychronakos ²⁹, E. Pompa Pacchi ^{75a,75b},
 D. Ponomarenko ¹¹³, L. Pontecorvo ³⁶, S. Popa ^{27a}, G.A. Popeneciu ^{27d},
 D.M. Portillo Quintero ^{156a}, S. Pospisil ¹³², P. Postolache ^{27c}, K. Potamianos ¹²⁶, P.A. Potepa ^{85a},
 I.N. Potrap ³⁸, C.J. Potter ³², H. Potti ¹, T. Poulsen ⁴⁸, J. Poveda ¹⁶³, M.E. Pozo Astigarraga ³⁶,
 A. Prades Ibanez ¹⁶³, M.M. Prapa ⁴⁶, J. Pretel ⁵⁴, D. Price ¹⁰¹, M. Primavera ^{70a},
 M.A. Principe Martin ⁹⁹, R. Privara ¹²², M.L. Proffitt ¹³⁸, N. Proklova ¹²⁸, K. Prokofiev ^{64c},
 G. Proto ^{76a,76b}, S. Protopopescu ²⁹, J. Proudfoot ⁶, M. Przybycien ^{85a}, W.W. Przygoda ^{85b},
 J.E. Puddefoot ¹³⁹, D. Pudzha ³⁷, D. Pyatiizbyantseva ³⁷, J. Qian ¹⁰⁶, D. Qichen ¹⁰¹, Y. Qin ¹⁰¹,
 T. Qiu ⁵², A. Quadt ⁵⁵, M. Queitsch-Maitland ¹⁰¹, G. Quetant ⁵⁶, G. Rabanal Bolanos ⁶¹,

D. Rafanoharana [ID⁵⁴](#), F. Ragusa [ID^{71a,71b}](#), J.L. Rainbolt [ID³⁹](#), J.A. Raine [ID⁵⁶](#), S. Rajagopalan [ID²⁹](#),
 E. Ramakoti [ID³⁷](#), K. Ran [ID^{48,14e}](#), N.P. Rapheeha [ID^{33g}](#), V. Raskina [ID¹²⁷](#), D.F. Rassloff [ID^{63a}](#), S. Rave [ID¹⁰⁰](#),
 B. Ravina [ID⁵⁵](#), I. Ravinovich [ID¹⁶⁹](#), M. Raymond [ID³⁶](#), A.L. Read [ID¹²⁵](#), N.P. Readioff [ID¹³⁹](#),
 D.M. Rebuzzi [ID^{73a,73b}](#), G. Redlinger [ID²⁹](#), K. Reeves [ID²⁶](#), J.A. Reidelsturz [ID¹⁷¹](#), D. Reikher [ID¹⁵¹](#),
 A. Rej [ID¹⁴¹](#), C. Rembser [ID³⁶](#), A. Renardi [ID⁴⁸](#), M. Renda [ID^{27b}](#), M.B. Rendel [ID¹¹⁰](#), F. Renner [ID⁴⁸](#),
 A.G. Rennie [ID⁵⁹](#), S. Resconi [ID^{71a}](#), M. Ressegotti [ID^{57b,57a}](#), E.D. Resseguie [ID^{17a}](#), S. Rettie [ID³⁶](#),
 J.G. Reyes Rivera [ID¹⁰⁷](#), B. Reynolds [ID¹¹⁹](#), E. Reynolds [ID^{17a}](#), M. Rezaei Estabragh [ID¹⁷¹](#), O.L. Rezanova [ID³⁷](#),
 P. Reznicek [ID¹³³](#), N. Ribaric [ID⁹¹](#), E. Ricci [ID^{78a,78b}](#), R. Richter [ID¹¹⁰](#), S. Richter [ID^{47a,47b}](#),
 E. Richter-Was [ID^{85b}](#), M. Ridel [ID¹²⁷](#), S. Ridouani [ID^{35d}](#), P. Rieck [ID¹¹⁷](#), P. Riedler [ID³⁶](#),
 M. Rijssenbeek [ID¹⁴⁵](#), A. Rimoldi [ID^{73a,73b}](#), M. Rimoldi [ID⁴⁸](#), L. Rinaldi [ID^{23b,23a}](#), T.T. Rinn [ID²⁹](#),
 M.P. Rinnagel [ID¹⁰⁹](#), G. Ripellino [ID¹⁶¹](#), I. Riu [ID¹³](#), P. Rivadeneira [ID⁴⁸](#), J.C. Rivera Vergara [ID¹⁶⁵](#),
 F. Rizatdinova [ID¹²¹](#), E. Rizvi [ID⁹⁴](#), C. Rizzi [ID⁵⁶](#), B.A. Roberts [ID¹⁶⁷](#), B.R. Roberts [ID^{17a}](#),
 S.H. Robertson [ID^{104,z}](#), M. Robin [ID⁴⁸](#), D. Robinson [ID³²](#), C.M. Robles Gajardo [ID^{137f}](#),
 M. Robles Manzano [ID¹⁰⁰](#), A. Robson [ID⁵⁹](#), A. Rocchi [ID^{76a,76b}](#), C. Roda [ID^{74a,74b}](#), S. Rodriguez Bosca [ID^{63a}](#),
 Y. Rodriguez Garcia [ID^{22a}](#), A. Rodriguez Rodriguez [ID⁵⁴](#), A.M. Rodríguez Vera [ID^{156b}](#), S. Roe [ID³⁶](#),
 J.T. Roemer [ID¹⁶⁰](#), A.R. Roepe-Gier [ID¹³⁶](#), J. Roggel [ID¹⁷¹](#), O. Røhne [ID¹²⁵](#), R.A. Rojas [ID¹⁰³](#),
 C.P.A. Roland [ID⁶⁸](#), J. Roloff [ID²⁹](#), A. Romaniouk [ID³⁷](#), E. Romano [ID^{73a,73b}](#), M. Romano [ID^{23b}](#),
 A.C. Romero Hernandez [ID¹⁶²](#), N. Rompotis [ID⁹²](#), L. Roos [ID¹²⁷](#), S. Rosati [ID^{75a}](#), B.J. Rosser [ID³⁹](#),
 E. Rossi [ID⁴](#), E. Rossi [ID^{72a,72b}](#), L.P. Rossi [ID^{57b}](#), L. Rossini [ID⁴⁸](#), R. Rosten [ID¹¹⁹](#), M. Rotaru [ID^{27b}](#),
 B. Rottler [ID⁵⁴](#), C. Rougier [ID^{102,ad}](#), D. Rousseau [ID⁶⁶](#), D. Rousso [ID³²](#), A. Roy [ID¹⁶²](#), S. Roy-Garand [ID¹⁵⁵](#),
 A. Rozanov [ID¹⁰²](#), Y. Rozen [ID¹⁵⁰](#), X. Ruan [ID^{33g}](#), A. Rubio Jimenez [ID¹⁶³](#), A.J. Ruby [ID⁹²](#),
 V.H. Ruelas Rivera [ID¹⁸](#), T.A. Ruggeri [ID¹](#), A. Ruggiero [ID¹²⁶](#), A. Ruiz-Martinez [ID¹⁶³](#), A. Rummeler [ID³⁶](#),
 Z. Rurikova [ID⁵⁴](#), N.A. Rusakovich [ID³⁸](#), H.L. Russell [ID¹⁶⁵](#), J.P. Rutherford [ID⁷](#), K. Rybacki [ID⁹¹](#),
 M. Rybar [ID¹³³](#), E.B. Rye [ID¹²⁵](#), A. Ryzhov [ID³⁷](#), J.A. Sabater Iglesias [ID⁵⁶](#), P. Sabatini [ID¹⁶³](#),
 L. Sabetta [ID^{75a,75b}](#), H.F-W. Sadrozinski [ID¹³⁶](#), F. Safai Tehrani [ID^{75a}](#), B. Safarzadeh Samani [ID¹⁴⁶](#),
 M. Safdari [ID¹⁴³](#), S. Saha [ID¹⁰⁴](#), M. Sahinsoy [ID¹¹⁰](#), M. Saimpert [ID¹³⁵](#), M. Saito [ID¹⁵³](#), T. Saito [ID¹⁵³](#),
 D. Salamani [ID³⁶](#), A. Salnikov [ID¹⁴³](#), J. Salt [ID¹⁶³](#), A. Salvador Salas [ID¹³](#), D. Salvatore [ID^{43b,43a}](#),
 F. Salvatore [ID¹⁴⁶](#), A. Salzburger [ID³⁶](#), D. Sammel [ID⁵⁴](#), D. Sampsonidis [ID^{152,f}](#), D. Sampsonidou [ID^{123,62c}](#),
 J. Sánchez [ID¹⁶³](#), A. Sanchez Pineda [ID⁴](#), V. Sanchez Sebastian [ID¹⁶³](#), H. Sandaker [ID¹²⁵](#), C.O. Sander [ID⁴⁸](#),
 J.A. Sandesara [ID¹⁰³](#), M. Sandhoff [ID¹⁷¹](#), C. Sandoval [ID^{22b}](#), D.P.C. Sankey [ID¹³⁴](#), T. Sano [ID⁸⁷](#),
 A. Sansoni [ID⁵³](#), L. Santi [ID^{75a,75b}](#), C. Santoni [ID⁴⁰](#), H. Santos [ID^{130a,130b}](#), S.N. Santpur [ID^{17a}](#), A. Santra [ID¹⁶⁹](#),
 K.A. Saoucha [ID¹³⁹](#), J.G. Saraiva [ID^{130a,130d}](#), J. Sardain [ID⁷](#), O. Sasaki [ID⁸³](#), K. Sato [ID¹⁵⁷](#), C. Sauer [ID^{63b}](#),
 F. Sauerburger [ID⁵⁴](#), E. Sauvan [ID⁴](#), P. Savard [ID^{155,ai}](#), R. Sawada [ID¹⁵³](#), C. Sawyer [ID¹³⁴](#), L. Sawyer [ID⁹⁷](#),
 I. Sayago Galvan [ID¹⁶³](#), C. Sbarra [ID^{23b}](#), A. Sbrizzi [ID^{23b,23a}](#), T. Scanlon [ID⁹⁶](#), J. Schaarschmidt [ID¹³⁸](#),
 P. Schacht [ID¹¹⁰](#), D. Schaefer [ID³⁹](#), U. Schäfer [ID¹⁰⁰](#), A.C. Schaffer [ID^{66,44}](#), D. Schaile [ID¹⁰⁹](#),
 R.D. Schamberger [ID¹⁴⁵](#), E. Schanet [ID¹⁰⁹](#), C. Scharf [ID¹⁸](#), M.M. Schefer [ID¹⁹](#), V.A. Schegelsky [ID³⁷](#),
 D. Scheirich [ID¹³³](#), F. Schenck [ID¹⁸](#), M. Schernau [ID¹⁶⁰](#), C. Scheulen [ID⁵⁵](#), C. Schiavi [ID^{57b,57a}](#),
 E.J. Schioppa [ID^{70a,70b}](#), M. Schioppa [ID^{43b,43a}](#), B. Schlag [ID^{143,q}](#), K.E. Schleicher [ID⁵⁴](#), S. Schlenker [ID³⁶](#),
 J. Schmeing [ID¹⁷¹](#), M.A. Schmidt [ID¹⁷¹](#), K. Schmieden [ID¹⁰⁰](#), C. Schmitt [ID¹⁰⁰](#), S. Schmitt [ID⁴⁸](#),
 L. Schoeffel [ID¹³⁵](#), A. Schoening [ID^{63b}](#), P.G. Scholer [ID⁵⁴](#), E. Schopf [ID¹²⁶](#), M. Schott [ID¹⁰⁰](#),
 J. Schovancova [ID³⁶](#), S. Schramm [ID⁵⁶](#), F. Schroeder [ID¹⁷¹](#), H-C. Schultz-Coulon [ID^{63a}](#), M. Schumacher [ID⁵⁴](#),
 B.A. Schumm [ID¹³⁶](#), Ph. Schune [ID¹³⁵](#), H.R. Schwartz [ID¹³⁶](#), A. Schwartzman [ID¹⁴³](#), T.A. Schwarz [ID¹⁰⁶](#),
 Ph. Schwemling [ID¹³⁵](#), R. Schwienhorst [ID¹⁰⁷](#), A. Sciandra [ID¹³⁶](#), G. Sciolla [ID²⁶](#), F. Scuri [ID^{74a}](#), F. Scutti [ID¹⁰⁵](#),
 C.D. Sebastiani [ID⁹²](#), K. Sedlaczek [ID⁴⁹](#), P. Seema [ID¹⁸](#), S.C. Seidel [ID¹¹²](#), A. Seiden [ID¹³⁶](#),
 B.D. Seidlitz [ID⁴¹](#), C. Seitz [ID⁴⁸](#), J.M. Seixas [ID^{82b}](#), G. Sekhniadze [ID^{72a}](#), S.J. Sekula [ID⁴⁴](#), L. Selam [ID⁴](#),
 N. Semprini-Cesari [ID^{23b,23a}](#), S. Sen [ID⁵¹](#), D. Sengupta [ID⁵⁶](#), V. Senthilkumar [ID¹⁶³](#), L. Serin [ID⁶⁶](#),
 L. Serkin [ID^{69a,69b}](#), M. Sessa [ID^{77a,77b}](#), H. Severini [ID¹²⁰](#), F. Sforza [ID^{57b,57a}](#), A. Sfyrla [ID⁵⁶](#),

E. Shabalina ⁵⁵, R. Shaheen ¹⁴⁴, J.D. Shahinian ¹²⁸, D. Shaked Renous ¹⁶⁹, L.Y. Shan ^{14a},
 M. Shapiro ^{17a}, A. Sharma ³⁶, A.S. Sharma ¹⁶⁴, P. Sharma ⁸⁰, S. Sharma ⁴⁸, P.B. Shatalov ³⁷,
 K. Shaw ¹⁴⁶, S.M. Shaw ¹⁰¹, Q. Shen ^{62c,5}, P. Sherwood ⁹⁶, L. Shi ⁹⁶, C.O. Shimmin ¹⁷²,
 Y. Shimogama ¹⁶⁸, J.D. Shinner ⁹⁵, I.P.J. Shipsey ¹²⁶, S. Shirabe ⁶⁰, M. Shiyakova ^{38,x},
 J. Shlomi ¹⁶⁹, M.J. Shochet ³⁹, J. Shojaii ¹⁰⁵, D.R. Shope ¹²⁵, S. Shrestha ^{119,al}, E.M. Shrif ^{33g},
 M.J. Shroff ¹⁶⁵, P. Sicho ¹³¹, A.M. Sickles ¹⁶², E. Sideras Haddad ^{33g}, A. Sidoti ^{23b},
 F. Siegert ⁵⁰, Dj. Sijacki ¹⁵, R. Sikora ^{85a}, F. Sili ⁹⁰, J.M. Silva ²⁰, M.V. Silva Oliveira ³⁶,
 S.B. Silverstein ^{47a}, S. Simion ⁶⁶, R. Simoniello ³⁶, E.L. Simpson ⁵⁹, H. Simpson ¹⁴⁶,
 L.R. Simpson ¹⁰⁶, N.D. Simpson ⁹⁸, S. Simsek ^{21d}, S. Sindhu ⁵⁵, P. Sinervo ¹⁵⁵, S. Singh ¹⁴²,
 S. Singh ¹⁵⁵, S. Sinha ⁴⁸, S. Sinha ^{33g}, M. Sioli ^{23b,23a}, I. Siral ³⁶, S.Yu. Sivoklov ^{37,*},
 J. Sjölin ^{47a,47b}, A. Skaf ⁵⁵, E. Skorda ⁹⁸, P. Skubic ¹²⁰, M. Slawinska ⁸⁶, V. Smakhtin ¹⁶⁹,
 B.H. Smart ¹³⁴, J. Smiesko ³⁶, S.Yu. Smirnov ³⁷, Y. Smirnov ³⁷, L.N. Smirnova ^{37,a},
 O. Smirnova ⁹⁸, A.C. Smith ⁴¹, E.A. Smith ³⁹, H.A. Smith ¹²⁶, J.L. Smith ⁹², R. Smith ¹⁴³,
 M. Smizanska ⁹¹, K. Smolek ¹³², A.A. Snesarev ³⁷, H.L. Snoek ¹¹⁴, S. Snyder ²⁹, R. Sobie ^{165,z},
 A. Soffer ¹⁵¹, C.A. Solans Sanchez ³⁶, E.Yu. Soldatov ³⁷, U. Soldevila ¹⁶³, A.A. Solodkov ³⁷,
 S. Solomon ⁵⁴, A. Soloshenko ³⁸, K. Solovieva ⁵⁴, O.V. Solovyanov ⁴⁰, V. Solovyev ³⁷,
 P. Sommer ³⁶, A. Sonay ¹³, W.Y. Song ^{156b}, J.M. Sonneveld ¹¹⁴, A. Sopczak ¹³², A.L. Sopio ⁹⁶,
 F. Sopkova ^{28b}, V. Sothilingam ^{63a}, S. Sottocornola ⁶⁸, R. Soualah ^{116b}, Z. Soumami ^{35e},
 D. South ⁴⁸, S. Spagnolo ^{70a,70b}, M. Spalla ¹¹⁰, D. Sperlich ⁵⁴, G. Spigo ³⁶, M. Spina ¹⁴⁶,
 S. Spinali ⁹¹, D.P. Spiteri ⁵⁹, M. Spousta ¹³³, E.J. Staats ³⁴, A. Stabile ^{71a,71b}, R. Stamen ^{63a},
 M. Stamenkovic ¹¹⁴, A. Stampekis ²⁰, M. Standke ²⁴, E. Stanecka ⁸⁶, M.V. Stange ⁵⁰,
 B. Stanislaus ^{17a}, M.M. Stanitzki ⁴⁸, M. Stankaityte ¹²⁶, B. Stapf ⁴⁸, E.A. Starchenko ³⁷,
 G.H. Stark ¹³⁶, J. Stark ^{102,ad}, D.M. Starko ^{156b}, P. Staroba ¹³¹, P. Starovoitov ^{63a}, S. Stärz ¹⁰⁴,
 R. Staszewski ⁸⁶, G. Stavropoulos ⁴⁶, J. Steentoft ¹⁶¹, P. Steinberg ²⁹, B. Stelzer ^{142,156a},
 H.J. Stelzer ¹²⁹, O. Stelzer-Chilton ^{156a}, H. Stenzel ⁵⁸, T.J. Stevenson ¹⁴⁶, G.A. Stewart ³⁶,
 J.R. Stewart ¹²¹, M.C. Stockton ³⁶, G. Stoicea ^{27b}, M. Stolarski ^{130a}, S. Stonjek ¹¹⁰,
 A. Straessner ⁵⁰, J. Strandberg ¹⁴⁴, S. Strandberg ^{47a,47b}, M. Strauss ¹²⁰, T. Strebler ¹⁰²,
 P. Strizenc ^{28b}, R. Ströhmer ¹⁶⁶, D.M. Strom ¹²³, L.R. Strom ⁴⁸, R. Stroynowski ⁴⁴,
 A. Strubig ^{47a,47b}, S.A. Stucci ²⁹, B. Stugu ¹⁶, J. Stupak ¹²⁰, N.A. Styles ⁴⁸, D. Su ¹⁴³,
 S. Su ^{62a}, W. Su ^{62d,138,62c}, X. Su ^{62a,66}, K. Sugizaki ¹⁵³, V.V. Sulin ³⁷, M.J. Sullivan ⁹²,
 D.M.S. Sultan ^{78a,78b}, L. Sultanaliyeva ³⁷, S. Sultansoy ^{3b}, T. Sumida ⁸⁷, S. Sun ¹⁰⁶, S. Sun ¹⁷⁰,
 O. Sunneborn Gudnadottir ¹⁶¹, M.R. Sutton ¹⁴⁶, M. Svatos ¹³¹, M. Swiatlowski ^{156a},
 T. Swirski ¹⁶⁶, I. Sykora ^{28a}, M. Sykora ¹³³, T. Sykora ¹³³, D. Ta ¹⁰⁰, K. Tackmann ^{48,w},
 A. Taffard ¹⁶⁰, R. Tafirout ^{156a}, J.S. Tafoya Vargas ⁶⁶, R.H.M. Taibah ¹²⁷, R. Takashima ⁸⁸,
 E.P. Takeva ⁵², Y. Takubo ⁸³, M. Talby ¹⁰², A.A. Talyshev ³⁷, K.C. Tam ^{64b}, N.M. Tamir ¹⁵¹,
 A. Tanaka ¹⁵³, J. Tanaka ¹⁵³, R. Tanaka ⁶⁶, M. Tanasini ^{57b,57a}, Z. Tao ¹⁶⁴, S. Tapia Araya ^{137f},
 S. Tapprogge ¹⁰⁰, A. Tarek Abouelfadl Mohamed ¹⁰⁷, S. Tarem ¹⁵⁰, K. Tariq ^{62b}, G. Tarna ^{102,27b},
 G.F. Tartarelli ^{71a}, P. Tas ¹³³, M. Tasevsky ¹³¹, E. Tassi ^{43b,43a}, A.C. Tate ¹⁶², G. Tateno ¹⁵³,
 Y. Tayalati ^{35e,y}, G.N. Taylor ¹⁰⁵, W. Taylor ^{156b}, H. Teagle ⁹², A.S. Tee ¹⁷⁰,
 R. Teixeira De Lima ¹⁴³, P. Teixeira-Dias ⁹⁵, J.J. Teoh ¹⁵⁵, K. Terashi ¹⁵³, J. Terron ⁹⁹,
 S. Terzo ¹³, M. Testa ⁵³, R.J. Teuscher ^{155,z}, A. Thaler ⁷⁹, O. Theiner ⁵⁶, N. Themistokleous ⁵²,
 T. Thevenaux-Pelzer ¹⁰², O. Thielmann ¹⁷¹, D.W. Thomas ⁹⁵, J.P. Thomas ²⁰, E.A. Thompson ^{17a},
 P.D. Thompson ²⁰, E. Thomson ¹²⁸, Y. Tian ⁵⁵, V. Tikhomirov ^{37,a}, Yu.A. Tikhonov ³⁷,
 S. Timoshenko ³⁷, E.X.L. Ting ¹, P. Tipton ¹⁷², S.H. Tlou ^{33g}, A. Tnourji ⁴⁰, K. Todome ^{23b,23a},
 S. Todorova-Nova ¹³³, S. Todt ⁵⁰, M. Togawa ⁸³, J. Tojo ⁸⁹, S. Tokár ^{28a}, K. Tokushuku ⁸³,
 O. Toldaiev ⁶⁸, R. Tombs ³², M. Tomoto ^{83,111}, L. Tompkins ^{143,q}, K.W. Topolnicki ^{85b},
 E. Torrence ¹²³, H. Torres ^{102,ad}, E. Torró Pastor ¹⁶³, M. Toscani ³⁰, C. Tosciri ³⁹, M. Tost ¹¹,

D.R. Tovey ¹³⁹, A. Traeet ¹⁶, I.S. Trandafir ^{27b}, T. Trefzger ¹⁶⁶, A. Tricoli ²⁹, I.M. Trigger ^{156a},
S. Trincaz-Duvoid ¹²⁷, D.A. Trischuk ²⁶, B. Trocmé ⁶⁰, C. Troncon ^{71a}, L. Truong ^{33c},
M. Trzebinski ⁸⁶, A. Trzupiek ⁸⁶, F. Tsai ¹⁴⁵, M. Tsai ¹⁰⁶, A. Tsiamis ^{152,f}, P.V. Tsiareshka ³⁷,
S. Tsigaridas ^{156a}, A. Tsirigotis ^{152,u}, V. Tsiskaridze ¹⁴⁵, E.G. Tskhadadze ^{149a},
M. Tsooulou ^{152,f}, Y. Tsujikawa ⁸⁷, I.I. Tsukerman ³⁷, V. Tsulaia ^{17a}, S. Tsuno ⁸³, O. Tsur ¹⁵⁰,
D. Tsybychev ¹⁴⁵, Y. Tu ^{64b}, A. Tudorache ^{27b}, V. Tudorache ^{27b}, A.N. Tuna ³⁶, S. Turchikhin ³⁸,
I. Turk Cakir ^{3a}, R. Turra ^{71a}, T. Turtuvshin ^{38,aa}, P.M. Tuts ⁴¹, S. Tzamarias ^{152,f}, P. Tzanis ¹⁰,
E. Tzovara ¹⁰⁰, K. Uchida ¹⁵³, F. Ukegawa ¹⁵⁷, P.A. Ulloa Poblete ^{137c}, E.N. Umaka ²⁹,
G. Unal ³⁶, M. Unal ¹¹, A. Undrus ²⁹, G. Unel ¹⁶⁰, J. Urban ^{28b}, P. Urquijo ¹⁰⁵, G. Usai ⁸,
R. Ushioda ¹⁵⁴, M. Usman ¹⁰⁸, Z. Uysal ^{21b}, L. Vacavant ¹⁰², V. Vacek ¹³², B. Vachon ¹⁰⁴,
K.O.H. Vadla ¹²⁵, T. Vafeiadis ³⁶, A. Vaitkus ⁹⁶, C. Valderanis ¹⁰⁹, E. Valdes Santurio ^{47a,47b},
M. Valente ^{156a}, S. Valentinetti ^{23b,23a}, A. Valero ¹⁶³, E. Valiente Moreno ¹⁶³, A. Vallier ^{102,ad},
J.A. Valls Ferrer ¹⁶³, D.R. Van Arneman ¹¹⁴, T.R. Van Daalen ¹³⁸, P. Van Gemmeren ⁶,
M. Van Rijnbach ^{125,36}, S. Van Stroud ⁹⁶, I. Van Vulpen ¹¹⁴, M. Vanadia ^{76a,76b}, W. Vandelli ³⁶,
M. Vandenbroucke ¹³⁵, E.R. Vandewall ¹²¹, D. Vannicola ¹⁵¹, L. Vannoli ^{57b,57a}, R. Vari ^{75a},
E.W. Varnes ⁷, C. Varni ^{17a}, T. Varol ¹⁴⁸, D. Varouchas ⁶⁶, L. Varriale ¹⁶³, K.E. Varvell ¹⁴⁷,
M.E. Vasile ^{27b}, L. Vaslin ⁴⁰, G.A. Vasquez ¹⁶⁵, F. Vazeille ⁴⁰, T. Vazquez Schroeder ³⁶,
J. Veatch ³¹, V. Vecchio ¹⁰¹, M.J. Veen ¹⁰³, I. Veliscek ¹²⁶, L.M. Veloce ¹⁵⁵, F. Veloso ^{130a,130c},
S. Veneziano ^{75a}, A. Ventura ^{70a,70b}, A. Verbytskyi ¹¹⁰, M. Verducci ^{74a,74b}, C. Vergis ²⁴,
M. Verissimo De Araujo ^{82b}, W. Verkerke ¹¹⁴, J.C. Vermeulen ¹¹⁴, C. Vernieri ¹⁴³,
P.J. Verschuuren ⁹⁵, M. Vessella ¹⁰³, M.C. Vetterli ^{142,ai}, A. Vgenopoulos ^{152,f},
N. Viaux Maira ^{137f}, T. Vickey ¹³⁹, O.E. Vickey Boeriu ¹³⁹, G.H.A. Viehhauser ¹²⁶, L. Vignani ^{63b},
M. Villa ^{23b,23a}, M. Villaplana Perez ¹⁶³, E.M. Villhauer ⁵², E. Vilucchi ⁵³, M.G. Vincter ³⁴,
G.S. Virdee ²⁰, A. Vishwakarma ⁵², C. Vittori ³⁶, I. Vivarelli ¹⁴⁶, V. Vladimirov ¹⁶⁷,
E. Voevodina ¹¹⁰, F. Vogel ¹⁰⁹, P. Vokac ¹³², J. Von Ahnen ⁴⁸, E. Von Toerne ²⁴,
B. Vormwald ³⁶, V. Vorobel ¹³³, K. Vorobev ³⁷, M. Vos ¹⁶³, K. Voss ¹⁴¹, J.H. Vossebeld ⁹²,
M. Vozak ¹¹⁴, L. Vozdecky ⁹⁴, N. Vranjes ¹⁵, M. Vranjes Milosavljevic ¹⁵, M. Vreeswijk ¹¹⁴,
R. Vuillermet ³⁶, O. Vujinovic ¹⁰⁰, I. Vukotic ³⁹, S. Wada ¹⁵⁷, C. Wagner ¹⁰³, J.M. Wagner ^{17a},
W. Wagner ¹⁷¹, S. Wahdan ¹⁷¹, H. Wahlberg ⁹⁰, R. Wakasa ¹⁵⁷, M. Wakida ¹¹¹, J. Walder ¹³⁴,
R. Walker ¹⁰⁹, W. Walkowiak ¹⁴¹, A. Wall ¹²⁸, A.Z. Wang ¹⁷⁰, C. Wang ¹⁰⁰, C. Wang ^{62c},
H. Wang ^{17a}, J. Wang ^{64a}, R.-J. Wang ¹⁰⁰, R. Wang ⁶¹, R. Wang ⁶, S.M. Wang ¹⁴⁸,
S. Wang ^{62b}, T. Wang ^{62a}, W.T. Wang ⁸⁰, X. Wang ^{14c}, X. Wang ¹⁶², X. Wang ^{62c},
Y. Wang ^{62d}, Y. Wang ^{14c}, Z. Wang ¹⁰⁶, Z. Wang ^{62d,51,62c}, Z. Wang ¹⁰⁶, A. Warburton ¹⁰⁴,
R.J. Ward ²⁰, N. Warrack ⁵⁹, A.T. Watson ²⁰, H. Watson ⁵⁹, M.F. Watson ²⁰, G. Watts ¹³⁸,
B.M. Waugh ⁹⁶, C. Weber ²⁹, H.A. Weber ¹⁸, M.S. Weber ¹⁹, S.M. Weber ^{63a}, C. Wei ^{62a},
Y. Wei ¹²⁶, A.R. Weidberg ¹²⁶, E.J. Weik ¹¹⁷, J. Weingarten ⁴⁹, M. Weirich ¹⁰⁰, C. Weiser ⁵⁴,
C.J. Wells ⁴⁸, T. Wenaus ²⁹, B. Wendland ⁴⁹, T. Wengler ³⁶, N.S. Wenke ¹¹⁰, N. Wermes ²⁴,
M. Wessels ^{63a}, K. Whalen ¹²³, A.M. Wharton ⁹¹, A.S. White ⁶¹, A. White ⁸, M.J. White ¹,
D. Whiteson ¹⁶⁰, L. Wickremasinghe ¹²⁴, W. Wiedenmann ¹⁷⁰, C. Wiel ⁵⁰, M. Wielers ¹³⁴,
C. Wiglesworth ⁴², L.A.M. Wiik-Fuchs ⁵⁴, D.J. Wilbern ¹²⁰, H.G. Wilkens ³⁶, D.M. Williams ⁴¹,
H.H. Williams ¹²⁸, S. Williams ³², S. Willocq ¹⁰³, B.J. Wilson ¹⁰¹, P.J. Windischhofer ³⁹,
F. Winklmeier ¹²³, B.T. Winter ⁵⁴, J.K. Winter ¹⁰¹, M. Wittgen ¹⁴³, M. Wobisch ⁹⁷, R. Wölker ¹²⁶,
J. Wollrath ¹⁶⁰, M.W. Wolter ⁸⁶, H. Wolters ^{130a,130c}, V.W.S. Wong ¹⁶⁴, A.F. Wongel ⁴⁸,
S.D. Worm ⁴⁸, B.K. Wosiek ⁸⁶, K.W. Woźniak ⁸⁶, K. Wraight ⁵⁹, J. Wu ^{14a,14e}, M. Wu ^{64a},
M. Wu ¹¹³, S.L. Wu ¹⁷⁰, X. Wu ⁵⁶, Y. Wu ^{62a}, Z. Wu ^{135,62a}, J. Wuerzinger ¹¹⁰,
T.R. Wyatt ¹⁰¹, B.M. Wynne ⁵², S. Xella ⁴², L. Xia ^{14c}, M. Xia ^{14b}, J. Xiang ^{64c}, X. Xiao ¹⁰⁶,
M. Xie ^{62a}, X. Xie ^{62a}, S. Xin ^{14a,14e}, J. Xiong ^{17a}, I. Xiotidis ¹⁴⁶, D. Xu ^{14a}, H. Xu ^{62a}, H. Xu ^{62a},

L. Xu ¹, R. Xu ¹²⁸, T. Xu ¹⁰⁶, Y. Xu ^{14b}, Z. Xu ^{62b}, Z. Xu ^{14a}, B. Yabsley ¹⁴⁷, S. Yacoob ^{33a}, N. Yamaguchi ⁸⁹, Y. Yamaguchi ¹⁵⁴, H. Yamauchi ¹⁵⁷, T. Yamazaki ^{17a}, Y. Yamazaki ⁸⁴, J. Yan ^{62c}, S. Yan ¹²⁶, Z. Yan ²⁵, H.J. Yang ^{62c,62d}, H.T. Yang ^{62a}, S. Yang ^{62a}, T. Yang ^{64c}, X. Yang ^{62a}, X. Yang ^{14a}, Y. Yang ⁴⁴, Y. Yang ^{62a}, Z. Yang ^{62a,106}, W-M. Yao ^{17a}, Y.C. Yap ⁴⁸, H. Ye ^{14c}, H. Ye ⁵⁵, J. Ye ⁴⁴, S. Ye ²⁹, X. Ye ^{62a}, Y. Yeh ⁹⁶, I. Yeletsikh ³⁸, B.K. Yeo ^{17a}, M.R. Yexley ⁹¹, P. Yin ⁴¹, K. Yorita ¹⁶⁸, S. Younas ^{27b}, C.J.S. Young ⁵⁴, C. Young ¹⁴³, Y. Yu ^{62a}, M. Yuan ¹⁰⁶, R. Yuan ^{62b,1}, L. Yue ⁹⁶, M. Zaazoua ^{35e}, B. Zabinski ⁸⁶, E. Zaid ⁵², T. Zakareishvili ^{149b}, N. Zakharchuk ³⁴, S. Zambito ⁵⁶, J.A. Zamora Saa ^{137d,137b}, J. Zang ¹⁵³, D. Zanzi ⁵⁴, O. Zaplatilek ¹³², C. Zeitnitz ¹⁷¹, H. Zeng ^{14a}, J.C. Zeng ¹⁶², D.T. Zenger Jr ²⁶, O. Zenin ³⁷, T. Ženiš ^{28a}, S. Zenz ⁹⁴, S. Zerradi ^{35a}, D. Zerwas ⁶⁶, M. Zhai ^{14a,14e}, B. Zhang ^{14c}, D.F. Zhang ¹³⁹, J. Zhang ^{62b}, J. Zhang ⁶, K. Zhang ^{14a,14e}, L. Zhang ^{14c}, P. Zhang ^{14a,14e}, R. Zhang ¹⁷⁰, S. Zhang ¹⁰⁶, T. Zhang ¹⁵³, X. Zhang ^{62c}, X. Zhang ^{62b}, Y. Zhang ^{62c,5}, Z. Zhang ^{17a}, Z. Zhang ⁶⁶, H. Zhao ¹³⁸, P. Zhao ⁵¹, T. Zhao ^{62b}, Y. Zhao ¹³⁶, Z. Zhao ^{62a}, A. Zhemchugov ³⁸, K. Zheng ¹⁶², X. Zheng ^{62a}, Z. Zheng ¹⁴³, D. Zhong ¹⁶², B. Zhou ¹⁰⁶, C. Zhou ¹⁷⁰, H. Zhou ⁷, N. Zhou ^{62c}, Y. Zhou ⁷, C.G. Zhu ^{62b}, J. Zhu ¹⁰⁶, Y. Zhu ^{62c}, Y. Zhu ^{62a}, X. Zhuang ^{14a}, K. Zhukov ³⁷, V. Zhulanov ³⁷, N.I. Zimine ³⁸, J. Zinsser ^{63b}, M. Ziolkowski ¹⁴¹, L. Živković ¹⁵, A. Zoccoli ^{23b,23a}, K. Zoch ⁵⁶, T.G. Zorbas ¹³⁹, O. Zormpa ⁴⁶, W. Zou ⁴¹, L. Zwalinski ³⁶.

¹Department of Physics, University of Adelaide, Adelaide; Australia.

²Department of Physics, University of Alberta, Edmonton AB; Canada.

³(^a)Department of Physics, Ankara University, Ankara; (^b)Division of Physics, TOBB University of Economics and Technology, Ankara; Türkiye.

⁴LAPP, Université Savoie Mont Blanc, CNRS/IN2P3, Annecy; France.

⁵APC, Université Paris Cité, CNRS/IN2P3, Paris; France.

⁶High Energy Physics Division, Argonne National Laboratory, Argonne IL; United States of America.

⁷Department of Physics, University of Arizona, Tucson AZ; United States of America.

⁸Department of Physics, University of Texas at Arlington, Arlington TX; United States of America.

⁹Physics Department, National and Kapodistrian University of Athens, Athens; Greece.

¹⁰Physics Department, National Technical University of Athens, Zografou; Greece.

¹¹Department of Physics, University of Texas at Austin, Austin TX; United States of America.

¹²Institute of Physics, Azerbaijan Academy of Sciences, Baku; Azerbaijan.

¹³Institut de Física d'Altes Energies (IFAE), Barcelona Institute of Science and Technology, Barcelona; Spain.

¹⁴(^a)Institute of High Energy Physics, Chinese Academy of Sciences, Beijing; (^b)Physics Department, Tsinghua University, Beijing; (^c)Department of Physics, Nanjing University, Nanjing; (^d)School of Science, Shenzhen Campus of Sun Yat-sen University; (^e)University of Chinese Academy of Science (UCAS), Beijing; China.

¹⁵Institute of Physics, University of Belgrade, Belgrade; Serbia.

¹⁶Department for Physics and Technology, University of Bergen, Bergen; Norway.

¹⁷(^a)Physics Division, Lawrence Berkeley National Laboratory, Berkeley CA; (^b)University of California, Berkeley CA; United States of America.

¹⁸Institut für Physik, Humboldt Universität zu Berlin, Berlin; Germany.

¹⁹Albert Einstein Center for Fundamental Physics and Laboratory for High Energy Physics, University of Bern, Bern; Switzerland.

²⁰School of Physics and Astronomy, University of Birmingham, Birmingham; United Kingdom.

²¹(^a)Department of Physics, Bogazici University, Istanbul; (^b)Department of Physics Engineering,

Gaziantep University, Gaziantep;^(c)Department of Physics, Istanbul University, Istanbul;^(d)Istinye University, Sariyer, Istanbul; Türkiye.

^{22(a)}Facultad de Ciencias y Centro de Investigaciones, Universidad Antonio Nariño,

Bogotá;^(b)Departamento de Física, Universidad Nacional de Colombia, Bogotá; Colombia.

^{23(a)}Dipartimento di Fisica e Astronomia A. Righi, Università di Bologna, Bologna;^(b)INFN Sezione di Bologna; Italy.

²⁴Physikalisches Institut, Universität Bonn, Bonn; Germany.

²⁵Department of Physics, Boston University, Boston MA; United States of America.

²⁶Department of Physics, Brandeis University, Waltham MA; United States of America.

^{27(a)}Transilvania University of Brasov, Brasov;^(b)Horia Hulubei National Institute of Physics and Nuclear Engineering, Bucharest;^(c)Department of Physics, Alexandru Ioan Cuza University of Iasi, Iasi;^(d)National Institute for Research and Development of Isotopic and Molecular Technologies, Physics Department, Cluj-Napoca;^(e)University Politehnica Bucharest, Bucharest;^(f)West University in Timisoara, Timisoara;^(g)Faculty of Physics, University of Bucharest, Bucharest; Romania.

^{28(a)}Faculty of Mathematics, Physics and Informatics, Comenius University, Bratislava;^(b)Department of Subnuclear Physics, Institute of Experimental Physics of the Slovak Academy of Sciences, Kosice; Slovak Republic.

²⁹Physics Department, Brookhaven National Laboratory, Upton NY; United States of America.

³⁰Universidad de Buenos Aires, Facultad de Ciencias Exactas y Naturales, Departamento de Física, y CONICET, Instituto de Física de Buenos Aires (IFIBA), Buenos Aires; Argentina.

³¹California State University, CA; United States of America.

³²Cavendish Laboratory, University of Cambridge, Cambridge; United Kingdom.

^{33(a)}Department of Physics, University of Cape Town, Cape Town;^(b)iThemba Labs, Western Cape;^(c)Department of Mechanical Engineering Science, University of Johannesburg,

Johannesburg;^(d)National Institute of Physics, University of the Philippines Diliman (Philippines);^(e)University of South Africa, Department of Physics, Pretoria;^(f)University of Zululand, KwaDlangezwa;^(g)School of Physics, University of the Witwatersrand, Johannesburg; South Africa.

³⁴Department of Physics, Carleton University, Ottawa ON; Canada.

^{35(a)}Faculté des Sciences Ain Chock, Réseau Universitaire de Physique des Hautes Energies - Université Hassan II, Casablanca;^(b)Faculté des Sciences, Université Ibn-Tofail, Kénitra;^(c)Faculté des Sciences Semlalia, Université Cadi Ayyad, LPHEA-Marrakech;^(d)LPMR, Faculté des Sciences, Université Mohamed Premier, Oujda;^(e)Faculté des sciences, Université Mohammed V, Rabat;^(f)Institute of Applied Physics, Mohammed VI Polytechnic University, Ben Guerir; Morocco.

³⁶CERN, Geneva; Switzerland.

³⁷Affiliated with an institute covered by a cooperation agreement with CERN.

³⁸Affiliated with an international laboratory covered by a cooperation agreement with CERN.

³⁹Enrico Fermi Institute, University of Chicago, Chicago IL; United States of America.

⁴⁰LPC, Université Clermont Auvergne, CNRS/IN2P3, Clermont-Ferrand; France.

⁴¹Nevis Laboratory, Columbia University, Irvington NY; United States of America.

⁴²Niels Bohr Institute, University of Copenhagen, Copenhagen; Denmark.

^{43(a)}Dipartimento di Fisica, Università della Calabria, Rende;^(b)INFN Gruppo Collegato di Cosenza, Laboratori Nazionali di Frascati; Italy.

⁴⁴Physics Department, Southern Methodist University, Dallas TX; United States of America.

⁴⁵Physics Department, University of Texas at Dallas, Richardson TX; United States of America.

⁴⁶National Centre for Scientific Research "Demokritos", Agia Paraskevi; Greece.

^{47(a)}Department of Physics, Stockholm University;^(b)Oskar Klein Centre, Stockholm; Sweden.

⁴⁸Deutsches Elektronen-Synchrotron DESY, Hamburg and Zeuthen; Germany.

- ⁴⁹Fakultät Physik , Technische Universität Dortmund, Dortmund; Germany.
- ⁵⁰Institut für Kern- und Teilchenphysik, Technische Universität Dresden, Dresden; Germany.
- ⁵¹Department of Physics, Duke University, Durham NC; United States of America.
- ⁵²SUPA - School of Physics and Astronomy, University of Edinburgh, Edinburgh; United Kingdom.
- ⁵³INFN e Laboratori Nazionali di Frascati, Frascati; Italy.
- ⁵⁴Physikalisches Institut, Albert-Ludwigs-Universität Freiburg, Freiburg; Germany.
- ⁵⁵II. Physikalisches Institut, Georg-August-Universität Göttingen, Göttingen; Germany.
- ⁵⁶Département de Physique Nucléaire et Corpusculaire, Université de Genève, Genève; Switzerland.
- ⁵⁷(^a)Dipartimento di Fisica, Università di Genova, Genova;(^b) INFN Sezione di Genova; Italy.
- ⁵⁸II. Physikalisches Institut, Justus-Liebig-Universität Giessen, Giessen; Germany.
- ⁵⁹SUPA - School of Physics and Astronomy, University of Glasgow, Glasgow; United Kingdom.
- ⁶⁰LPSC, Université Grenoble Alpes, CNRS/IN2P3, Grenoble INP, Grenoble; France.
- ⁶¹Laboratory for Particle Physics and Cosmology, Harvard University, Cambridge MA; United States of America.
- ⁶²(^a)Department of Modern Physics and State Key Laboratory of Particle Detection and Electronics, University of Science and Technology of China, Hefei;(^b)Institute of Frontier and Interdisciplinary Science and Key Laboratory of Particle Physics and Particle Irradiation (MOE), Shandong University, Qingdao;(^c)School of Physics and Astronomy, Shanghai Jiao Tong University, Key Laboratory for Particle Astrophysics and Cosmology (MOE), SKLPPC, Shanghai;(^d)Tsung-Dao Lee Institute, Shanghai; China.
- ⁶³(^a)Kirchhoff-Institut für Physik, Ruprecht-Karls-Universität Heidelberg, Heidelberg;(^b)Physikalisches Institut, Ruprecht-Karls-Universität Heidelberg, Heidelberg; Germany.
- ⁶⁴(^a)Department of Physics, Chinese University of Hong Kong, Shatin, N.T., Hong Kong;(^b)Department of Physics, University of Hong Kong, Hong Kong;(^c)Department of Physics and Institute for Advanced Study, Hong Kong University of Science and Technology, Clear Water Bay, Kowloon, Hong Kong; China.
- ⁶⁵Department of Physics, National Tsing Hua University, Hsinchu; Taiwan.
- ⁶⁶IJCLab, Université Paris-Saclay, CNRS/IN2P3, 91405, Orsay; France.
- ⁶⁷Centro Nacional de Microelectrónica (IMB-CNM-CSIC), Barcelona; Spain.
- ⁶⁸Department of Physics, Indiana University, Bloomington IN; United States of America.
- ⁶⁹(^a)INFN Gruppo Collegato di Udine, Sezione di Trieste, Udine;(^b)ICTP, Trieste;(^c)Dipartimento Politecnico di Ingegneria e Architettura, Università di Udine, Udine; Italy.
- ⁷⁰(^a)INFN Sezione di Lecce;(^b)Dipartimento di Matematica e Fisica, Università del Salento, Lecce; Italy.
- ⁷¹(^a)INFN Sezione di Milano;(^b)Dipartimento di Fisica, Università di Milano, Milano; Italy.
- ⁷²(^a)INFN Sezione di Napoli;(^b)Dipartimento di Fisica, Università di Napoli, Napoli; Italy.
- ⁷³(^a)INFN Sezione di Pavia;(^b)Dipartimento di Fisica, Università di Pavia, Pavia; Italy.
- ⁷⁴(^a)INFN Sezione di Pisa;(^b)Dipartimento di Fisica E. Fermi, Università di Pisa, Pisa; Italy.
- ⁷⁵(^a)INFN Sezione di Roma;(^b)Dipartimento di Fisica, Sapienza Università di Roma, Roma; Italy.
- ⁷⁶(^a)INFN Sezione di Roma Tor Vergata;(^b)Dipartimento di Fisica, Università di Roma Tor Vergata, Roma; Italy.
- ⁷⁷(^a)INFN Sezione di Roma Tre;(^b)Dipartimento di Matematica e Fisica, Università Roma Tre, Roma; Italy.
- ⁷⁸(^a)INFN-TIFPA;(^b)Università degli Studi di Trento, Trento; Italy.
- ⁷⁹Universität Innsbruck, Department of Astro and Particle Physics, Innsbruck; Austria.
- ⁸⁰University of Iowa, Iowa City IA; United States of America.
- ⁸¹Department of Physics and Astronomy, Iowa State University, Ames IA; United States of America.
- ⁸²(^a)Departamento de Engenharia Elétrica, Universidade Federal de Juiz de Fora (UFJF), Juiz de Fora;(^b)Universidade Federal do Rio De Janeiro COPPE/EE/IF, Rio de Janeiro;(^c)Instituto de Física, Universidade de São Paulo, São Paulo;(^d)Rio de Janeiro State University, Rio de Janeiro; Brazil.

- ⁸³KEK, High Energy Accelerator Research Organization, Tsukuba; Japan.
- ⁸⁴Graduate School of Science, Kobe University, Kobe; Japan.
- ⁸⁵(^a) AGH University of Krakow, Faculty of Physics and Applied Computer Science, Krakow; (^b) Marian Smoluchowski Institute of Physics, Jagiellonian University, Krakow; Poland.
- ⁸⁶Institute of Nuclear Physics Polish Academy of Sciences, Krakow; Poland.
- ⁸⁷Faculty of Science, Kyoto University, Kyoto; Japan.
- ⁸⁸Kyoto University of Education, Kyoto; Japan.
- ⁸⁹Research Center for Advanced Particle Physics and Department of Physics, Kyushu University, Fukuoka ; Japan.
- ⁹⁰Instituto de Física La Plata, Universidad Nacional de La Plata and CONICET, La Plata; Argentina.
- ⁹¹Physics Department, Lancaster University, Lancaster; United Kingdom.
- ⁹²Oliver Lodge Laboratory, University of Liverpool, Liverpool; United Kingdom.
- ⁹³Department of Experimental Particle Physics, Jožef Stefan Institute and Department of Physics, University of Ljubljana, Ljubljana; Slovenia.
- ⁹⁴School of Physics and Astronomy, Queen Mary University of London, London; United Kingdom.
- ⁹⁵Department of Physics, Royal Holloway University of London, Egham; United Kingdom.
- ⁹⁶Department of Physics and Astronomy, University College London, London; United Kingdom.
- ⁹⁷Louisiana Tech University, Ruston LA; United States of America.
- ⁹⁸Fysiska institutionen, Lunds universitet, Lund; Sweden.
- ⁹⁹Departamento de Física Teórica C-15 and CIAFF, Universidad Autónoma de Madrid, Madrid; Spain.
- ¹⁰⁰Institut für Physik, Universität Mainz, Mainz; Germany.
- ¹⁰¹School of Physics and Astronomy, University of Manchester, Manchester; United Kingdom.
- ¹⁰²CPPM, Aix-Marseille Université, CNRS/IN2P3, Marseille; France.
- ¹⁰³Department of Physics, University of Massachusetts, Amherst MA; United States of America.
- ¹⁰⁴Department of Physics, McGill University, Montreal QC; Canada.
- ¹⁰⁵School of Physics, University of Melbourne, Victoria; Australia.
- ¹⁰⁶Department of Physics, University of Michigan, Ann Arbor MI; United States of America.
- ¹⁰⁷Department of Physics and Astronomy, Michigan State University, East Lansing MI; United States of America.
- ¹⁰⁸Group of Particle Physics, University of Montreal, Montreal QC; Canada.
- ¹⁰⁹Fakultät für Physik, Ludwig-Maximilians-Universität München, München; Germany.
- ¹¹⁰Max-Planck-Institut für Physik (Werner-Heisenberg-Institut), München; Germany.
- ¹¹¹Graduate School of Science and Kobayashi-Maskawa Institute, Nagoya University, Nagoya; Japan.
- ¹¹²Department of Physics and Astronomy, University of New Mexico, Albuquerque NM; United States of America.
- ¹¹³Institute for Mathematics, Astrophysics and Particle Physics, Radboud University/Nikhef, Nijmegen; Netherlands.
- ¹¹⁴Nikhef National Institute for Subatomic Physics and University of Amsterdam, Amsterdam; Netherlands.
- ¹¹⁵Department of Physics, Northern Illinois University, DeKalb IL; United States of America.
- ¹¹⁶(^a) New York University Abu Dhabi, Abu Dhabi; (^b) University of Sharjah, Sharjah; United Arab Emirates.
- ¹¹⁷Department of Physics, New York University, New York NY; United States of America.
- ¹¹⁸Ochanomizu University, Otsuka, Bunkyo-ku, Tokyo; Japan.
- ¹¹⁹Ohio State University, Columbus OH; United States of America.
- ¹²⁰Homer L. Dodge Department of Physics and Astronomy, University of Oklahoma, Norman OK; United States of America.

- ¹²¹Department of Physics, Oklahoma State University, Stillwater OK; United States of America.
- ¹²²Palacký University, Joint Laboratory of Optics, Olomouc; Czech Republic.
- ¹²³Institute for Fundamental Science, University of Oregon, Eugene, OR; United States of America.
- ¹²⁴Graduate School of Science, Osaka University, Osaka; Japan.
- ¹²⁵Department of Physics, University of Oslo, Oslo; Norway.
- ¹²⁶Department of Physics, Oxford University, Oxford; United Kingdom.
- ¹²⁷LPNHE, Sorbonne Université, Université Paris Cité, CNRS/IN2P3, Paris; France.
- ¹²⁸Department of Physics, University of Pennsylvania, Philadelphia PA; United States of America.
- ¹²⁹Department of Physics and Astronomy, University of Pittsburgh, Pittsburgh PA; United States of America.
- ¹³⁰^(a)Laboratório de Instrumentação e Física Experimental de Partículas - LIP, Lisboa;^(b)Departamento de Física, Faculdade de Ciências, Universidade de Lisboa, Lisboa;^(c)Departamento de Física, Universidade de Coimbra, Coimbra;^(d)Centro de Física Nuclear da Universidade de Lisboa, Lisboa;^(e)Departamento de Física, Universidade do Minho, Braga;^(f)Departamento de Física Teórica y del Cosmos, Universidad de Granada, Granada (Spain);^(g)Departamento de Física, Instituto Superior Técnico, Universidade de Lisboa, Lisboa; Portugal.
- ¹³¹Institute of Physics of the Czech Academy of Sciences, Prague; Czech Republic.
- ¹³²Czech Technical University in Prague, Prague; Czech Republic.
- ¹³³Charles University, Faculty of Mathematics and Physics, Prague; Czech Republic.
- ¹³⁴Particle Physics Department, Rutherford Appleton Laboratory, Didcot; United Kingdom.
- ¹³⁵IRFU, CEA, Université Paris-Saclay, Gif-sur-Yvette; France.
- ¹³⁶Santa Cruz Institute for Particle Physics, University of California Santa Cruz, Santa Cruz CA; United States of America.
- ¹³⁷^(a)Departamento de Física, Pontificia Universidad Católica de Chile, Santiago;^(b)Millennium Institute for Subatomic physics at high energy frontier (SAPHIR), Santiago;^(c)Instituto de Investigación Multidisciplinario en Ciencia y Tecnología, y Departamento de Física, Universidad de La Serena;^(d)Universidad Andres Bello, Department of Physics, Santiago;^(e)Instituto de Alta Investigación, Universidad de Tarapacá, Arica;^(f)Departamento de Física, Universidad Técnica Federico Santa María, Valparaíso; Chile.
- ¹³⁸Department of Physics, University of Washington, Seattle WA; United States of America.
- ¹³⁹Department of Physics and Astronomy, University of Sheffield, Sheffield; United Kingdom.
- ¹⁴⁰Department of Physics, Shinshu University, Nagano; Japan.
- ¹⁴¹Department Physik, Universität Siegen, Siegen; Germany.
- ¹⁴²Department of Physics, Simon Fraser University, Burnaby BC; Canada.
- ¹⁴³SLAC National Accelerator Laboratory, Stanford CA; United States of America.
- ¹⁴⁴Department of Physics, Royal Institute of Technology, Stockholm; Sweden.
- ¹⁴⁵Departments of Physics and Astronomy, Stony Brook University, Stony Brook NY; United States of America.
- ¹⁴⁶Department of Physics and Astronomy, University of Sussex, Brighton; United Kingdom.
- ¹⁴⁷School of Physics, University of Sydney, Sydney; Australia.
- ¹⁴⁸Institute of Physics, Academia Sinica, Taipei; Taiwan.
- ¹⁴⁹^(a)E. Andronikashvili Institute of Physics, Iv. Javakhishvili Tbilisi State University, Tbilisi;^(b)High Energy Physics Institute, Tbilisi State University, Tbilisi;^(c)University of Georgia, Tbilisi; Georgia.
- ¹⁵⁰Department of Physics, Technion, Israel Institute of Technology, Haifa; Israel.
- ¹⁵¹Raymond and Beverly Sackler School of Physics and Astronomy, Tel Aviv University, Tel Aviv; Israel.
- ¹⁵²Department of Physics, Aristotle University of Thessaloniki, Thessaloniki; Greece.
- ¹⁵³International Center for Elementary Particle Physics and Department of Physics, University of Tokyo,

Tokyo; Japan.

¹⁵⁴Department of Physics, Tokyo Institute of Technology, Tokyo; Japan.

¹⁵⁵Department of Physics, University of Toronto, Toronto ON; Canada.

¹⁵⁶(^a)TRIUMF, Vancouver BC; (^b)Department of Physics and Astronomy, York University, Toronto ON; Canada.

¹⁵⁷Division of Physics and Tomonaga Center for the History of the Universe, Faculty of Pure and Applied Sciences, University of Tsukuba, Tsukuba; Japan.

¹⁵⁸Department of Physics and Astronomy, Tufts University, Medford MA; United States of America.

¹⁵⁹United Arab Emirates University, Al Ain; United Arab Emirates.

¹⁶⁰Department of Physics and Astronomy, University of California Irvine, Irvine CA; United States of America.

¹⁶¹Department of Physics and Astronomy, University of Uppsala, Uppsala; Sweden.

¹⁶²Department of Physics, University of Illinois, Urbana IL; United States of America.

¹⁶³Instituto de Física Corpuscular (IFIC), Centro Mixto Universidad de Valencia - CSIC, Valencia; Spain.

¹⁶⁴Department of Physics, University of British Columbia, Vancouver BC; Canada.

¹⁶⁵Department of Physics and Astronomy, University of Victoria, Victoria BC; Canada.

¹⁶⁶Fakultät für Physik und Astronomie, Julius-Maximilians-Universität Würzburg, Würzburg; Germany.

¹⁶⁷Department of Physics, University of Warwick, Coventry; United Kingdom.

¹⁶⁸Waseda University, Tokyo; Japan.

¹⁶⁹Department of Particle Physics and Astrophysics, Weizmann Institute of Science, Rehovot; Israel.

¹⁷⁰Department of Physics, University of Wisconsin, Madison WI; United States of America.

¹⁷¹Fakultät für Mathematik und Naturwissenschaften, Fachgruppe Physik, Bergische Universität Wuppertal, Wuppertal; Germany.

¹⁷²Department of Physics, Yale University, New Haven CT; United States of America.

^a Also Affiliated with an institute covered by a cooperation agreement with CERN.

^b Also at An-Najah National University, Nablus; Palestine.

^c Also at Borough of Manhattan Community College, City University of New York, New York NY; United States of America.

^d Also at Bruno Kessler Foundation, Trento; Italy.

^e Also at Center for High Energy Physics, Peking University; China.

^f Also at Center for Interdisciplinary Research and Innovation (CIRI-AUTH), Thessaloniki; Greece.

^g Also at Centro Studi e Ricerche Enrico Fermi; Italy.

^h Also at CERN, Geneva; Switzerland.

ⁱ Also at Département de Physique Nucléaire et Corpusculaire, Université de Genève, Genève; Switzerland.

^j Also at Departament de Física de la Universitat Autònoma de Barcelona, Barcelona; Spain.

^k Also at Department of Financial and Management Engineering, University of the Aegean, Chios; Greece.

^l Also at Department of Physics and Astronomy, Michigan State University, East Lansing MI; United States of America.

^m Also at Department of Physics, Ben Gurion University of the Negev, Beer Sheva; Israel.

ⁿ Also at Department of Physics, California State University, East Bay; United States of America.

^o Also at Department of Physics, California State University, Sacramento; United States of America.

^p Also at Department of Physics, King's College London, London; United Kingdom.

^q Also at Department of Physics, Stanford University, Stanford CA; United States of America.

^r Also at Department of Physics, University of Fribourg, Fribourg; Switzerland.

^s Also at Department of Physics, University of Thessaly; Greece.

^t Also at Department of Physics, Westmont College, Santa Barbara; United States of America.

^u Also at Hellenic Open University, Patras; Greece.

- ^v Also at Institutio Catalana de Recerca i Estudis Avancats, ICREA, Barcelona; Spain.
- ^w Also at Institut für Experimentalphysik, Universität Hamburg, Hamburg; Germany.
- ^x Also at Institute for Nuclear Research and Nuclear Energy (INRNE) of the Bulgarian Academy of Sciences, Sofia; Bulgaria.
- ^y Also at Institute of Applied Physics, Mohammed VI Polytechnic University, Ben Guerir; Morocco.
- ^z Also at Institute of Particle Physics (IPP); Canada.
- ^{aa} Also at Institute of Physics and Technology, Ulaanbaatar; Mongolia.
- ^{ab} Also at Institute of Physics, Azerbaijan Academy of Sciences, Baku; Azerbaijan.
- ^{ac} Also at Institute of Theoretical Physics, Ilia State University, Tbilisi; Georgia.
- ^{ad} Also at L2IT, Université de Toulouse, CNRS/IN2P3, UPS, Toulouse; France.
- ^{ae} Also at Lawrence Livermore National Laboratory, Livermore; United States of America.
- ^{af} Also at National Institute of Physics, University of the Philippines Diliman (Philippines); Philippines.
- ^{ag} Also at Technical University of Munich, Munich; Germany.
- ^{ah} Also at The Collaborative Innovation Center of Quantum Matter (CICQM), Beijing; China.
- ^{ai} Also at TRIUMF, Vancouver BC; Canada.
- ^{aj} Also at Università di Napoli Parthenope, Napoli; Italy.
- ^{ak} Also at University of Colorado Boulder, Department of Physics, Colorado; United States of America.
- ^{al} Also at Washington College, Maryland; United States of America.
- ^{am} Also at Yeditepe University, Physics Department, Istanbul; Türkiye.
- * Deceased